Watershed modeling for
regional water budget analysis

Neil Hellas
Department of Bioresource Engineering
McGill University, Montréal

November 2007

A thesis submitted to McGill University
in partial fulfillment of the requirements of the degree of
Master of Science

Abstract

Watershed models can play an important role in regional planning. Their ability to consider large, spatially diverse regions and assess the impact of different land use scenarios on water resources can lead to better, more informed decision making. Recent legislation in Ontario has led to the adoption of watershed models as part of drinking water source protection planning processes.

In this study, the ability of the SWAT model to simulate the hydrology of the Raisin River watershed, an area of 556km^2 located in eastern Ontario, is examined. The model was calibrated using data from 1985 to 1994 and validated using data from 1995 to 2004. Weekly average flow rates were used to evaluate the model, producing a Nash Sutcliffe coefficient of 0.798 for the period of calibration and 0.788 for the validation period.

Model error is most significant during the annual snowmelt period, suggesting deficiencies in the way snowmelt is modeled. Baseflow predictions are correct on an annual basis but exhibit more volatility than the observed flow. The Nash Sutcliffe coefficient is a common measure of hydrologic model performance but suffers from being strongly biased to certain times of the year. Specifically, it is insensitive to periods of low flow which are important for source protection planning. The possibility of transforming the observed and predicted flow rates to compensate is discussed.

The methodology presented takes advantage of readily available standardised data, permitting a similar modeling exercise to be easily undertaken for a different region. Results and analysis as presented could be used directly in the development of source protection plans. Spatial and temporal variation of water budget components (runoff, recharge and evapotranspiration) throughout the watershed is discussed. The impact of land use and soil type on the water budget is also highlighted.

Résumé

Les modèles de bassin d'eau peuvent jouer un rôle important dans la planification régionale. Leur capacité de considérer de grandes régions, diverses en espace et évaluer l'impact de scénarios d'utilisation de différentes terres sur des ressources en eau peut mener à des prises de décisions meilleures et plus informées. La récente législation en Ontario a mené à l'adoption de modèles de bassin d'eau faisant partie de processus de planification de protection de source d'eau potable.

Dans cette étude, la capacité du modèle SWAT (Outil d'évaluation du sol et de l'eau) pour simuler l'hydrologie du bassin de la Rivière Raisin, un secteur de 556km^2 situé à l'est de l'Ontario, est examiné. Le modèle a été calibré au cours de la période de 1985 à 1994 et validé au cours de la période de 1995 à 2004. Des débits hebdomadaires moyens ont été utilisés pour évaluer le modèle, produisant un coefficient Nash Sutcliffe de 0.798 pendant la période de calibrage et 0.788 pendant la période de validation.

L'erreur modèle est la plus significative pendant la période de fonte de neige annuelle, suggérant des manques dans la manière que la fonte de neige est modelée. Les prédictions du débit de base sont correctes sur une base annuelle, mais exposent plus de volatilité que le flux observé. Le coefficient Nash Sutcliffe est une mesure commune de performance du modèle hydrologique, mais souffre en étant fortement influencé par certains temps de l'année. Spécifiquement, il est insensible aux périodes de bas débit qui sont importantes pour la planification de la protection de source. La possibilité de transformer les débits observés et prévus pour indemniser est discutée.

La méthodologie présentée profite de données standardisées aisément disponibles, permettant à un exercice de modélisation semblable d'être facilement entrepris pour une région différente. Les résultats et l'analyse tel que présentés pourraient être utilisés directement dans le développement de plans de protection de source. La variation spatiale et temporelle de composants budgétaires d'eau (l'écoulement, la recharge et l'évapotranspiration) partout dans le bassin d'eau est discutée. L'impact d'utilisation de terre et le type de sol sur le bilan hydrique est aussi mis en évidence.

Acknowledgements

This thesis was made possible by the help of several people. Thanks to the people from several conservation authorities who were willing describe their experiences and requirements of watershed-scale hydrologic models. In particular, Shah Alamgir and John Meek from the Raisin River Conservation Authority were pivotal in providing background and context for this project. The help of the Walter Hitschfeld Geographic Information Centre staff in obtaining data from the National Topographic Database is appreciated. André Villeneuve from Agriculture Agri-food Canada provided additional clarification on the Canadian Soil Information System data. Tom Arsenault from Water Survey Canada provided clarification on stream gauge records within the study area. Yves Gauthier assisted with translation. Thanks to Dr. Shiv Prasher for providing constructive advice during the development of this thesis. Finally, thanks to Dr. Robert Bonnell for advising on this project and for his review of this and other manuscripts.

Table of Contents

List of Figures

List of Maps

List of Tables

List of Abbreviations

7Q	Annual minimum 7 day moving average flow rate
AGNPS	Agricultural Non-Point Source pollution model
ARS	United States Department of Agriculture – Agricultural Research Service
AWC	Available water content
CA	Conservation authority
CanSIS	Canadian Soil Information System
CN	Curve number
DEM	Digital elevation model
ESCO	Soil evaporation compensation coefficient
ET	Actual evapotranspiration
GWDLY	Groundwater delay coefficient
HRU	Hydrologic response unit
ML	Maximum likelihood
MUSLE	Modified Universal Soil Loss Equation
NDVI	Normalised difference vegetative index
NS	Nash Sutcliffe coefficient
NTDB	National Topographic Database
PET	Potential evapotranspiration
RVA	Range of variability approach
SPP	Source protection plan
SURLAG	Surface lag coefficient
SWAT	Soil and Water Assessment Tool
TIMP	Snowpack temperature lag coefficient
USLE	Universal Soil Loss Equation

1. Introduction

Watershed models are useful tools for planners and engineers. They can help identify ecologically significant areas and can link the impacts of land use to water quantity and quality in a basin. Identifying areas susceptible to pollution and quantifying the components of the water budget are key tasks which must be undertaken for support of good planning. Forecasting and the ability to consider large, diverse areas are also important aspects to consider. All of these are applications to which watershed models are well suited.

In any large geographic region, spatial heterogeneity of land cover, soil type and elevation lead to localised effects on the water budget components. Further, areas in downstream sections of a watershed are impacted by the upper reaches of the basin. When estimating the water budget components for an entire region, the particular contributions of localised areas can often be obscured. This has notable impacts on land use planning and environmental protection as decisions taken can ignore local specificity.

On the other hand, spatially-based watershed models may provide regional planners with an effective tool for analysing regional water budgets (Leon et al. 2004). Regional water authorities, such as Ontario's Conservation Authorities (CAs) have used models to identify target areas or potential goals for land use management. A challenge to implementing watershed scale models is the potential amount of data required or available to be collected. At this scale it becomes intractable to physically sample all components of the watershed. A compromise must be made by aggregating data and using remotely sensed data.

In addition to data requirements, the expertise to select, implement and analyse models is needed. Not all CAs have, in the past, had the resources to develop modeling experience, thus the use of spatial models is inconsistent across the province. Now, there is a regulatory requirement that the water budget for each watershed used as a source of drinking water is quantified and understood. The implementation of spatial, watershed scale models is expected to occur.

In Ontario, the recently legislated Clean Water Act (S.O. 2006 c.22) requires regional authorities to develop source water protection plans (SPPs). These plans are to include a watershed description, analysis of surface and groundwater availability, an understanding of

water demand, and an assessment of the risks to the water supply and water quality. The means by which quantity and quality risks are determined for SPPs is not prescribed, but the use of watershed assessment models is identified as potentially necessary to quantify the risk of identified threats.

In this thesis, the hydrology of the Raisin River watershed is modeled using the Soil and Water Assessment Tool (SWAT) (Neitsch et al. 2002). This process should lead to specific outcomes detailed herein:

1. The model is calibrated and validated, and the sensitivity of the results to the model parameters investigated.
2. A methodology of processing and analysing the data is given such that a similar study could be done for another region.
3. The limitations of the model in predicting certain aspects of the water cycle is shown. The difficulties associated with using single-valued metrics to quantify model performance are also investigated.
4. The hydrologic results presented can be combined with other SPP discoveries as part of a comprehensive risk assessment of the region's water supply.

The modeling exercise has been undertaken with standardised public data which can be considered a baseline of information available for many regions in Canada. By presenting a methodology which can be reproduced in other watersheds, comparable results could be obtained for other areas. These results include quantifying the runoff, evapotranspiration and aquifer recharge, both spatially and temporally. Each of these are important elements of SPP, illustrating that this model and methodology are useful for SPP development. The implementation provides the possibility of further investigation into changes of climate or land use on the supply, demand and safety of the water supply.

Region of study

The area under study is the Raisin River watershed in eastern Ontario, within the United Counties of Stormont, Dundas and Glengarry (Figure 1). This basin of 556km^2 is predominantly forest (44%) and pasture land (32%) with some areas under agricultural production(11%) (CH2MHill 2001). Much of the region is zoned as rural (SDG 2005). Most

of the urban and industrial development in the region is located south of the watershed, in the city of Cornwall.

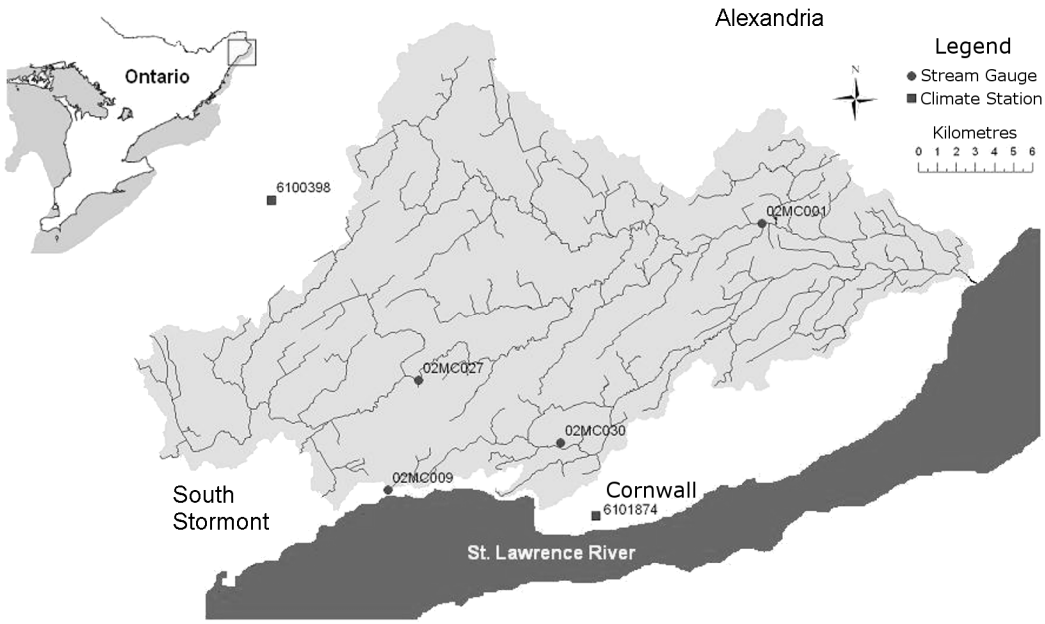

Figure 1 – Location and outline of the Raisin River watershed

The climate in the region is typical of south eastern Ontario, with mean monthly temperatures ranging from -10ºC to 22ºC. The watershed receives roughly 1020mm of precipitation a year, of which approximately 235mm falls as snow.

Most of watershed is part of the physiographic region identified as the Glengarry Till Plain (Chapman and Putnam 1984). The landscape is characterised by its rolling hills and winding streams; drumlins, small hills which are remnants of glacier movement during the last ice age, are common. Singer et al. (2003) captured the geologic details of the till, noting that depth to bedrock is generally less than 10m but is up to 35m near the St. Lawrence. Due to its stony, porous nature, there is great soil water capacity and good groundwater flow. This geology informs us that baseflow is likely to be a significant contribution to the regional water budget. Nearly all of the region's potable water supply is from groundwater[1]. Most wells in the area (more than 87%) are drilled into bedrock thus the quantity and location of recharge to deep (sub-bedrock) aquifers is of interest to the local population.

A small area at the outlet of the basin has a different surficial geology, with up to 14m of deposits confining the aquifer underneath (Singer et al. 2003). Modeling this different

[1] John Meek, Raisin River Conservation Authority, personal communication, Oct. 5, 2005

physiographic region is accomplished through the specification of different groundwater parameters. However, because this area is downstream of all flow measurement stations, the impact of its differing physiography is not considered part of the model calibration and validation process.

2. Literature Review

Context

Institutional management of natural resources has often been in reaction to an existing or looming environmental catastrophe. For example, increased agricultural mechanisation coupled with drought in the U.S. mid-west during the 1930s was a key driver for the creation of the Soil Conservation Service. In Ontario, development and deforestation during the same period resulted in increased soil erosion and flooding. Conservationists pushed for government action, which led to the passing of the Conservation Authorities Act in 1946 (R.S.O. 1990, c.C.27).

The objective of the conservation authorities (CAs) is "to further the conservation, restoration, development and management of natural resources" within their watershed (R.S.O. 1990, c.C.27). The boundaries of the CAs were determined using environmental (watershed), rather that political boundaries, which is well suited to this goal. The inclusion of local representatives in decision making processes is also a part of the authority's mandate, which is a necessary component of integrated water resources management at this scale (Burton 2003).

Other provincial legislation has dealt with standards for drinking water (S.O. 2002, c.32) as well as the use and discharge of water and water infrastructure design (R.S.O. 1990, c.O.40). After a tragedy involving the contamination of a municipal water supply, the Ontario government commissioned an inquiry to examine how water could be better managed within the province (O'Connor 2002). One outcome of this inquiry was additional government legislation concerning water management and risk assessment in the province. The Clean Water Act (S.O. 2006, c.22) received Royal Ascent in 2006. This Act entrusts the CAs with a new responsibility for the protection of drinking water sources within their watersheds.

A key characteristic of the new law is the introduction of source water protection planning. All sources of drinking water are to be assessed for risks to availability as well as their potential exposure to pollution. Each conservation authority (or other source protection organisation, such as groups of authorities or municipalities) is required to

develop and maintain a plan for source water protection. A number of requirements are laid out for the development of source protection plans, including:

- quantifying the existing quantity and quality of water within the watershed
- identifying groundwater recharge areas
- determining regions around surface intakes and wells that should be protected
- describing actual and potential threats to the water supply

To aid in plan development, the Ministry has released draft technical documentation with the intent that each watershed authority or municipality will assess their water supply in a common way (MOE 2006). The use of watershed models is proposed as a means to predict the quality and quantity of water in each area. Models can provide planners and responsible authorities with indications of the present and future risks their water supplies face. Further, estimates to the impact of changes to the landscape, through development or natural causes can be predicted. Knowledge of the water cycle can be estimated temporally and spatially given an appropriately chosen model.

In this thesis, the implementation of a watershed scale hydrologic model is undertaken. This process begins by assessing different hydrologic models for suitability and exploring the variety of approaches to model implementation. A survey of similar modeling experiences is presented. Data requirements and the relationship of model structure to predictive capability are also examined.

Models

Models are an abstraction or simplification of complicated systems. They are tools which allow some understanding of the behaviour and interaction between system components. The suitability of a model for a particular application depends on the end user, the available data, time and resources available for the study and most importantly, the questions which are being answered.

Grayson and Blöschl (2000) classify models in three ways:

1. by their algorithmic approach
2. whether they are deterministic or stochastic

3. as being spatially lumped or distributed

A model's algorithmic approach reflects how it is constructed. For example, physically based models use theory based processes or equations to describe different components, while empirically based models use past observations to characterise the behaviour. Deterministic models require all data and parameters to be specified or calculated, while stochastic models allow values to vary as part of the simulation.

Distributed models use inputs and parameters which are spatially explicit, allowing the model to more accurately represent heterogeneous areas. Lumped models approximate spatial differences by "lumping" together areas or parameters. This enables the model to be implemented with fewer data requirements but possibly with a loss of spatial detail. The degree to which a spatial model should be lumped or distributed depends on the scale at which the model is to be used and the availability of input data.

Models with a large number of parameters may be able to better represent the complex nature of the water cycle (Refsgaard and Storm 1996), however the use of many parameters may lead to difficulty in calibration and validation. Acquiring sufficient data in order to tune and validate these parameters may be a challenge. Importantly, a model with highly detailed components will not show improved accuracy if input data or other dependant components are not detailed. Conversely, a model with few parameters may be overly general and may not be able to satisfactorily represent the wide range of conditions expected to be modeled. Since each watershed has its own unique characteristics, some components of the water cycle may be more important than others; this may ultimately affect the choice of model.

We can further classify hydrologic models as to whether they are continuous (long term) or event based (short term) (Singh 1988). Like spatial scale, identifying the time scale for which the simulations will be used is important to know before implementing a model. Hydrologic processes occur at different time scales. For example, storm-generated floods occur over periods of hours or days, while aquifer recharge may occur over weeks or years. Knowledge of the end requirements will ensure that a model appropriate for the necessary time scale is chosen. In order to understand the long term behaviour of a water system continuous time models must be used. Event based models, which examine the result of single, transient occurrences are used for predicting such entities as expected peak flows but do not provide a long term view which is necessary for planning. It is necessary to use

continuous models for water budget planning or the assessment of source protection measures.

Hydrologic models

Several continuous, integrated watershed assessment models have been developed. Descriptions of a number of models are given by their authors in Singh (1995). Singh and Woolhieser (2002) reviewed a number of watershed models with an emphasis on their history and evolution. Borah and Bera (2003) reviewed different watershed assessment models and compiled their particular mathematical basis. An overview of commonly cited and recommended continuous-time models is given below.

SWAT

SWAT was developed for the USDA Agricultural Research Service (ARS). It is an extension of previously existing ARS models, the Simulator for Water Resources in Rural Basins (SWRRB) (Arnold and Williams 1995) and ROTO (Routing Outputs To the Outlet) (Arnold et al. 1995). Key components of the SWRRB model were derived from other ARS models, such as CREAMS (Chemicals, Runoff and Erosion from Agricultural Management Systems) (Knisel 1982) for surface hydrology, EPIC (Erosion Productivity Impact Calculator) (Williams et al. 1984) for erosion and sediment and GLEAMS (Groundwater Loading Effects of Agricultural Management Systems) (Leonard et al. 1987) for groundwater modeling.

SWAT is a continuous time model which simulates runoff, erosion and nutrient transport through a watershed. The watershed to be modeled is divided into subbasins. Each subbasin is further divided into hydrologic response units (HRUs) which contain a unique combination of land use and soil type. Each HRU has different properties which affect runoff and infiltration, both in quantity and quality. In each simulated time interval (one day), changes in the water balance are calculated at the HRU level, then aggregated to the subbasin level. Runoff and baseflow from each subbasin are directed to the main channel, then routed to the watershed outlet. A complete description of the SWAT model is given by Neitsch et al. (2002).

The SWAT model predicts surface runoff and infiltration using either the SCS curve number method (SCS 1972) or the Green-Ampt Mein-Larson infiltration method (Mein and Larson 1973). Potential evapotranspiration (PET) is modeled using either the Hargreaves (Hargreaves 1985), Penman-Montieth (Montieth 1965) or Priestley-Taylor (Priestley and Taylor 1972) method. Percolation through the soil profile is based on one-dimensional saturated flow rates through the user-defined soil profile. Channel routing is based on a variable storage method (Williams 1969) or the Muskingum method. Snowmelt – a process important for the area under study – is calculated using a degree-day method.

The key design features of SWAT are that it is physically based and, for basic simulations, requires minimal input data. Since it was designed as a continuous time model, its authors state it is not capable of effective single-event simulation.

HSP-F

Hydrological Simulation Program – Fortran (HSP-F) (Bicknell et al. 1997) is an evolution of the Stanford Watershed Model (Crawford and Linsley, 1966). It models a continuous time simulation of watershed hydrology as well as erosion, sediment and chemical transport. The time step of HSP-F is variable, depending on the resolution of the input data available. The size of watersheds modeled with HSP-F range from fields of a few hectares to large basins of thousands of square kilometres.

Most of the hydrological processes in HSP-F are modeled conceptually rather than physically. Infiltration and surface runoff are determined based on Philip's equation (Philip 1957). The model considers the soil profile to have an upper and lower storage zone, below which water percolates to groundwater aquifers. Channel routing is based on storage or kinematic wave techniques. HSP-F does not model PET, which must be provided by the user. Snowmelt is calculated using an energy balance formula, though the most recent version of HSP-F has added a degree-day formula to reduce the amount of input climate data required.

MIKE SHE

MIKE-SHE (Refsgaard and Storm 1995) is another continuous time, physically based comprehensive model. This model is an integration of the Système Hydrologique Européen

(SHE) model (Abbott et al. 1986) which conceptualises the land phases of the hydrologic cycle and MIKE 11 (Havnø et al. 1995), a river flow model. A key feature which distinguishes it is the ability to model different sections of a watershed at different spatial and temporal scales, allowing the user to take advantage of different available inputs or more rigorously simulate regions of particular interest. As a fully distributed model it requires large amounts of input data, though users may lump together sections and focus only on components of interest. MIKE-SHE is capable of both event and continuous simulation.

The model is based on physical equations. Diffusive wave equations are used to model one-dimensional channel flow and two-dimensional overland flow. Water movement through the soil profile is based on Richard's equation in one dimension for unsaturated flow and in three-dimensions for saturated flow. The model is grid based, and these differential equations must be solved numerically for each grid cell in the simulation.

AnnAGNPS

The Annual Agricultural Non-point Source Pollution model (AnnAGNPS) (Binger et al. 2001) is a continuous time version of the event based AGNPS model (Young et al. 1989). This model, like SWAT, derives many key equations from the ARS CREAMS model.

The AnnAGNPS model divides a watershed into homogeneous "cells", with each cell discharging surface water and loadings to the stream network. Surface runoff is calculated using the SCS curve number approach. Erosion is estimated using a revision of the Universal Soil Loss Equation (USLE) (Renard et al. 1997). The model is intended for understanding surface water processes, particularly how pollutant loads such as sediment and chemicals are transported by surface and channel processes through a watershed. It does not have the capacity to model groundwater recharge or baseflow.

Model comparison and selection

El-Nasr et al. (2005) compared MIKE-SHE to SWAT over a 465km^2 Belgian agricultural watershed. The lumped groundwater component of SWAT was not considered comparable to the fully distributed MIKE-SHE model, thus only surface flow components were compared. Both models were found to predict streamflow well, but MIKE-SHE modeled

the variation in streamflow better. However, the heavy data requirement of MIKE-SHE was cited as a hurdle to implementing the model.

Van Liew et al. (2003) compared SWAT to HSP-F in several adjacent watersheds located in Oklahoma. Results showed that SWAT performed better across the simulated set of climatic situations. The HSP-F model exhibited better calibration results, attributed to its different runoff model, though calibration of runoff required detailed site specific information. However, SWAT showed better validation results, suggesting that the model is more robust to different climatic situations. The authors also noted that the calibration and input data procedures are much easier in SWAT.

The same conclusions about SWAT and HSP-F were made by Saleh and Du (2004) when comparing the models for a watershed in central Texas. It was also noted that the ability of SWAT to consider different agricultural land management practices resulted in better predictions of nutrient loadings than HSP-F.

A comparison between HSP-F and SWAT was performed by Singh et al. (2005), which determined that SWAT generally predicted periods of low flow better than HSP-F. Further, the smaller number of calibration parameters and the inclusion of PET calculations in the model made SWAT particularly useful. Again, HSP-F results were not as consistent as SWAT between the calibration and validation periods, suggesting that the large number of parameters prevented effective calibration. However, the hourly time step of HSP-F resulted in less variation of daily simulated flow error.

The MIKE-SHE model has very high input data requirements, which limits its ability to be applied in areas with little existing data and few resources with which to gather data. It is also a commercial product which is an additional hurdle to implementation. The HSP-F model has reasonable data requirements and can simulate using small time steps, but appears to be less robust than the SWAT model. For these reasons, the SWAT model was chosen for implementation.

Previous SWAT implementations

Borah and Bera (2004) reviewed about 20 implementations of SWAT. By comparing the results obtained, they noted that the model lacks accuracy in predicting daily extreme events or extreme months. We have no expectation that SWAT should perform well in daily event

simulations, given its daily time step and the authors' own caveats that the model is not intended for short term analysis (Nietsch et al. 2002). However, extreme events tend to be of great interest to those who manage watersheds. Chu and Shirmohammadi (2004) confirmed that SWAT's daily hydrologic predictions often fail to meet extreme values.

Land use planning and practices

In assessing management plans or policy changes, the long term impact is often used as a measure of success. A number of studies have used SWAT to determine the impacts of changes to land management or policy.

Agriculture has been identified as the largest contributor to freshwater pollution in the United States (US-EPA 2002). Thus the effects of agricultural practices on sediment and nutrient transport are of particular interest to resource managers. This is one of the key capabilities of SWAT which has been examined by many researchers. Bärlund et al. (2007) implemented SWAT to assess agricultural best management practices (BMPs). The model was shown to predict flow and sediment reasonably well but accurate predictions of nutrient movement required detailed input data. Jayakrishnan et al. (2005) discussed applications of the SWAT model over very large areas, including the impacts of national-scale agricultural management policies and SWATs applicability to TMDL (total maximum daily load) studies. Santhi et al. (2006) also used SWAT to evaluate the potential of BMPs to reduce sediment and nutrient loading of waterways. Kang et al. (2006) applied SWAT to an agricultural region in Korea to determine appropriate TMDL levels. Grizzetti et al. (2003) evaluated SWAT for the prediction of nutrient (nitrogen and phosphorus) retention and loading on a 1680km^2 watershed in Finland. They found that the model's ability to generate predictions spatially and temporally was an improvement over previously used statistical methods.

Impacts of larger policy or economic initiatives have also been assessed using the SWAT model. Attwood et al. (2000) linked SWAT with an economic model to predict the effect of national agricultural initiatives. Nelson et al. (2006) used SWAT to determine the change in water quality and crop viability as land was put into switchgrass production. This permitted the effects of different agricultural practices to be examined and allowed the economics of switchgrass production to be estimated. Bekele and Nicklow (2005) used SWAT to

determine the linkages between agricultural profits and ecological services such as nutrient and sediment loading.

When managing the resources of a large geographic area, it can be useful to identify the regions of particular importance or concern. Rosenthal and Hoffman (1999) implemented SWAT for a large watershed in Texas which was lacking in water quality monitoring sites. Ecologically significant points in the river system were identified and thus particular sites could be targeted for the installation of water quality equipment.

Climate change analysis

The Ontario Ministry of Environment has indicated that, initially, source protection planning does not need to consider the impacts of climate change (MOE 2006). However, this will likely change once initial studies have been completed. It is therefore useful to know if SWAT has the capability to simulate the effects of climate change.

The relationships between CO_2 and plant growth have been integrated into SWAT (Williams et al. 1996). These changes in plant growth cause changes to land cover, which has long term impacts on soil erosion. Eckhardt and Ulrich (2003) used SWAT to perform climate change analysis, to observe the impact of temperature change and CO_2 level on annual hydrology. This amounted to a reduction in spring peak flow and lowering of summer flow.

Effects of input data on model performance

The SWAT model is sensitive to spatial resolution of the input data, and numerous studies have attempted to quantify the impact of spatial resolution on model results. For example, Chaplot (2005) examined SWAT's sensitivity to digital elevation model (DEM) and soil map resolution. It was noted that higher resolutions provide better model results and that DEM resolution should be at least 50m for accurate simulation. This corresponds to results seen by Romanowicz et al. (2005), who examined the impact of soil and land use resolution on an uncalibrated SWAT implementation. They also noted improved model results with higher resolution data. Chaubey et al. (2005) also looked at DEM resolution impact on SWAT. They found that a minimum resolution of 100m was necessary for simulation and that predicted runoff decreased when DEM resolution decreased.

Since SWAT has different sensitivities to different inputs, the resolution of some inputs is more important than others. Di Luzio et al (2005) examined the impact of input quality on model output. An accurate DEM was considered most important, followed by land use (for runoff and sediment) and soil type. The problems of using a DEM with insufficient resolution are described by Tarboton et al. (1991). In particular, poor resolution can hide existing flowpaths and create localised land depressions that are not real. Sensitivity of SWAT to land use inputs was also discussed by Eckhardt et al. (2003).

Chaplot et al. (2005) looked at the effect of rain gauge density on SWAT. It was expected that using more rain gauges would improve model accuracy as others have shown that SWAT is highly sensitive to climate and precipitation data (Hernandez et al. 2000, Muttiah and Wurbs 2002, Reungsang et al. 2005). However, since the results were assessed on a monthly basis, the variation between gauges was masked. In other words, additional precipitation data provided better input to the model on a daily basis, but over the period of a month the variation from station to station was minimal. Thus it is important when considering the resolution of input data to take into account the differences in both space and time.

Subbasin size

The SWAT model divides the watershed under study into a series of subbasins. The size of subbasins chosen has an effect on the model's predictions of erosion and consequently on nutrient transport and loading. This is due to the use of the Modified Universal Soil Loss Equation (MUSLE) (Williams 1984), which exhibits non-linear behaviour with changes in area:

$$sed = 11.8 \cdot (Q_{surf} \cdot q_{peak} \cdot area_{hru})^{0.56} \cdot K_{USLE} \cdot C_{USLE} \cdot P_{USLE} \cdot LS_{USLE} \cdot CFRG \qquad 1$$

where sed is the sediment produced in a given day (tonnes), Q_{surf} is the runoff volume (mm/ha), q_{peak} is the peak rate of runoff (m^3/s), $area_{hru}$ is the HRU area (ha). K, C, P and LS are the erodibility, cover, practice and topographical factors from the USLE equation and $CFRG$ is the coarse fragment factor.

SWAT calculates the peak runoff rate using the Rational formula:

$$q_{peak} = \frac{C \cdot i \cdot A}{3.6} \qquad 2$$

where C is the runoff coefficient, i is the rainfall intensity (mm/hour), A is the area (km^2) and q_{peak} is measured in m^3/s. Substituting this into the MUSLE, we find that:

$$sed \propto A^{1.12} \qquad 3$$

Increases to the area of an HRU will result in a greater than linear increase in the amount of sediment predicted. This contradicts a number of studies cited by Parsons et al. (2006). Kinnell (2004a, 2004b) points out a number of other problems inherent in the mathematics of MUSLE. Specifically, the MUSLE assumes a constant sediment delivery ratio. Changes to the amount of predicted erosion have a linear impact on the amount of sediment predicted, yet Kinnell argues these are independent processes which cannot be captured in the same equation. The equation is based on empirical data and may be reasonable for conditions similar to those used in its development. However, the ability to translate the results to situations outside of this are questioned.

FitzHugh and Mackay (2000) examined the effect of varying subbasin size in SWAT. Changes in HRU area greatly affected sediment predictions. As expected, the curve number based runoff predictions were not affected by different delineation of sizes. These findings were also reached by Chen and Mackay (2004) and Binger et al. (1997). As shown, the MUSLE assumes that delivered sediment increases non-linearly with area. However, this assumption is broken by the way that SWAT linearly aggregates runoff and sediment predicted at the HRU level into the subbasin level. Thus, errors in sediment prediction which might be attributed to incorrect input data may actually be products of this (somewhat inconsistent) model structure.

SWAT Processes

Snowmelt

The snowmelt process in SWAT is based on a degree day method.

$$melt = b \cdot cov \cdot \left(\frac{T_{snow} + T_{\max}}{2} - T_{melt} \right) \qquad 4$$

where T_{snow} is the temperature of the snowpack (ºC), T_{max} is the maximum air temperature on a given day (ºC), T_{melt} is the temperature at which snow begins to melt (ºC), *cov* is the percent of the land area covered by snow and *b* is the melt factor (mm/day ºC) and *melt* is expressed in mm per day.

The average of the snowpack temperature and the daily maximum air temperature is compared to the base melting temperature to determine the amount of melt in a given day. Snowpack temperature is modeled based on the mean daily air temperature and a user-defined parameter which lags the daily temperature with that of the snowpack:

$$T_{snow(d)} = T_{snow(d-1)} \cdot (1 - \ell) + T_{avg} \cdot \ell \qquad 5$$

where T_{avg} is the mean daily air temperature, $T_{snow(d)}$ is the temperature of the snowpack on a given day and ℓ is the user-specified lag factor (TIMP) which ranges from 0 to 1. Limitations of the degree-day method are discussed by Dunne and Leopold (1978). A more thorough, physically based representation of snowmelt considers the energy balance of the snow, including solar radiation, energy loss to the atmosphere, etc. The energy balance method, implemented in HSP-F, is more accurate but requires significant amounts of climate data to solve.

Fontaine et al. (2002) introduced improvements to the SWAT model to consider some additional aspects snowmelt. The use of elevation to determine the temperature at which precipitation becomes snow was added for the benefit of mountainous regions. It was also suggested that lag factor, ℓ, should vary inversely with snow depth rather than remain fixed.

Benaman et al. (2005) report the results of implementing SWAT for a New York state watershed where snowmelt is a significant component of the annual hydrologic cycle. With large amounts of data available for calibration and validation, it was determined that the model was not particularly well suited to modeling snowmelt. Monthly flow estimates in the snowmelt months were generally under predicted. Underestimation of flow impacts the prediction of sediment. As shown earlier, the quantity of runoff is a factor in the MUSLE equation. Benaman and Shoemaker (2005) examined sediment prediction for high flow

events, typical of snowmelt runoff and attributed the under predictions to the poor modeling of snowmelt and snowmelt induced erosion.

Wang and Melesse (2005) examine the sensitivity and performance of SWATs snowmelt structure on a basin in Minnesota. They suggested that the model does not predict as well when the annual snowfall is less than normal.

Baseflow and recharge effects

While soil processes are mostly physical representations in SWAT, its implementation of aquifer storage and discharge is a simple conceptual framework. Recharge is based on infiltration from the overlying soil layers. Baseflow discharge is a linear function of the aquifer water level. Model parameters exist to allow water to move back into the soil profile under dry soil conditions ("revap"), and the user may also specify what fraction of recharge is lost from the system to deep aquifer storage.

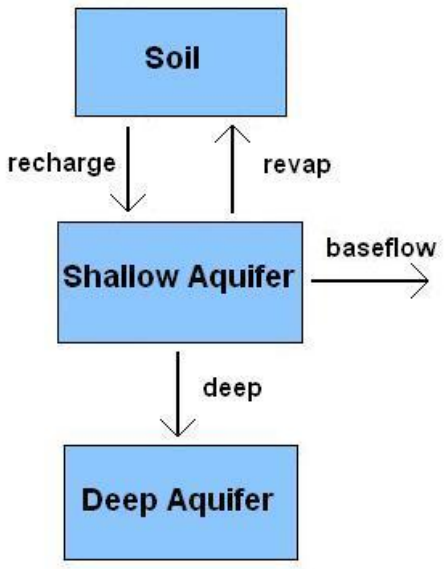

$$recharge(t) = (1 - e^{-1/\delta}) \cdot percolation(t) + (e^{-1/\delta}) \cdot recharge(t-1) \quad (6)$$

$$baseflow(t) = recharge(t) \cdot (1 - e^{-\partial}) + baseflow(t-1) \cdot (e^{-\partial}) \quad (7)$$

$$revap(t) = K_{REVAP} \cdot PET(t) \quad (8)$$

$$deep(t) = K_{DEEP} \cdot recharge(t) \quad (9)$$

Figure 2 – Conceptual schematic illustrating the groundwater process in SWAT. Water movement in and out of aquifers is simulated using equations 6 through 9.

Arnold et al. (2000) used SWAT predict baseflow and aquifer recharge in a large area (roughly 500000 km^2) of the upper Mississippi basin. This was tested against an interpreted

hydrograph (to determine the fraction of baseflow) and a calculated water balance (to determine the amount of recharge). It was shown that SWAT could predict the baseflow and recharge reasonably well on a monthly basis. This is contradicted by Romanowicz et al. (2005) which concluded that SWAT was poor at modeling baseflow and recharge in a Belgian agricultural region. Also, Sun and Cornish (2005) attempted to use SWAT to estimate recharge amounts in an arid part of Australia. Preferential flow due to cracking was identified as a model limitation which prevented accurate recharge estimation.

Chu and Shirmohammadi (2004) identified another limitation of SWAT in that baseflow from outside the watershed is not considered. This can lead to errors in the simulation in physiographic regions where this is a contributing factor. This result was also obtained by Spruill et al. (2000) when evaluating SWAT on a karst watershed.

In order to compensate for SWAT's limited groundwater conceptualisation, Sophocleous et al. (1999) and Sophocleous and Perkins (2000) proposed a methodology to integrate SWAT with MODFLOW, a fully distributed groundwater model. However, the potential increase in model accuracy comes at a trade off of requiring more input data, which may not necessarily be available.

Calibration and Validation of hydrologic models

Calibration is the estimation of model parameters that cannot be directly determined. This can be a manual or automated process, or some combination of the two. Validation is the process where the model performance is assessed to see if it can perform acceptably well using different data than it was calibrated with. A systematic framework for model calibration and validation is given by Refsgaard and Storm (1996). A methodology for calibrating the SWAT model is described by Santhi et al. (2001).

Hill (1998) described a number of mathematical techniques for calibrating and evaluating hydrologic models. The ASCE (1993) has recommended a series of common measurements for evaluating hydrologic models, allowing published implementations to be more easily compared with one another. For continuous time models, they recommend the use of deviation of volume (DV), the Nash Sutcliffe coefficient (Nash and Sutcliffe, 1970) (NS) and the deviation of gain from the daily mean (DG):

$$DV(\%) = \frac{\overline{O} - \overline{P}}{\overline{O}} \times 100 \qquad \textbf{10}$$

$$NS = 1 - \frac{\sum_i (P_i - O_i)^2}{\sum_i (O_i - \overline{O})^2} \qquad \textbf{11}$$

$$DG = 1 - \frac{\sum_i (P_i - O_i)^2}{\sum_i (O_i - \overline{O_i})^2} \qquad \textbf{12}$$

In each equation, $\overline{P}$ and $\overline{O}$ represent the mean predicted and observed values over the period of simulation, P_i and O_i represent the predicted and observed values at a given timestep, and $\overline{O_i}$ represents the mean observed value for a given period of the year over all years of the simulation. Coffey et al. (2004) describes the application of these qualitative measurements to hydrologic models, particularly SWAT. Notably, monthly values tend to be used rather than daily values because they are more often normally distributed and have less autocorrelation.

When calibrating a model, we can choose only one objective function to maximise (von Neumann and Morgenstern 1953), yet the use of a single metric for evaluating hydrologic models can be misconstrued (Legates and McCabe 1999). Any metric may have a particular bias to some values, thus the incorporation of other, independent factors to generate a new metric can be useful (Wang and Melesse 2005). However, deviation from standardised measures makes comparison with other studies difficult. Nevertheless, distributed and physically based models have numerous variables and independent components, thus must be validated using an array of independent data and criteria (Refsgaard and Storm 1996).

Arnold and Allen (1996) also identify the shortcomings of validating a comprehensive watershed model using just stream flow. Instead, using a combination of PET, water yield, runoff, baseflow and soil moisture was proposed. Similar techniques were described by Grayson et al. (1992) and Cao et al. (2006). Incorporation of a variety of aspects of the watershed as a means of validating across independent parameters should ultimately improve model accuracy.

Spatially based models have the ability to describe localised effects occurring throughout a watershed. Aspinall and Pearson (2000) discuss the need for understanding model variables

in their spatial context, that is, considering the landscape and geographic variability which surrounds a spatial parameter. Jetten et al. (2003) examine erosion models, including SWAT, to determine their capability in predicting erosion spatially. This is considered key since the use of single outlet measurements for calibration and validation tend to obscure local effects.

Ecological flow regimes

Single-valued metrics are convenient ways to quantify model performance, yet the main benefit of comprehensive watershed models is that they can predict many different variables. There is evidence that the use of multiple types of stream flow measures are required to describe a flow regime in a way that is useful for resource management, such as suitability for aquatic habitat or susceptibility to pollution. For example, source protection planning places weight on periods of low flow, as this is when the quantity of available water is less and there is greater risk of unavailability (Ontario Ministry of the Environment 2006). Conversely, periods of high flow, particularly during snow melt periods, are when most erosion and pollution occurs (Dunne and Leopold 1978). Stream habitats can be affected by the durations and intensity of flow surges and recessions (Bradford and Maude). For these reasons, alternate measures of stream flow have been proposed (Richter et al. 1997). Such multi-variate flow measures, or ecological flow regimes, give us an understanding of the quantity and variance of flow. Multiple metrics cannot be directly used for model calibration, but can be used to assess the existing characteristics of a flow regime and to determine the ability of a model to mimic that regime.

Automated calibration techniques

A key concern with highly parameterised models is that manual calibration can be difficult and time consuming to perform. The use of automated techniques to find an optimal parameter set allows a model to be implemented faster and with potentially less expert knowledge required. However, they also require that the model implementer understands what the suitable parameter ranges are and whether the final result is reasonable or not.

For a 133km^2 watershed in Illinois, Muleta and Nicklow (2005) performed an automated calibration of SWAT using a genetic algorithm to optimise 35 parameters. A key part of the process was to identify the possible variability in each input parameter. This variability was

used as a means to restrict the ranges used for calibration as well as to determine the uncertainty in the final calibration point. Al-Abed and Whiteley (2002) described a similar approach to automated calibration of HSP-F over the Grand River watershed in Ontario. By determining which parameters the model was most sensitive to, calibration effort could be directed towards those parameters, potentially reducing final uncertainty of the model.

Eckhardt and Arnold (2001) and Eckhardt et al. (2005) showed that SWAT could be calibrated using a shuffled complex evolution algorithm. This allowed for a large number of parameters to be used in calibration and thousands of parameter sets to be tested. Yet ultimately, the model performance was similar to other SWAT implementations and exhibited a tendency to underestimate extreme runoff peaks. Artificial neural networks (ANNs) are another automated technique which has been used to calibrate SWAT (Srinivastava et al. 2006, Heuvelmans et al. 2006).

Some automated calibration routines have been integrated into the most recent version of SWAT. These were reviewed by Van Liew et al. (2005). It was concluded that the routines perform less well than manual calibration, but with properly selected parameter bounds the results are satisfactory.

Land cover and remotely sensed data

In order to survey the land over a watershed scale, remote sensing techniques can provide fast, inexpensive access to necessary data. There are many examples of remotely sensed data being used for hydrological studies (Pietroniro and Leconte 2000, 2005). One of the significant inputs to the SWAT model is land use which can be easily acquired by remote means. While soil types within a basin tend to be constant over the time scale of simulations, land use can change quickly and dramatically. Examples include deforestation to enable agriculture, or the development of urbanised areas on agricultural land. However, remotely sensed images cannot be used directly by the model. They must first be classified into the land covers or land uses of interest to the modeler.

Techniques to classify image data can be supervised or unsupervised, (Richards and Jia 1999). Supervised classification relies on the user to identify known areas of each desired land cover (training sets). The rest of the image is then classified to one of the predetermined land cover classes based on the similarities of the spectral signature. In an

unsupervised classification scheme, the image is organised into spectrally similar classes. The user must then determine which land cover each class represents.

Unsupervised classification is useful when it is difficult to define training sets for the images under investigation. The effectiveness of five popular unsupervised classifications schemes were described by Duda and Canty (2002). Cihlar et al. (2001) has proposed another unsupervised algorithm for multispectral data

Supervised classification schemes are commonly used in hydrological studies when there is some knowledge of the region's land cover. The maximum likelihood classifier was used by Su (2000) on Landsat data to determine land cover changes for input to basin scale studies. Jobin et al. (2003) and Cherrill et al. (1994) also used the maximum likelihood scheme on Landsat data. Haapanen et al. (2004) used a minimum distance algorithm to discriminate between forest types in Finland and the Great Lakes region.

Both supervised and unsupervised schemes can be effective, but appropriate combinations of the two can yield more accurate results (Richards and Jia, 1999). Cihlar et al. (2003) proposed a combined supervised-unsupervised methodology to automate the generation of a Canada-wide land cover map. A similar process was used by Latifovic et al. (2004) as part of the Global Land Cover 2000 project and the development of land cover maps for North and Central America. Kerr and Cihlar (2003) used the combined process to derive land use and agricultural intensity for areas in Canada. A combined methodology to generate input to the AGNPS model is described by Marzen et al. (2000)

Steele et al. (1998) point out that the spatial variation in an image is not consistent, and depends on a number of factors such as terrain and land use. Chica-Olmo and Abarca-Hernandez (2000) exploit this notion and note that the signatures of individual Landsat pixels are not independent of the signatures of their neighbours. By using spatial autocorrelation they were able to improve image classification from their Landsat images. Aspinall and Pearson (2000) identify the need to link landscape features in their spatial context in order to properly implement watershed models.

Prenzel and Treitz (2005) compare "structure" (land cover) based and "function" (land use) based classification schemes. When we wish to examine the anthropogenic impacts on a watershed, it is the land use (function) that we should consider. However, remotely sensed

images provide inherently structural (land cover) information. It is suggested that both structural and functional can work equally well since some functional groups (for example, grassland) are both functional and structural in nature. However, in order to make an effective classification scheme, the separation between a class' functional and structural definition must be understood. In some cases, further linkages between socio-economic factors and land management practices can be made (Jobin et al. 2003) which may also aid in connecting structural and functional definitions.

As noted earlier, the spatial resolution of input data is an important factor in model performance. Goetz et al. (2003) assessed various classification schemes for use with high resolution (4m) IKONOS imagery. Key limitations that were noted included shadowing and an increased level of spatial variability within areas of the same land cover type. The imagery could identify spaces between trees and the shadows cast by trees, whereas this level of detail is not seen when using Landsat (30m) imagery. Such details may be useful for highly localised studies but are a hindrance to determining large scale land cover classifications.

Physical properties of the land can be exploited when classifying multi-spectral images. For example, the tasselled-cap index (Crist and Kauth 1986) uses the changing reflectance of plants throughout their growing season to identify different crops and their stage of growth. Combined with some knowledge of local crop calendars, this technique can be used to determine land covers (Oetter et al. 2000), or distinguish between forest types (Dymond et al. 2002). Soil moisture is another physical property which can be directly related to spectral response. Cosh et al. (2004) outlined a procedure for relating point sampled soil moisture to satellite data. Differences in soil moisture can also be used to infer levels of soil drainage (Peng et al. 2003), which is a key input to hydrologic models.

3. Materials

Overview of data

Input required for modeling with SWAT can be divided into two major groups. First, spatial data describing the landscape under study. This includes topographical, land cover and soil information. The second group consists of temporal data describing the climate. Daily precipitation and temperature values are required, while other climate parameters were defined seasonally. To calibrate and validate the model, daily streamflow records were used.

A summary of the data sources used can be found in Table 11. An overview of the data and the preprocessing necessary for SWAT is described in this section.

Spatial data

Three data sources provided most of the spatial information for the watershed: Landsat imagery, a digital elevation model (DEM) and soil maps. As well, the National Topographic Database (NTDB) provided the location of waterbodies and wetlands.

For consistency, all spatial data was analysed using the Universal Transverse Mercator (UTM) coordinate system and the North American 1983 (NAD83) reference datum. This necessitated reprojecting the soil maps which had been digitised to the NAD27 reference. In the Raisin River area, the coordinate error resulting from reprojecting NAD27 to NAD83 is less than 1m (CCRS 2007). As the spatial analysis was performed at a 30m resolution, this difference was considered negligible.

Landsat images

Landsat imagery was used to derive land cover classes. Of the images available only two (Nov 1 1999 and May 29 1992) were generally cloud free, allowing full view of the watershed. The images from 2001 have partial cloud cover but could be used as aids to the labelling of classes. Each Landsat image is shown in Map 1 through Map 4.

Digital elevation model (DEM)

The digital elevation model (DEM) of the watershed from the NTDB 1:50000 map series was used. The source data was converted from geographic coordinates to UTM NAD83,

resulting in a square grid resolution of 19.764m. Vertical resolution of the DEM is 1m. The topography of the watershed is illustrated in Map 5.

Water and Wetlands

The watercourses and waterbodies layers of the NTDB were used to identify the stream network and delineate the watershed. The vector-based stream network consists of linear elements for reaches less than 25m wide (the watercourses layer) and polygon ("double line") elements for wider reaches (the waterbodies layer). The waterbodies layer also contributed to identifying ponds in the region. The wetlands layer was used in the process of classifying land cover. These maps were developed from analysis of air photos coupled with some field verification (Natural Resources Canada 2001).

Soil

Soil maps of the local townships were developed in the 1950s (Matthews and Richards 1954, Matthews et al. 1957) and have since been digitised into the Canadian Soil Information System (CanSIS). The soil descriptions in this database include general layer information such as approximate depths and soil texture.

Specific soil layer information collected by CanSIS is limited. The layer database does not contain all the soil classes found in the region, nor are there many samples from classes which were available. Thus, some of the detailed soil information required by the SWAT model was estimated using information found in the Canadian soil classification standards (Agriculture and Agri-food Canada 1998). Available water content was estimated based on typical values for the soil texture (Schwab et al. 1993). Values of saturated hydraulic conductivity recommended for design purposes by the Ontario government (Stone 2006) were used.

A complete listing of all soil parameters for all soil classes provided in Appendix D.

Temporal data

Climate

Daily minimum and maximum temperature and daily precipitation amounts were obtained from the Environment Canada weather stations at Cornwall and Avonmore (see Map 5).

These stations were chosen as they have continuous data over the period of study. Each subbasin was assigned the climate data from the nearest weather station. For the occurrences of missing data points from a climate station (Table 1), values from the other station were used: precipitation values were used directly, while temperature values were adjusted for the average 1.4ºC difference between the two stations.

Number of missing records (Total records = 9132)	Cornwall	Avonmore
Precipitation	0	34
Min. Temperature	8	107
Max. Temperature	13	115

Table 1 - Records missing from climate stations, 1980 - 2004

Typical rainfall intensities per month for southern Ontario were obtained from Dickenson (1977). These values are used by the model to calculate rainfall induced erosion. Typical monthly solar radiation values, required for potential evapotranspiration estimation, came from CanSIS.

Stream gauge data

There are three stream gauges in the watershed with daily flow records (Map 5). Only gauge 02MC001 has continuous daily records. It captures nearly 70% of the watershed area and was used for calibrating and validating the model. The other gauges, with only seasonal records, were used for validation.

Station	Williamstown	Black River	South Raisin
Station ID	02MC001	02MC027	02MC030
Location	45º 9' 19"N	45º 4' 50"N	45º 3' 5"N
	74º 38' 16"W	74º 52' 4"W	74º 46' 25"W
Contributing Area	363km^2	26km^2	129km^2
Data record	Continuous	Seasonal	Seasonal

Table 2 – Stream gauges within the Raisin River watershed

Data preprocessing

In order to prepare the data for use with SWAT, some preprocessing steps were taken. A description of those tasks is given here.

Stream network

It was first necessary to identify what part of the stream network fell within the basin. This was accomplished by manually all streams which were not connected to the main branch of the Raisin River.

Waterbodies were converted to linear elements by identifying the centreline between enclosing arcs. Occurrences of multiple vectors representing a single stream section between branch nodes were consolidated to a single vector by simplifying the stream arcs.

The stream vectors had to be corrected to point in the downstream direction. This was accomplished by first manually identifying the watershed outlet. Once the outlet was identified all the headwater reaches could be programmatically identified. The path from the headwater reaches to the outlet was traced and the direction of reaches corrected to point downstream. A problem with this methodology occurs when the stream forks and then converges at some point downstream. To resolve the proper flow direction in these situations, the DEM was used to identify the most elevated node; flow was considered to flow away from that node.

Width and Depth estimation

The SWAT ArcView interface (BRC 2002) contains empirically based equations for determining stream width and depth as a function of contributing area. These equations were used to estimate the unknown reach dimensions.

Reaches which were waterbodies in the NTDB had their average widths estimated using the area of the reach divided by the length. Width, in metres, for reaches less than 25m (the NTDB watercourses layer) was estimated as:

$$width = 1.29 \cdot CA^{0.6} \qquad \textbf{13}$$

where CA is the contributing area of the reach in square kilometres (BRC 2002). The width equation provided similar results to the polygon method (Figure 3) suggesting that the equation is reasonable for this watershed.

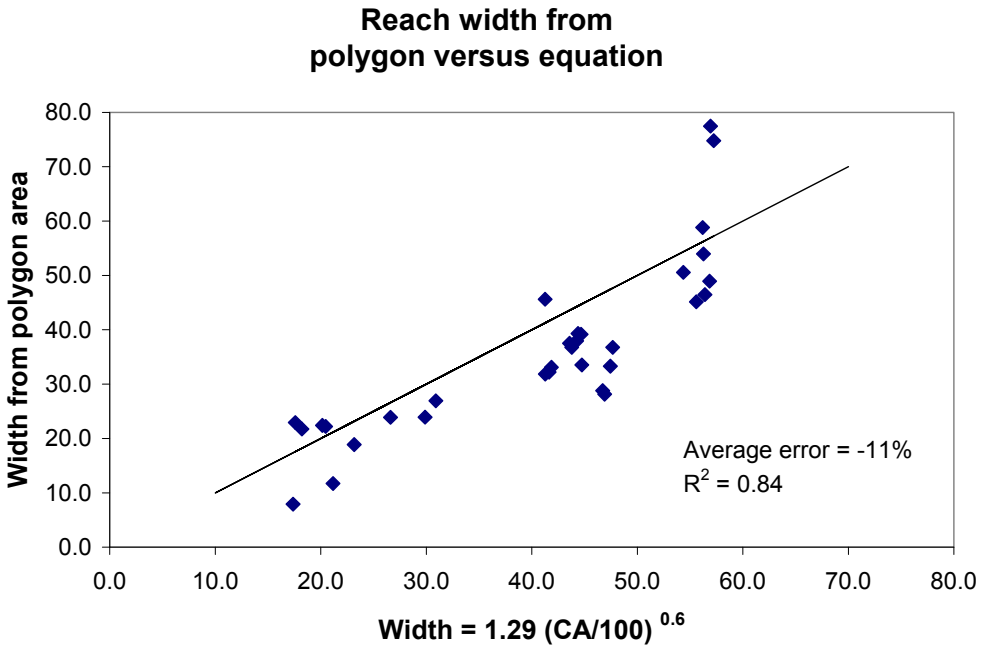

Figure 3 - Reach width (m) determined from empirical equation or polygon area. Solid line represents equivalence between the two methods.

Average depth (m) for all reaches was estimated as (BRC 2002):

$$depth = 0.8419 \cdot CA^{0.2911} \qquad 14$$

The elevation at the head and outlet of each reach was determined using the DEM in order to provide an estimate of the channel slope.

DEM and basin delineation

The direction of surface flow was calculated by determining the direction of steepest downward slope from each pixel in the DEM. The vector stream network was converted to a raster of the same resolution as the flow direction grid (19.764m). Using each reach as a distinct outlet, subbasin delineation was performed with the flow direction grid.

A probable stream network could have been estimated using the flow direction grid and used in place of the NTDB stream network. However, the use of the NTDB to define the outlets for delineation allows consideration of narrow streams which may not be reflected in the resolution of the topographical map.

Sinks

This initial delineation process highlighted areas of the watershed which did not appear to contribute surface flow to the stream network and were not included in any subbasins. If the DEM is correct, these localised depressions (or "sinks") will collect surface runoff, possibly forming ponds or wetland areas. In order to include these regions in the delineation process, the depressions were filled.

The sink areas in the DEM up to a certain depth (initially 1m) were identified and filled using GIS. The new flow direction grid was calculated and subbasin delineation performed. If there remained any areas within the watershed which were not included as part of a subbasin, the depth limit for sinks was increased by 1m and the process repeated. Sinks up to 4m were identified and filled. In total, 445 hectares of sinks were filled to an average depth of 1.1m.

A set of 307 subbasins with an average area of 181 ha each (mostly between 20 and 200ha) were generated (see Figure 4). In aggregate these subbasins represent the entire watershed of 556km^2.

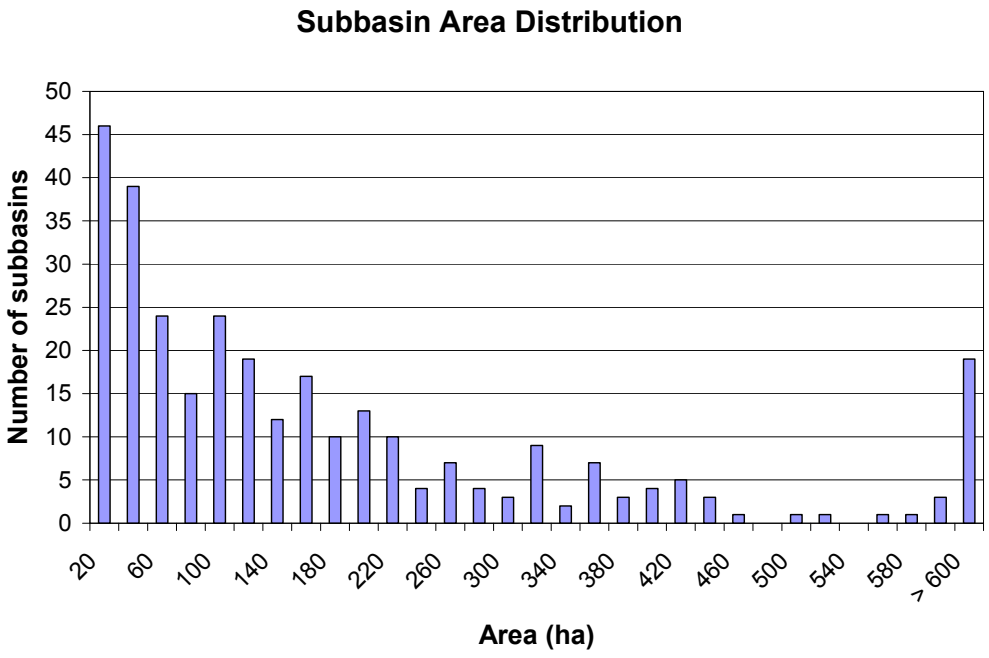

Figure 4 - Subbasin area distribution

Land cover classification

The classification process began by determining the potential classes that land cover should be categorised into. To represent the hydrology of this landscape, water, wetland, forest, unmanaged land (generally grassy fields, some of which may be used for pasture) and agriculture were chosen as the necessary master classes.

Initially, the Landsat image from November 1999 was used for land cover classification. A key consideration in using this image is that it was taken late in the year. In early November, agricultural crops have been harvested and leaves on deciduous trees have changed colour or fallen. Thus the image cannot be used to distinguish based on summer foliage. However, it can be used to distinguish between broad land cover categories as long as those categories remain spectrally different into the fall.

The image was classified using an isocluster approach (Richards and Jia 2005) on the six 30m resolution bands of the image. Twenty spectral classes were used for the isocluster process - higher than the final number of classes sought. Each clustered class was then labelled as the appropriate final class manually. This process of class aggregation allows land covers which are not spectrally consistent to be defined as the set of a number of different spectral classes.

The initial number of classes chosen is a trade off between classification certainty and the amount of manual intervention required. As the number of classes chosen for isoclustering increases, the certainty with which each pixel is classified increases. Yet as the number of classes increases, the manual effort required to assign each class to the correct land cover increases. In the limiting case, there is a distinct class for every pixel: each pixel is certain to belong to the predicted class, but the entire image must be labelled pixel by pixel defeating the purpose of automated clustering.

Labelling of the classified image was done by visual observation of the other available satellite images and other land use maps (SDG 2005, CH2MHill 2001). Field visits were used to confirm that the forested area was generally mixed deciduous and coniferous, that most fields are unmanaged and that agriculture land is generally corn production.

Agricultural land was modeled as corn and hay as these are the crops typically grown in the area. While the area does have some soybean production, the model is insensitive to the

field crop chosen for simulation. Specifically, most of the agricultural land is concentrated in the south east of the watershed, outside of the catchments of the stream gauges used for validation. Altering the simulation to use either corn or soybean results in negligible differences in daily and monthly hydrologic values (runoff, infiltration and actual evapotranspiration) for the basin. Thus the choice of corn, soybean or some mixture of the two was not considered important.

What we have labelled unmanaged land was graded into good, fair or poor conditions (Unmanaged I, II and III) based on the relative normalised difference vegetative index (NDVI) values of the distinctly identified groups. The NDVI, originally proposed by Rouse (1973) is a measure of greenness and is defined as:

$$NDVI = \frac{NIR - RED}{NIR + RED} \qquad 15$$

where NIR is the reflectivity in the near infrared band and RED is the reflectivity in the red band.

The area has very little urban or built up areas. Roads and other impermeable surfaces were absorbed into the other, vegetative classes. Curve number values may be increased during calibration to account for the additional runoff that these areas would provide.

Water and wetlands identified in classification are also identified in the NTDB layers. This information is considered more accurate as it is sourced from higher resolution imagery. The areas from the NTDB were overlaid on the classified image.

The clustering and labelling process was repeated using the Landsat image from May 1992. It was noted that the 1992 image was harder to label following classification. The amount of new green foliage tended to make classes appear more similar.

Classification certainty

The classification process is based on the maximum likelihood (ML) estimator, which assesses each pixel independently using a Bayesian approach (Richards and Jia, 2006). This process assumes that each class is comprised of a set of pixels which are normally distributed. Thus the probability of a pixel belonging to a class can be determined using only class means and covariances. The function indicating the relative likelihood that pixel x belongs to class i is given as:

$$g_i(\vec{x}) = -\ln|\Sigma_i| - (\vec{x} - \overrightarrow{m_i})^t \Sigma_i^{-1} (\vec{x} - \overrightarrow{m_i})$$

where $\vec{x}$ is the vector representing a given pixel, $\overrightarrow{m_i}$ is the mean vector of class *i* and Σ_i is the covariance matrix for class *i*. The pixel is classified as class *i* for which the value of $g_i(\vec{x})$ is highest.

Classes which were labelled the same were aggregated together. The probability of a pixel belonging to an aggregated class is the sum of the probabilities of the pixel belonging to each of the classes that comprise the aggregated class.

Though pixels in the original spectral classes were assumed to be normally distributed, pixels within aggregate classes would not be normally distributed. The distribution of pixels within each aggregate class should exhibit peaks in the distribution, one peak for each class which was aggregated together.

Figure 5 illustrates the classification confidence of the 1992 and 1999 images following labelling and aggregation. The increased difficulty labelling the image from 1992 was validated by the results showing that the classification confidence for this image is somewhat lower than that of the 1999 image.

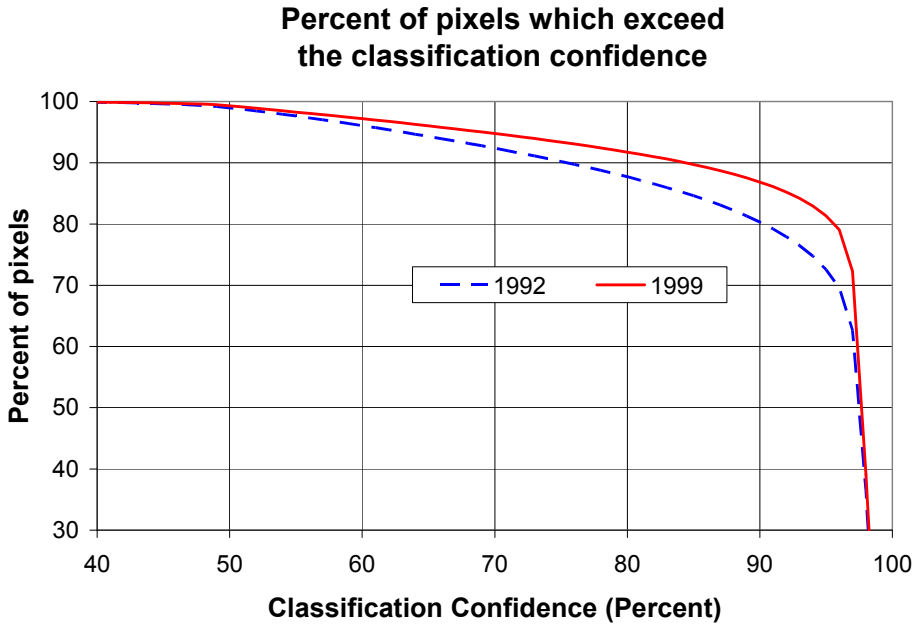

Figure 5 - Classification accuracy of Landsat images based on the maximum likelihood estimator

Classification confidence is a measure relating a pixel to the properties of a classes (in the case of the ML classifier, the mean and covariance). Labelling confidence, however, relates a spectral class to the properties of a land cover label. Since spectral or quantitative properties of each land cover are undefined, we could only assess the labelling accuracy by comparing with other land use classifications.

Documents prepared for an eastern Ontario water study (CH2MHill 2001) identified land uses over a large region encompassing the Raisin River watershed. Though the classification schemes were slightly different (the other study did not include wetlands, but did include bare soil) and the resolution of the available data much lower, we could compare the fraction of land cover within the watershed that some land covers represent.

Label	CH2MHill (2001)	Classification (Landsat 1999)
Forest	44	38
Open space/Pasture	32	44
Agriculture	11	12

Table 3 – Percentage land use within the watershed, regional study versus classified image

Regional planning documents (SDG 2005) highlight significant woodlands and wetlands. 72% of this area was labelled forest or wetland on the November 1999 image. Much of the rest (25%) was labelled Unmanaged-III due to its low NDVI value. Some of this can be attributed to the spatial correlation between the forest and this class. It tends to be located at the edge of forests, and may actually represent a transition region or a mixed class.

Label	As percentage of regionally significant woodlands and wetlands (SDG 2005)
Forest	62
Wetland	10
Unmanaged – III	25

Table 4 – Land cover classes as a percentage of regionally significant woodlands and wetlands

Soil preprocessing

The soil maps for Stormont and Glengarry were merged to create an overall soil map for the region under study. This map was clipped to the watershed boundary. GIS tables containing the overall and layer specific properties were created.

Each soil class was assigned to one of four broader categories indicating its overall drainage ability. These hydrologic soil groups (NRCS 1996) were used to specify the curve number for various land uses over the range of soil types.

The soil map was transformed to a raster format in the same resolution as the land cover map (30m). The soil classes and hydrologic groups in the watershed are shown in Map 7 and Map 8.

Ponds and wetlands

The NTDB waterbodies layer was used to identify ponds within the watershed. Any waterbody not part of the stream network was considered a pond.

All areas that were identified as sinks in the DEM (445ha over the watershed of 556km^2) were modeled using the SWAT "wetland" landcover type. Wetland depth was assumed to be the same as the average filled depression depth, or 1.1m. SWAT models wetlands using a "normal" and "maximum" storage depth. Outflow from the wetland occurs whenever the water volume is greater than the normal depth. The maximum depth was also set to 1.1m, such that the model would release all water in excess the normal depth to surface runoff.

The contributing area to the ponds and wetlands within each subbasin was calculated using the unfilled DEM. This information was used by the model to determine the fraction of surface flow to be directed to stream, ponds or wetlands.

HRU level data

SWAT models each area as a combination of land cover and soil type known as hydrologic response units (HRUs). Each subbasin is comprised of a set of HRUs which define the amount of runoff generated in each subbasin.

The land cover, soil and subbasin maps were combined to identify each unique HRU. The HRU map took on the resolution of the lowest resolution input layer, the 30m land

cover map. The resulting distribution of land use and soil group is shown in Figure 6. The DEM was used to determine the mean slope within each HRU, required for runoff and erosion calculations.

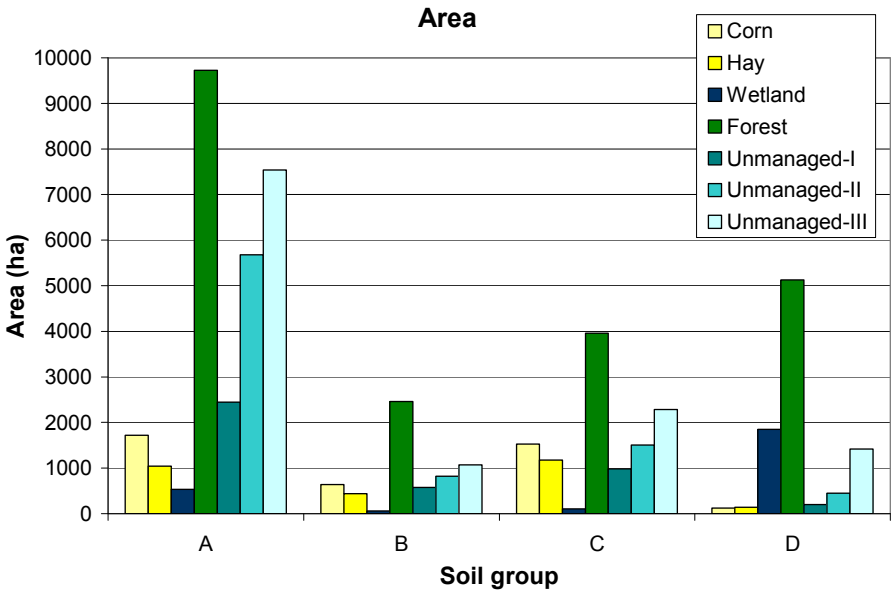

Figure 6 – Distribution of watershed area by land use and soil group

4. Methodology

Simulation

The SWAT model was run for five years (1980 to 1985) to allow state variables such as soil water to reach equilibrium. Results from the model for the period of 1985 to 1994 were used to calibrate the model. The period of 1995 to 2004 was used to validate the model.

Calibration

Hydrologic calibration was performed by comparing the predicted streamflow at the location of gauge 02MC001 to observed values. Average daily flow values were separated into runoff and baseflow values using a recursive digital filter suggested by Nathan and McMahon (1990):

$$q_t = \beta * q_{t-1} + \frac{1+\beta}{2} * Q_t \qquad \textbf{16}$$

where Q_t is the flow at time t, q_t is the filtered runoff, and β is the filter coefficient of 0.925 (determined by Nathan and McMahon and verified through visual observation of the hydrograph). The average of two passes of this filter was used to estimate the fraction of runoff and verified by observing the hydrograph graphically. An example hydrograph illustrating the separation is given in Figure 7.

A recommended metric (ASCE 1993) for quantifying the performance of hydrologic models is the Nash Sutcliffe coefficient (NS). This was chosen as our objective function for calibration. The equation for NS is given as:

$$NS = 1 - \frac{\sum_i (P_i - O_i)^2}{\sum_i (O_i - \overline{O})^2} \qquad \textbf{17}$$

where O_i and P_i are the observed and predicted values at a given time interval, and $\overline{O}$ is the mean value of all observed values over the calibration period.

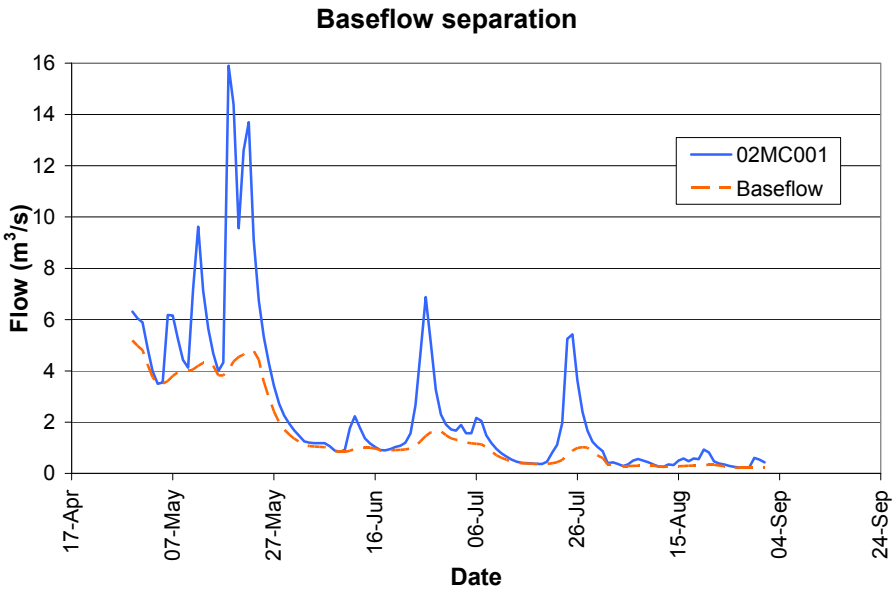

Figure 7 - Baseflow separation example using the filter of Nathan and McMahon (1990)

Weekly average flow was used to compare model output with observed. This removes some of the error associated with the different definitions of "daily" in model inputs and outputs. For example, precipitation is provided as daily total and occasionally reported on the following day, while stream flow is provided as daily average. Such errors make it inappropriate to examine model performance on the same time scale as its time step (Jackson et al. 2000). As well, the purpose of the model is not to predict watershed response on a daily basis but to assess the watershed with a longer term view.

Calibration procedure

Thirteen parameters were used to calibrate the SWAT model. These parameters reflected different parts of the water cycle including runoff (two parameters), soil and evapotranspiration properties (three parameters), groundwater (three parameters) and the snowfall and snowmelt cycle (five parameters) (Figure 8). A list of the calibration parameters, their calibration range and final value is given in Table 12. A detailed description of the calibration parameters is provided in Chapter 5.

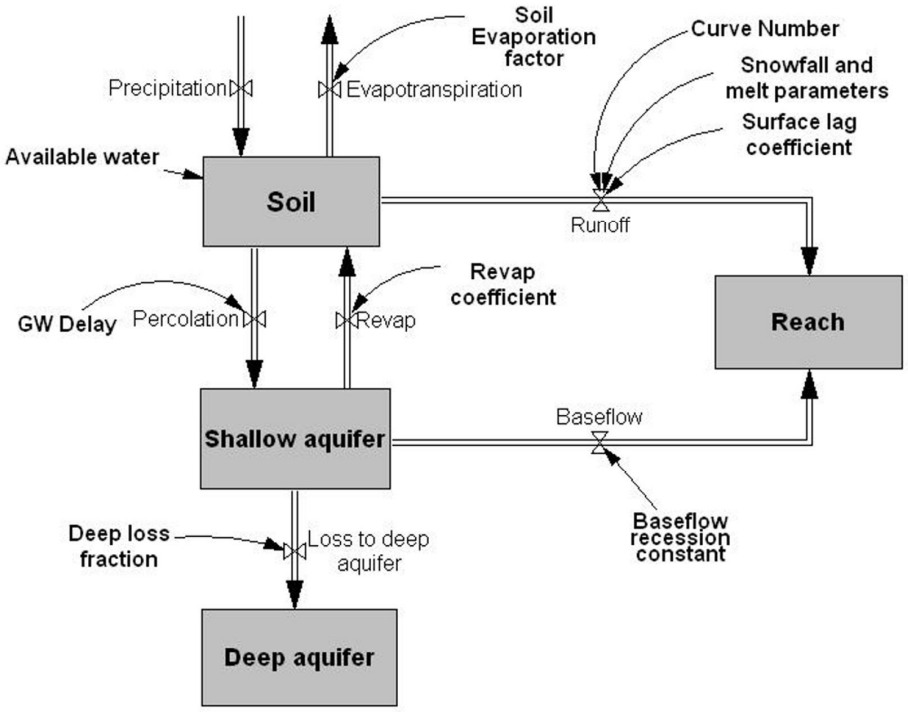

Figure 8 - SWAT hydrologic cycle and parameters used for calibration

The initial value for the groundwater recession coefficient was estimated using the master recession curve procedure described in Arnold et al. (1995). Using the flow values from gauge 02MC001, all recession periods of ten days or longer between the months of December to March were identified. This was considered to be the season when recharge would be at its lowest. The flow values were shifted up or down so that each recession period ended at the same flow, $1 m^3/s$. The natural logarithm of the flow was plotted against the day of the recession period. The slope of this graph, estimated through linear regression, represents the recession coefficient. To remove runoff or other flow peaks, all values over the regression line were removed and the regression line recalculated on the remaining values (Figure 9). The slope of this line was used as an initial estimate of the groundwater recession coefficient.

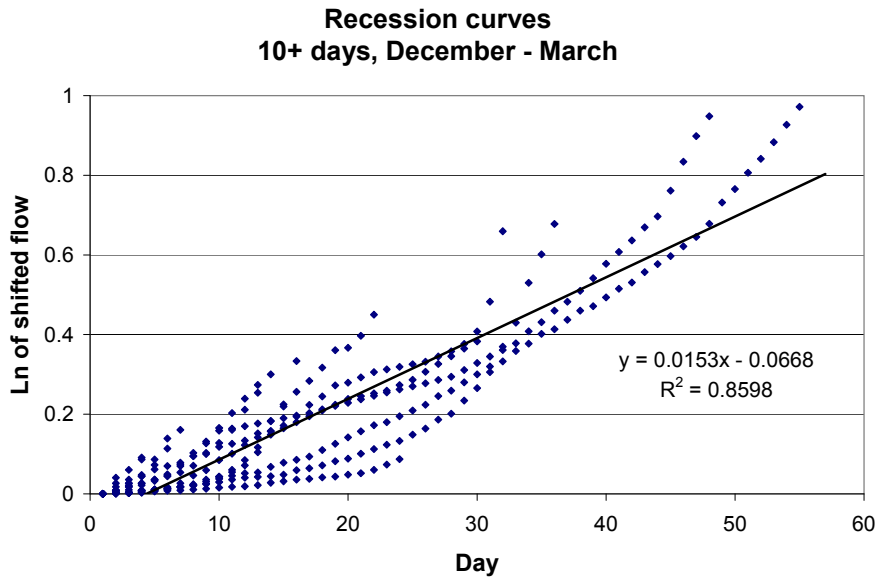

Figure 9 - Recession curves for 02MC001. Solid line is determined by linear regression; the slope of this line is used as an initial estimate for the groundwater recession coefficient.

The curve number and AWC parameters were set using typical values for the land use and soil type respectively, using data from the SWAT user manual (Neitsch et al. 2002) and Schwab et al. (1993). The rest of the calibration parameters were set to the recommended or default values specified in the SWAT user manual.

Annual flow was first calibrated to be within the desired range by adjusting curve numbers, loss to the deep aquifer and the surface lag coefficient. Next, adjustments affecting seasonal performance were made. These steps were performed iteratively making finer adjustments with each iteration.

Annual Calibration

Initial calibration steps were taken to adjust the predicted annual flow, runoff and baseflow to within 5% of the observed values. This process is outlined in Figure 44. Curve number (CN) and the surface lag coefficient (SURLAG) were used to adjust annual runoff values, while the deep aquifer loss fraction was adjusted to calibrate the annual baseflow.

Curve numbers were increased in 5% increments order to predict reasonable annual runoff. However, as curve numbers were increased the model performance began to drop

off. In particular, the predictions of runoff peaks in the summer period were too high. Once curve numbers were increased by 15% the daily NS coefficient for the summer period fell below 0 (Table 5). At this point the model is generating poorer flow estimates than always choosing the average flow. Since the goal of accurately predicting annual runoff needed to be balanced against the desire for reasonable model predictions throughout the year, the curve number values were limited to 10% higher than original.

Increase in curve number	Model performance by season – calibration period (Daily NS) | (Average flow error %)							
	Jan 1 – Apr 30		Jun 1 – Sept 1		Oct 1 – Nov 30		Annual	
5%	0.629	-7	0.260	-5	0.377	27	0.608	-1
10%	0.624	-7	0.153	13	0.284	31	0.592	2
15%	0.616	-6	-0.058	46	0.143	42	0.561	8

Table 5 - Seasonal impact on model performace due to an increase in curve number

Decreasing the SURLAG parameter from its initial value resulted in lagging the surface flow, smoothing the hydrograph and decreasing the ratio of runoff to baseflow calculated by the baseflow separation filter. Thus the SURLAG parameter has a significant effect on the interpretation of runoff and baseflow, though it does not change the total flow.

By decreasing the SURLAG parameter less variation in the model error was observed, reflected in the higher calculations of NS. Further decreases to SURLAG would increase NS, but decrease the amount of annual runoff enough to require a further increase in CN. However, as noted above, we have limited the increase in CN in order to maintain acceptable predictions throughout the year.

The deep aquifer loss fraction affects the predicted baseflow in a nearly linear way, thus it is simple to calibrate the model to predict good baseflow on an annual basis. Within a fairly large range from the calibration point, changes to this parameter have little impact on the NS value.

Seasonal calibration

The remaining parameters used in calibration affect the annual quantities of runoff and baseflow to a lesser extent. Most impact the water cycle on a predominantly seasonal basis. These parameters were used for fine tuning of the model as outlined in Figure 46. The procedure used to adjust an individual variable is shown in Figure 45. The SURLAG and

deep loss coefficients used in annual calibration were also used in seasonal calibration. Small adjustments to these variables could be made as the model was seasonally calibrated.

The revap and soil evaporation (ESCO) parameters are connected to evapotranspiration predictions thus their primary impact is seen in the summer months. The impact of soil available water content (AWC) is also dominant in the summer.

Small changes in the groundwater delay coefficient (GWDLY) around the calibration point have little effect on the annual flow statistics, however there is some seasonal effect. Seasonal baseflow peaks, primarily in the spring, recede slower with an increase in the GWDLY parameter. Baseflow recession is much more sensitive to the groundwater recession coefficient, impacting predictions primarily during winter and summer low flow periods.

Model response for the snow fall and snow melt variables was isolated primarily to the months of March to May. It was noted that these five parameters could be calibrated without affecting the ideal value of other parameters, minimizing the need for iterative calibration. The specifics of adjusting snow melt parameters is shown in Figure 47.

Model Sensitivity

The sensitivity of the model to each parameter near the calibration point was examined. The change in streamflow (total, runoff and baseflow) and the value of the weekly NS coefficient was observed as each parameter was varied in turn. A detailed examination of SWAT parameters and sensitivity is provided in Chapter 5 and summarised in Table 6. These results identify how important calibration accuracy will be on the model results. Parameters to which the model is insensitive will have little impact on results. Conversely, sensitive parameters must be accurately calibrated to produce good results.

Parameter	Annual	Runoff	Baseflow	NS
CN	Medium	High	Low	Medium
SURLAG	Low	High	High	High
AWC	Medium	Medium	Medium	Low
ESCO	Medium	Medium	Medium	Low
Revap	Medium	Low	High	Low
Deep loss	Medium	Low	High	Low
GW delay	Low	Low	Low	Low
GW recession	Low	High	High	Medium
Snowfall temperature	Low	Low	Low	Low
Snowpack temperature lag	Low	Low	Medium	Low
Snowmelt temperature	Low	Low	Medium	Medium
Dec. 21 melt rate	Low	Low	Medium	High
June 21 melt rate	Low	Low	Medium	High

Table 6 - SWAT parameter sensitivity

5. SWAT Parameters and Sensitivity

Sensitivity

While the SWAT model is deterministic, it is not feasible to have an analytic solution to determine the sensitivity of the model to each parameter. Nor is it possible to know analytically if the calibration point we have determined is the most optimum. However, we can determine the sensitivity of the model to individual parameters by graphical means. Changing only one parameter at a time and observing the change in model output gives us the sensitivity of the model to the parameter in question.

If the model is highly sensitive to a particular parameter, then predictions will be greatly affected by small errors in the parameter estimation. If the model is insensitive to a parameter, we can forego detailed calibration as small changes will not affect the model output.

Sensitivity of the model was determined by observing the change in prediction of flow at the location of gauge 02MC001 over the validation period of the model (1995 – 2004). Changes to the annual flow error (total, runoff and baseflow) and changes in NS (daily and weekly) as each parameter was varied around the calibration point were used as measures of sensitivity.

Each parameter was calibrated to the highest weekly NS value over the calibration period (1985-1994). By examining model sensitivity over the validation period, we can observe if the calibrated value for each parameter is also the optimal value for the validation period. A difference in optimal value between the two periods is another measure of uncertainty in the parameter. However, uncertainty in calibrated values is only of importance if the model is sensitive to that particular parameter.

Runoff Parameters

The curve number (CN) and surface lag coefficient (SURLAG) parameters directly affect the prediction of runoff. CN controls the amount of predicted runoff while SURLAG controls the rate at which runoff moves from land to stream.

Curve Number

CN is used in the prediction of runoff by way of the SCS method (SCS 1972). Changes to CN affect the fraction of precipitation which becomes runoff. As well, CN controls the level of initial abstraction which is the threshold for precipitation to become runoff.

Annual runoff increases roughly 7% for each 5% increase in CN (Figure 10). As noted in the calibration procedure, an increase of curve number beyond 10% results in lower model performance due to overpredicted summer runoff peaks.

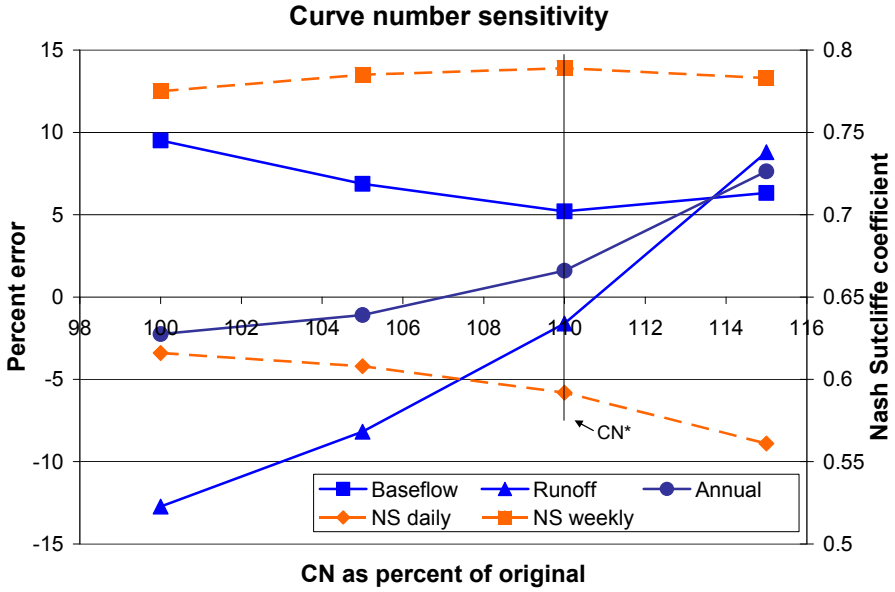

Figure 10 - Curve number sensitivity around the calibrated value (CN*)

Surface lag coefficient

The SURLAG variable affects the interpretation of runoff by shifting the annual flow from baseflow to runoff:

$$Q_{surf} = \left(Q'_{surf} + Q_{stor,i-1}\right) \cdot \left(1 - e^{-SURLAG/t_{conc}}\right) \qquad 18$$

Q_{surf} is the surface runoff discharged to the stream on a given day (in mm), Q'_{surf} is the runoff generated on that day (mm) and $Q_{stor,i-1}$ is the amount of runoff lagged from previous days (mm). The SURLAG parameter is used as a fraction of the time of concentration, t_{conc} (hours), which is calculated at the HRU level.

Increasing SURLAG results in the exponential term approaching zero, and the discharged runoff will approach the generated runoff on each day. As SURLAG decreases, more runoff is lagged. The method used to separate runoff from baseflow – a high pass filter with a fixed cutoff – is sensitive to this. The lag has the effect of making some runoff appear as slow-moving baseflow. Consequently, our interpretation of runoff and baseflow changes, though total flow does not (Figure 11).

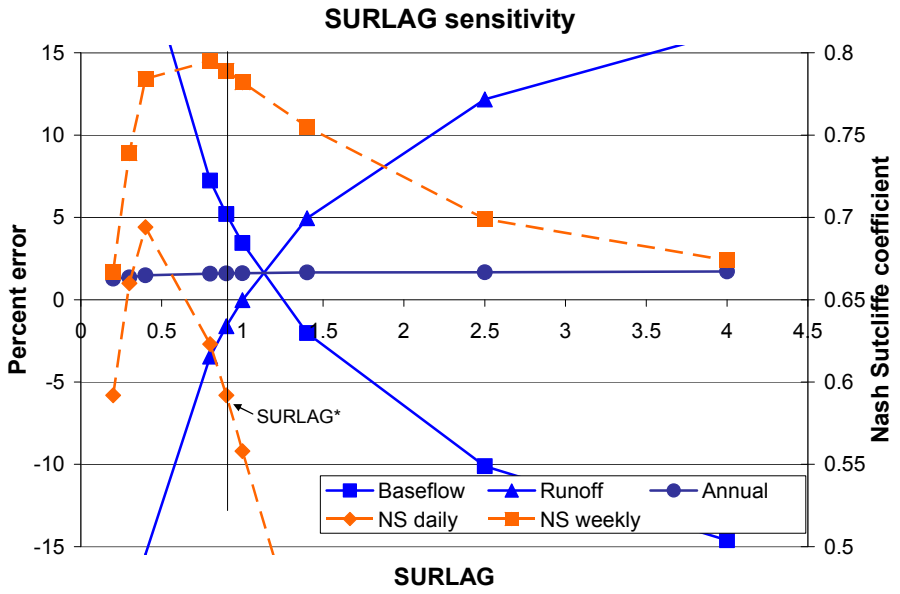

Figure 11 - Surface lag coefficient sensitivity around the calibrated value (SURLAG*). Runoff, baseflow and model performance are very sensitive to SURLAG near the calibration point.

Runoff parameter interdependence

To consider the possibility that CN and SURLAG were interdependent, the parameters were varied together. By lowering the CN values below the calibration point and re-examining the sensitivity of the SURLAG parameter, we can observe if there is a change in the model performance. This could be suggestive of a change in model state whereby a different hydrologic process begins to dominate. Figure 12 highlights the change in model performance as a function of SURLAG for two values of CN. We see that the sensitivity of the model to SURLAG does not change substantially with a change in CN, nor does the optimal value for SURLAG differ. This finding gives us confidence that the calibrated values for runoff parameters are optimal and not the result of some interdependence.

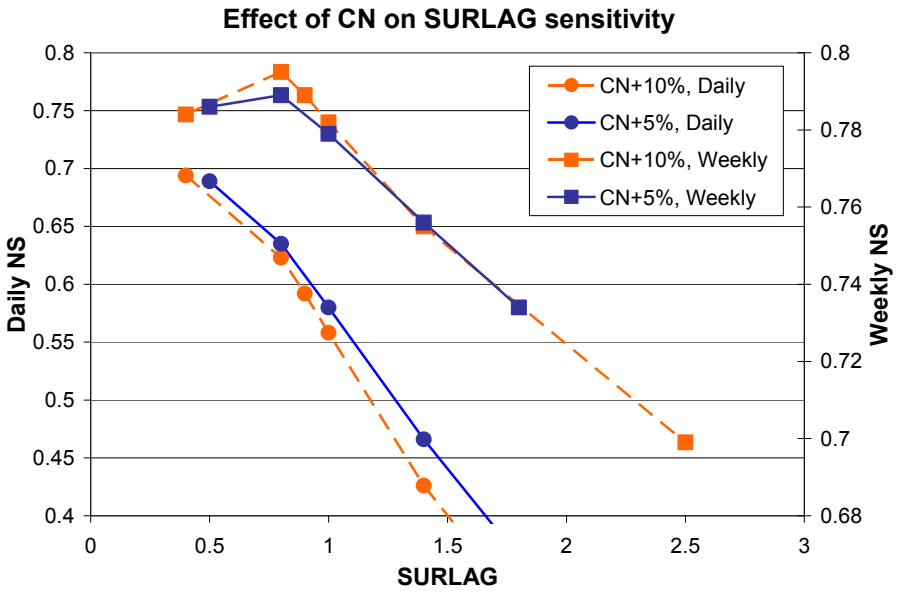

Figure 12 - Effect of CN on SURLAG sensitivity. Changes to CN do not appear to have a significant impact on the sensitivity of the model to SURLAG.

Soil and Evapotranspiration parameters

Three parameters were used to calibrate soil water and evapotranspiration. Available water controls the soil water content, while the revap and soil evaporation compensation coefficients control actual evapotranspiration.

Available water content

Available water content (AWC) defines the soil water available to plants and is also used by the model to estimate field capacity. An increase in AWC leads to a greater possibility of fulfilling plant ET requirements. This decreases the amount of water available for recharge and baseflow (Figure 13). Additionally, when calculating runoff volumes the runoff coefficient is adjusted for soil moisture conditions as a function of AWC. Overall we observe a decrease in runoff with an increase in AWC.

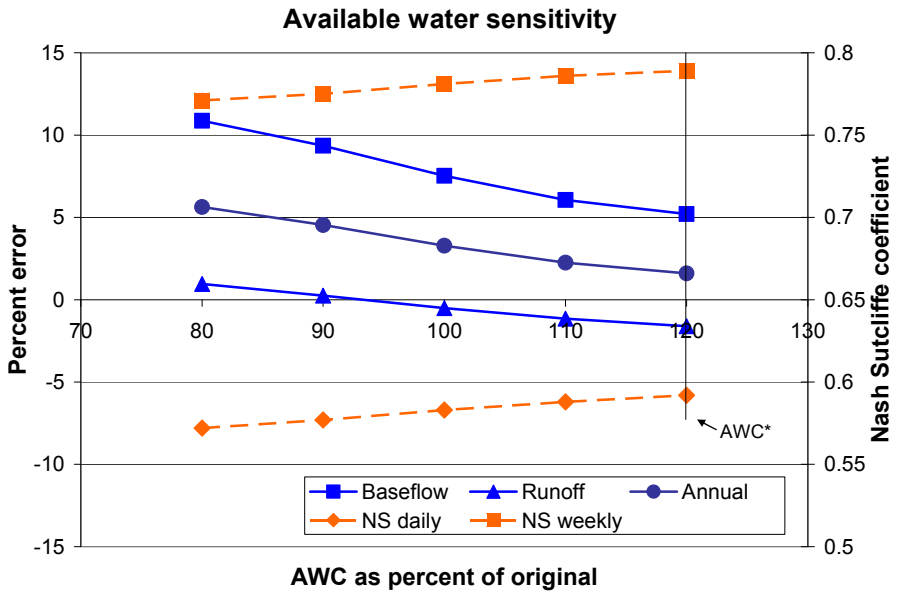

Figure 13 - Available water content sensitivity. Model performance increases slightly as AWC is increased to the calibrated value (AWC*)

Revap

The REVAP parameter affects the amount of water which plants can extract from the shallow aquifer to satisfy their evapotranspiration demand. When the soil profile is dry, SWAT allows water to move upwards from the shallow aquifer back into the soil profile in order to satisfy ET demand. The revap coefficient is defined as the fraction of the daily PET that can be satisfied in this manner. As the REVAP coefficient increases, the amount of water which may be channelled from the shallow aquifer back to the soil profile increases. This decreases the amount of water in the shallow aquifer and thus decreases the amount of baseflow discharged. The effect of this coefficient is particularly apparent in the early spring and summer. A higher REVAP coefficient causes the spring baseflow peak to recede faster.

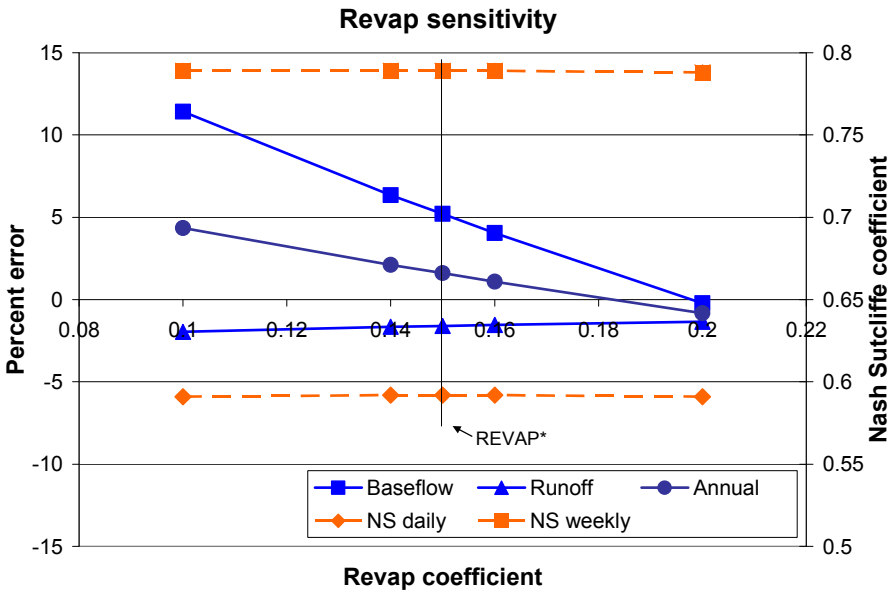

Figure 14 - Revap coefficient sensitivity. Model performance is not affected by changes to REVAP near the calibration point (REVAP*), however baseflow is strongly affected.

Soil evaporation compensation coefficient

The soil evaporation compensation coefficient (ESCO) impacts the prediction of actual evapotranspiration. As ESCO decreases, evapotranspiration demand is satisfied from deeper in the soil profile. Thus, increases in ESCO tend to decrease the amount of actual ET, which in turn increases the amount of soil water, runoff, recharge and baseflow.

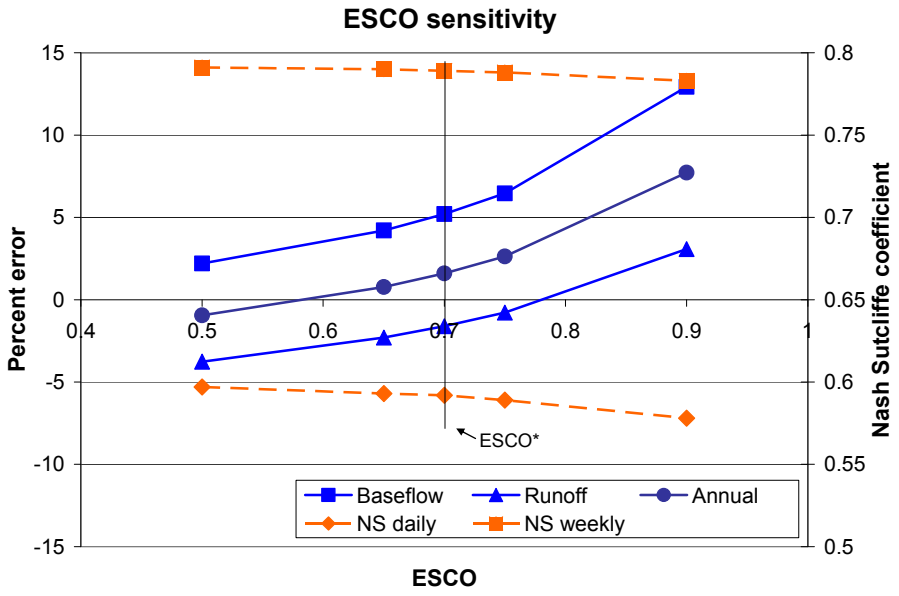

Figure 15 - ESCO sensitivity. Increases in ESCO decrease predictions of actual evapotranspiration, thus increasing predicted water yield.

The model performance is not particularly sensitive to the values of ESCO nor REVAP, primarily because the impact of these parameters is greatest during the summer, low flow months. This is the same period in which the NS metric is least sensitive (see Chapter 6).

Groundwater parameters

Groundwater delay coefficient

The groundwater delay coefficient (GWDLY) affects the rate of recharge as water moves from the soil profile into the shallow aquifer:

$$R_i = R_{i-1} \cdot e^{-1/\delta} + S_i \cdot \left(1 - e^{-1/\delta}\right) \qquad 19$$

where R_i is the recharge on a given day (mm), S_i is the amount of water moving from the soil profile in a given day (mm) and δ is GWDLY (days). This parameter is meant to account for any geologic transition that may exist between the bottom of the soil profile and the shallow aquifer. As GWDLY decreases, the exponential term becomes vanishingly small and there is little delay between soil profile and aquifer.

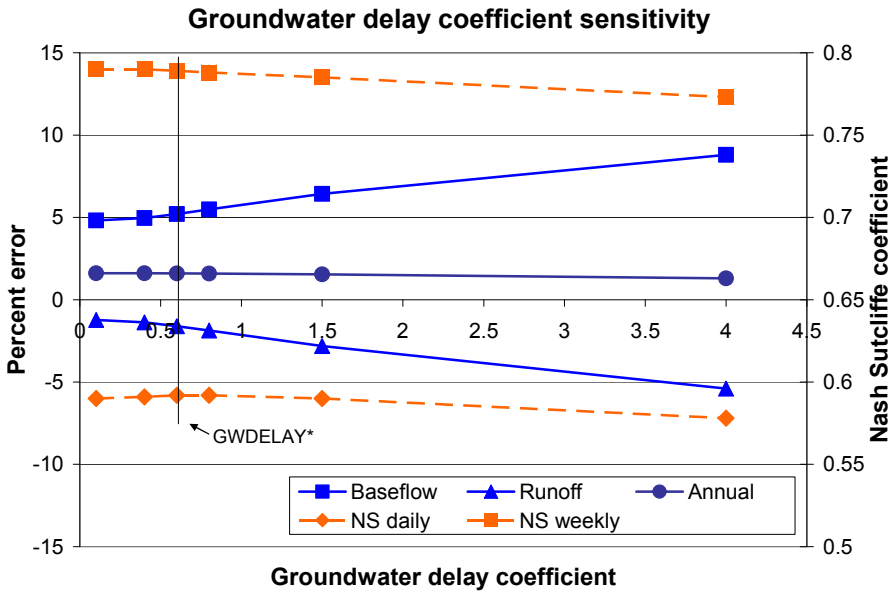

Figure 16 - Groundwater delay coefficient sensitivity. The model is insensitive to changes in the coefficient near the calibration point (GWDELAY*).

For the calibrated delta value of 0.6, the exponential term is close to 0.189. Small changes in the coefficient around the calibration point have little effect on the annual flow statistics however there is a slight seasonal effect. The spring baseflow peak recedes slightly faster with a decrease in the GWDLY parameter.

Deep aquifer loss fraction

The deep aquifer loss fraction directly adjusts the amount of shallow aquifer recharge by removing water from the system. As baseflow is a linear function of shallow aquifer storage, this has a direct impact on the amount of baseflow predicted.

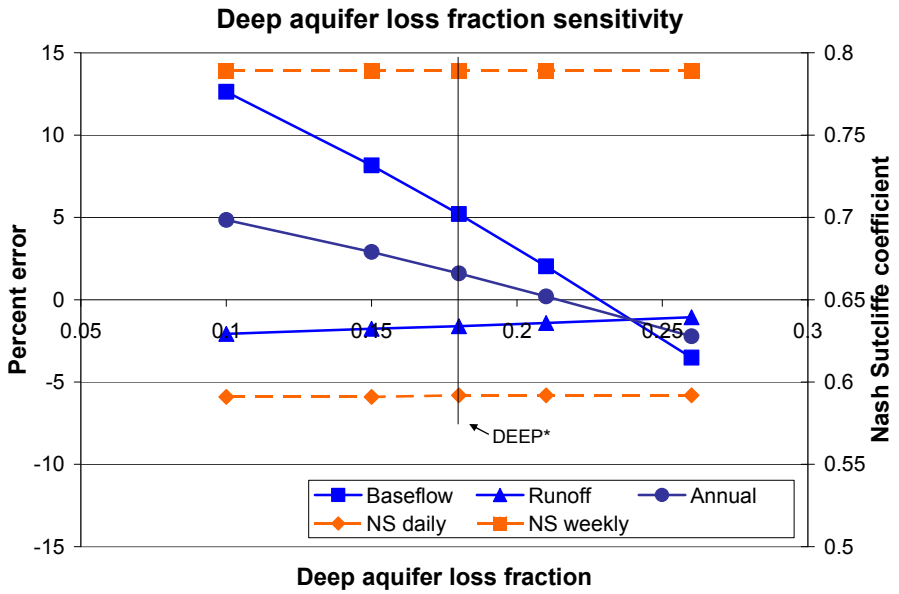

Figure 17 - Deep aquifer loss sensitivity. Changes to this coefficient strongly affect baseflow predictions.

Groundwater recession coefficient

The groundwater recession parameter controls the rate that water which enters the shallow aquifer becomes baseflow. The baseflow on a given day is calculated as:

$$Q_{gw,i} = Q_{gw,i-1} \cdot e^{-\alpha \cdot t} + R_i \cdot \left(1 - e^{-\alpha \cdot t}\right) \qquad 20$$

where R_i and $Q_{gw,i}$ are the recharge and baseflow on a given day (mm), α is the recession coefficient and t is the time step (one day). Under conditions of no recharge, the second term becomes zero and baseflow decays in an exponential manner. As alpha increases, recharge becomes baseflow more quickly. As alpha decreases, the baseflow is lagged for a longer period of time. This change in baseflow speed is interpreted as a shift between runoff and baseflow (Figure 18).

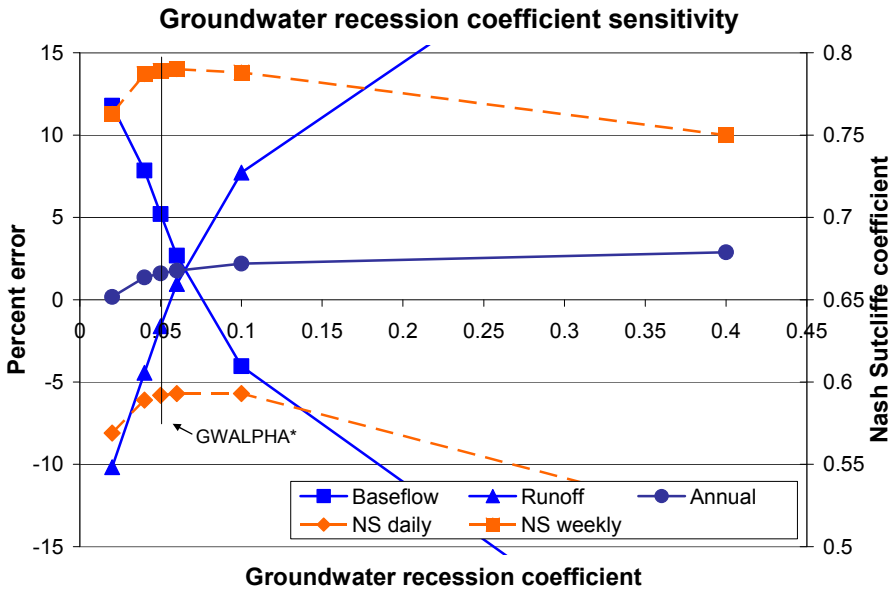

Figure 18 - Groundwater recession coefficient sensitivity. Changes to this coefficient strongly affect the runoff-baseflow separation determined by Equation 16.

Snow parameters

Snowmelt is the dominant hydrologic event of the year, thus knowledge of the snowfall and melt parameters is important. Due to the high sensitivity of the NS coefficient to high flow values, the snowmelt period is strongly represented in our measure of model performance. As such, the snowmelt parameters play a key role in model performance, which has been noted in other SWAT implementations for similar climates (Wang and Melesse 2005).

Snowfall temperature

The model is generally insensitive to snowfall temperature (Figure 19). The time of year when temperatures are such that precipitation could be either snow or rain is limited to short periods in the fall and spring. In the late fall streamflow is waning and the impact of precipitation is small. In the spring, the dominant factor is the melting of several months of accumulated snow. At neither time does incorrectly predicting precipitation as rain or snow make a significant impact to the results.

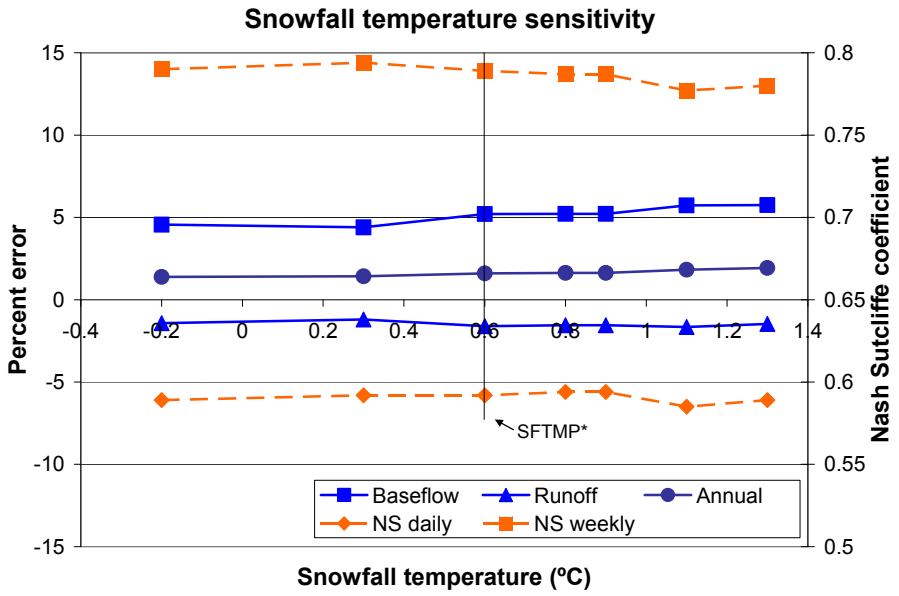

Figure 19 - Snowfall temperature sensitivity. The appears insensitive to changes in the snowfall temperature.

Snowpack temperature lag coefficient

The snowpack temperature lag coefficient (TIMP) is the amount that the snow pack temperature lags the ambient air temperature. This affects the rate at which melting begins.

Model performance is somewhat sensitive to this parameter (Figure 20). Perhaps more importantly is that the same optimal value for TIMP was found during the validation period, giving us certainty in the selected value.

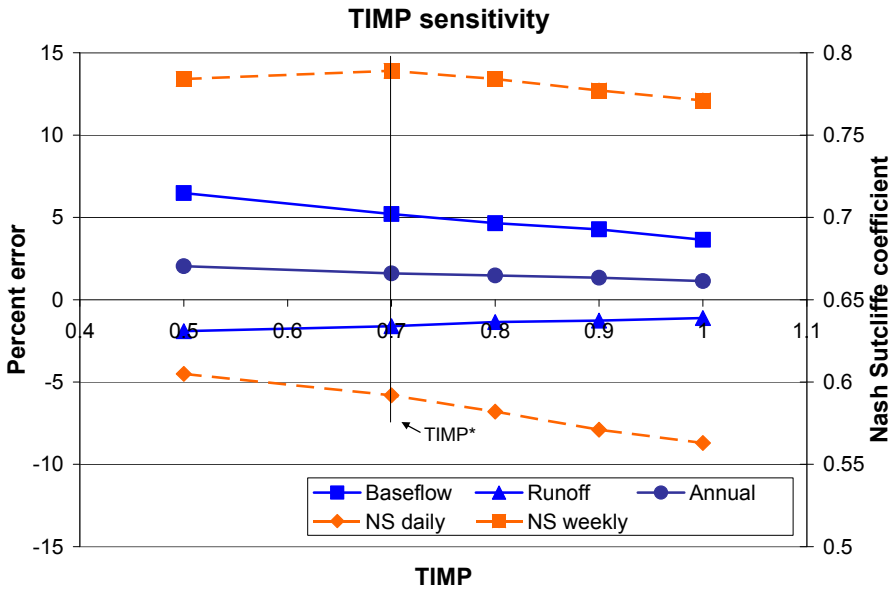

Figure 20 – Sensitivity of the model to changes in the snowpack temperature lag coefficient near the calibration point (TIMP*)

Snowmelt temperature

The snowmelt temperature has a strong impact on model performance as snowmelt is the dominant annual hydrologic event. This parameter specifies the threshold temperature over which snow melts (see page 15). As well, the degree-day method uses the difference between the current temperature and the melt temperature to determine the amount of melt for a given day. What appears to be the optimal value of snowmelt temperature during the validation period is very close (within 0.1ºC) to the value determined in calibration.

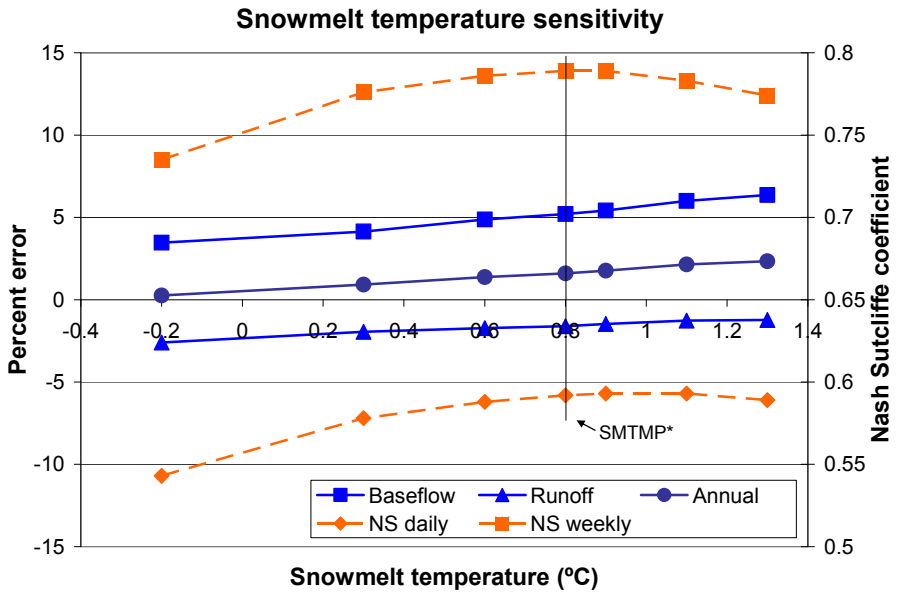

Figure 21 - Snowmelt temperature sensitivity near the calibration point (SMTMP*)

Snowmelt rates

The snowmelt rates for the winter and summer solstices (December 21 and June 21) are used to define the snowmelt rate through the year. This is based on the premise that there will be less snowmelt due to the lower solar radiation in the winter than in the summer. The melt rate on a given day is determined by interpolation between the two days.

Model sensitivity to the melt rates are shown in Figure 22 and Figure 23. Increasing the June 21 melt rate would improve model performance during validation. This would increase runoff during the spring but without increasing runoff during other times of the year. This is in agreement with our calibration findings of a need to increase annual runoff but not increase runoff peaks.

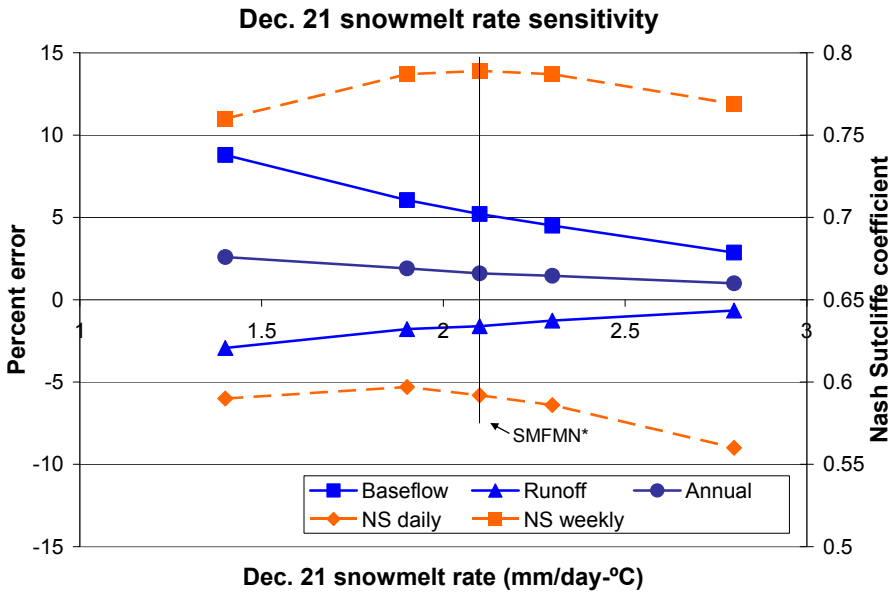

Figure 22 – Model sensitivity to changes in the minimum melt rate

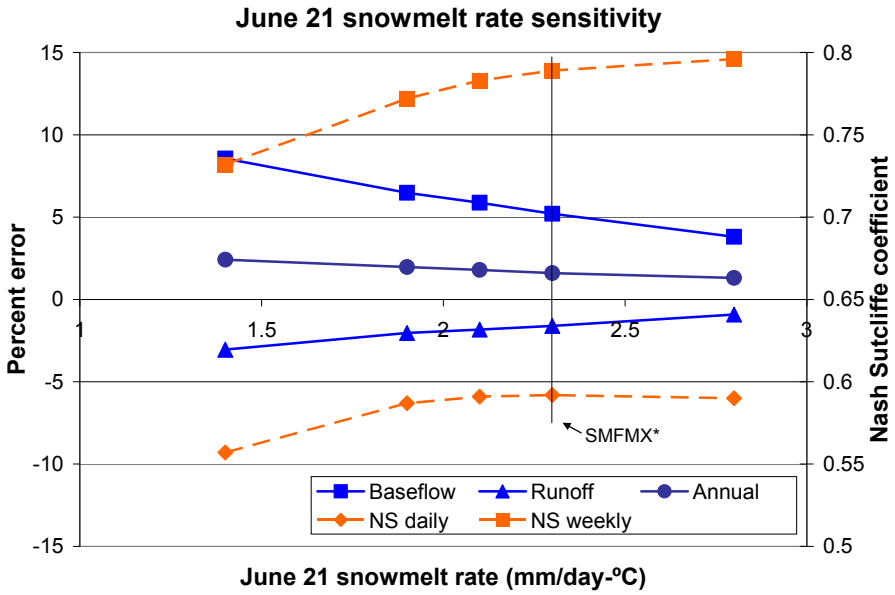

Figure 23 - Model sensitivity to changes in the maximum melt rate

Interaction of snowmelt temperature and snowmelt rate

To determine the interaction of the most sensitive melt parameters, the melt temperature and melt rates were varied simultaneously. As expected, increasing the melt temperature required increased melt rates in order to compensate and generate enough snowmelt (Table 7). As well, the sensitivity of the model to melt rate greatly increases as the melt temperature

is varied from the calibrated value of 0.8 ºC. Given the limited accuracy of the degree-day method to predict snowmelt, a greater sensitivity to the parameter values may not be desirable.

Melt temperature (ºC)	Dec. 21 melt rate (mm/ºC · day)	June 21 melt rate (mm/ºC · day)		
		2.0	2.3	2.6
0.5	1.8	0.795	0.802	0.799
	2.1	0.798	0.795	0.787
	2.4	0.789	0.780	0.766
0.8	1.8	0.779	0.794	0.800
	2.1	0.792	0.799	0.797
	2.4	0.794	0.794	0.787
1.1	1.8	0.756	0.775	0.788
	2.1	0.776	0.789	0.796
	2.4	0.788	0.795	0.795

Table 7 - Effect of melt temperature and melt rate on model performance, measured using the Nash-Sutcliffe coefficient for weekly average values (validation period).

6. Data transformation

In this section we consider the relationship between the series of streamflow measurements and the metric used for analysis, the Nash Sutcliffe coefficient (NS). We will examine how the distribution of streamflow values affect the NS calculation and the possibility of transforming the data to improve the usefulness of NS.

The equation for NS is:

$$NS = 1 - \frac{\sum_i (P_i - O_i)^2}{\sum_i (O_i - \overline{O})^2} \qquad \textbf{21}$$

where O_i and P_i are the observed and predicted values at a given time interval, and $\overline{O}$ is the mean value of all observed values over the period of interest.

The fractional part of this equation is the ratio of mean squared model error to the variance in the observed values. NS is thus a measure of how the model performs compared to the variance in the observed values. Conceptually we can think of the variance specifying a reasonable level of model error. The coefficient indicates whether the model does better than average by virtue of its sign. NS values greater than 0 indicate that the model performs better than merely choosing the average value all the time and this threshold is used to determine whether or not a model is a reasonable predictor.

The daily and weekly values are not normally distributed (Table 8) and as such are not well described by variance. A skewed distribution will have a variance which does not reflect what a typical deviation is. Additionally, for streamflow values the variance of values changes throughout the year. As the median weekly error increases, so does the variance in the weekly values.

Regardless of whether the variance in observed values is a good measure or not, the NS calculation can still be used for model calibration. The denominator of the fractional part is constant for all calibration sets, and we expect the numerator to decrease as the model performance improves. From one calibration run to the next, we can observe the relative difference in NS to determine if the mean squared model error has improved.

02MC001 flow (m^3/s)	Daily		Weekly		Monthly	
	1985-1994	**1995-2004**	**1985-1994**	**1995-2004**	**1985-1994**	**1995-2004**
Mean	4.97	5.19	4.97	5.19	4.98	5.19
Median	1.50	1.55	1.68	1.80	2.15	2.67
Variance	100.15	106.51	78.90	81.79	49.76	38.76
Skewness	4.29	4.56	3.73	4.08	3.00	1.69
Kurtosis	23.28	28.38	17.73	24.26	11.72	2.50

Table 8 – Statistical metrics describing flow distribution at the site of gauge 02MC001 for daily, weekly and monthly average flows.

However, if the variance term does not describe the dataset well, it becomes difficult to compare the resulting coefficient with other published models. The primary goal of the ASCE 1993 report was to identify a set of metrics which could be commonly used amongst hydrologic models, which would enable comparative review of models possible. By using a poor definition of variance, we are essentially changing the equation of NS, and removing the possibility of comparing models from different flow regimes.

In order to create a normal distribution of daily and weekly flow values, we considered a transformation of the data. By applying this transformation to both observed and modeled values, the NS calculation would better reflect its intended purpose.

Box Cox transformation

The Box-Cox transformation (Box and Cox 1964) is a power transformation which can be used to change the statistical distribution of a data set while maintaining the order of values. The form of the transform is:

$$x' = \begin{bmatrix} x^{\lambda} & for\ \lambda \neq 0 \\ \ln(x) & for\ \lambda = 0 \end{bmatrix} \qquad 22$$

The value of lamda is determined to create the desired distribution, in this case, a distribution which is symmetric about the mean and which has a consistent spread based on the flow rate. We use linear regression to determine what value of lamda will make the most normal distribution.

In order to transform the data so that the spread is reasonably consistent over the range, the spread versus level graphical procedure suggested by Emerson and Strenio (1983) was used. Weekly values at gauge 02MC001 during the calibration period were analysed to determine the median and quartile weekly flow rates. The difference between the first and third quartiles is defined as the fourth spread. Supposing that the spread of the original data is proportional to some power of the median value:

$$s = aM^{b} \qquad 23$$

where s is the spread, M is the median value and a and b are constants. In this case,

$$\ln[s] = \ln[a] + b\ln[M] \qquad 24$$

and the slope of the $\ln[s]$ versus $\ln[M]$ will be the power term, b. This is shown in Figure 24, where the spread level plot for weekly streamflow values for gauge 02MC001 has a slope of 0.854. To transform this data set for constant spread requires a power transformation of 1-b, or 0.146. As recommended by the author, utilising a power transform of 0 (for a logarithmic transform) or 0.5 (for a square root transform) is recommended. Thus the data suggests that we should use a log transform in order to stabilise the spread over the range of values.

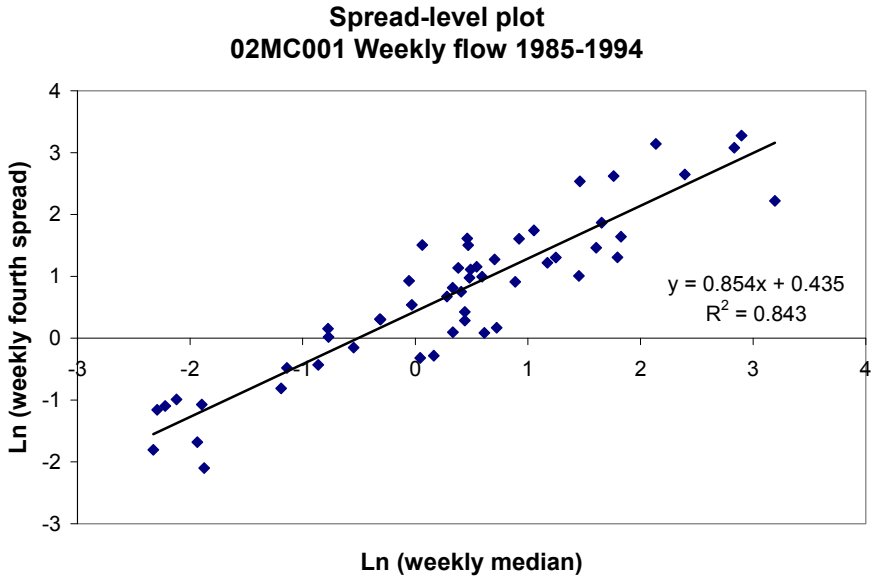

Figure 24 - Spread level plot for 02MC001. Solid line determined through linear regression.

With the goal to recreate the NS metric in such a way that it can be applied and realistically compared among other areas, using a straight log transformation would be most appropriate,

rather than having different values of lamda being calculated at each site and potentially reducing the ability to compare using this statistic. However, this procedure is useful to determine that a log transformation is appropriate.

Results of Transform

The impact of the log transformation on NS values is shown in Table 9. For a given percentage error, NS is sensitive to the magnitude of the observed value, while NS using log-transformed values is insensitive to observed value. The point at which the two measures are equally sensitive is dependant on the variance of the observed values and the variance of the transformed values, as well as the percentage error in predicted value.

Model performance (NS) at 02MC001	1985-1994	1995-2004
Weekly average flow	0.798	0.788
ln (Weekly average flow)	0.528	0.523

Table 9 - Effect of logarithmic transform on the Nash-Sutcliffe (NS) performance coefficient

The skew of the original data values means that many data points are extreme values to which NS is sensitive, a common feature of streamflow records (Legates and McCabe 1999). In particular, model errors at high-flow periods are more heavily weighted in the NS calculation. Under the transformed scenario, high flow periods (mainly, spring flow) are less heavily weighted while low flows (late summer) are given more significance. The results in Table 9 confirm that the model predicts reasonably well during all times of the year. The use of NS as a means to assess model performance throughout the year is questionable given the unequal weighting it gives to the different seasons.

Point where impact of transform is zero

The logarithmic transformation will, in general, give higher weight to periods of low flow and less weight to periods of high flow. However, the impact is dependent on the level of prediction error.

Consider the fractional part of the NS equation. For a single data point, the relative contribution to the coefficient can be considered as:

$$NS_i = \frac{(P_i - O_i)^2}{Var(O)} \qquad 25$$

There is a percentage error, ε, to each prediction, such that:

$$P_i = (1+\varepsilon)\cdot O_i \qquad 26$$

Thus we can represent the contribution of each prediction in terms of the observed value and the percentage error:

$$NS_i = \frac{((1+\varepsilon)\cdot O_i - O_i)^2}{Var(O)}$$

$$NS_i = \frac{(\varepsilon \cdot O_i)^2}{Var(O)} \qquad 27$$

The NS coefficient is affected by the magnitude of the observed values. An error in prediction during a period of high flow will have more impact on the final NS coefficient than an error during a period of low flow. Errors in prediction during periods of low flow will tend to be masked by the high sensitivity of NS to flow, thus the coefficient does not reflect the performance of the model equally throughout the flow regime.

In the transformed space, the contribution that each prediction makes to the coefficient is:

$$NS_{\ln,i} = \frac{(\ln[P_i] - \ln[O_i])^2}{Var(\ln[O])}$$

$$NS_{\ln,i} = \frac{(\ln[1+\varepsilon] + \ln[O_i] - \ln[O_i])^2}{Var(\ln[O])}$$

$$NS_{\ln,i} = \frac{(\ln[1+\varepsilon])^2}{Var(\ln[O])} \qquad 28$$

This is valid for all values of ε greater than -1, which is to say all predicted values must be greater than 0.

Note that the contribution each prediction has in the transformed space is a function only of the error in prediction. Each prediction with a given error is weighted the same regardless of magnitude. Use of this transformed coefficient would provide a measure of model accuracy which considers all flow regimes and times of the year equally. However, a limitation of the transform is that positive errors, or over-predictions, will be weighted less

than negative errors, or under-predictions (Figure 25). For prediction errors which are sufficiently small (less than 10%) the difference is negligible. However, the difference between positive and negative errors quickly diverges such that large underpredictions are weighted very high.

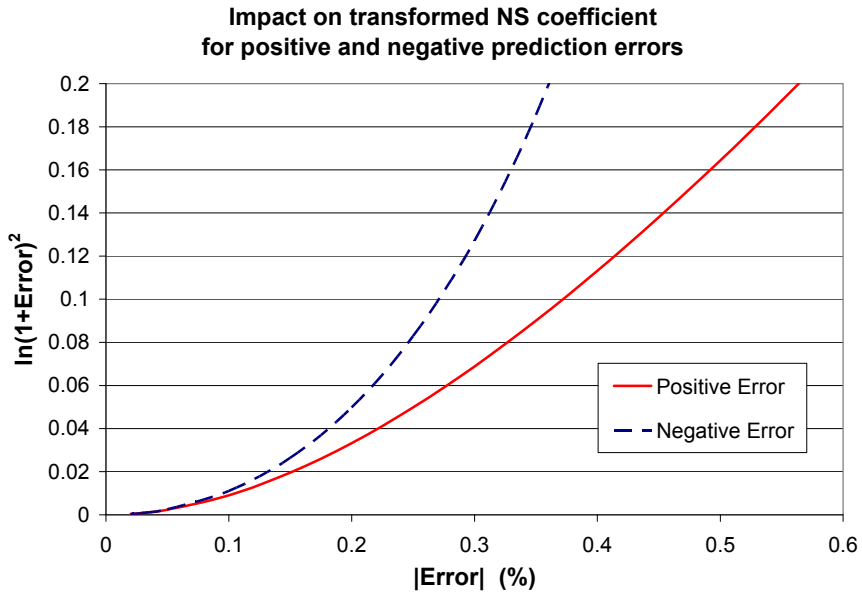

Figure 25 – Sensitivity of the log-transformed Nash Sutcliffe coefficient to over and under predictions

By transforming the data, the effect that each prediction has on the NS coefficient will change. Periods of high flow which were previously given more weight will count for less. Conversely, predictions during low flow periods will have more impact. The flow where the contribution to both coefficients will be the same can be determined where:

$$NS_i = NS_{\ln,i}$$

$$\frac{(\varepsilon \cdot O_i)^2}{Var(O)} = \frac{(\ln[1+\varepsilon])^2}{Var(\ln[O])}$$

$$O_i = \frac{\sigma(O)}{\sigma(\ln[O])} \cdot \frac{(\ln[1+\varepsilon])}{\varepsilon} \qquad 29$$

This is illustrated in Figure 26, where the effect of a 10% prediction error in average weekly flow is shown for both the original and transformed NS coefficients using the values from the calibration period for gauge 02MC001. The transformed and original coefficients

are about the same when the average flow is near 5m^3/s, or approximately (and coincidently) near the mean of the observed values.

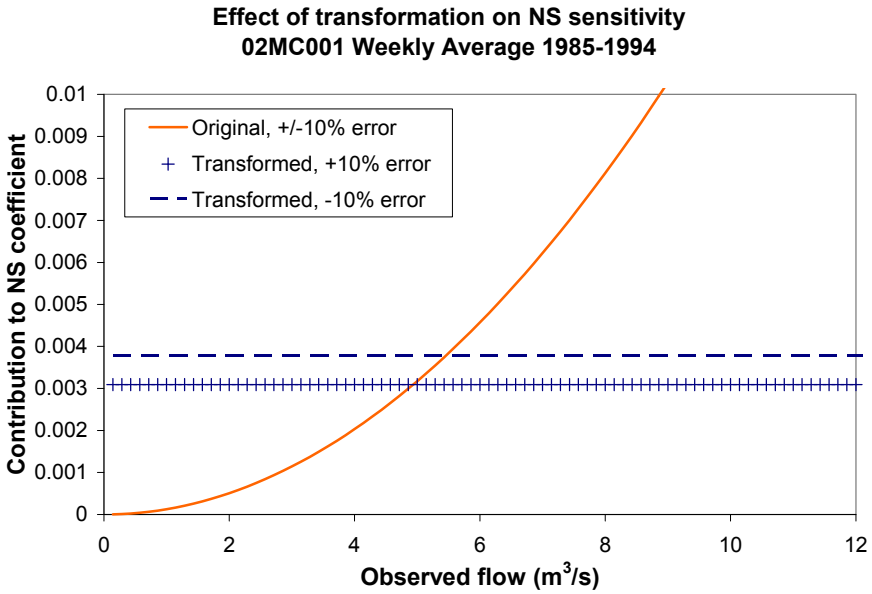

Figure 26 – Sensitivity of the Nash Sutcliffe coefficient (original and log-transformed) to the magnitude of observed flow given a constant (10%) prediction error.

7. Results

Each area of the watershed makes a unique contribution to the balance of runoff, baseflow, ET and recharge in the basin. Identifying the contributions that each subbasin makes to the water balance can highlight areas of environmental significance. The key parameters which influence the water cycle are land cover and soil type. Land cover is one variable which can be easily altered by development or planning policies, so knowledge of the contribution each land cover makes to the water balance in the basin provides useful information on the trade offs that are made when land use changes occur. Soil type is not readily altered, but the model can inform us about how different areas of the watershed with different soil types will impact the water cycle differently.

In this section, model predictions of streamflow are first compared with observed data. Predictions of other water budget components are also examined spatially and temporally. An assessment of the water balance predictions in the context of source water protection planning is presented. Finally, the ability to predict low flow conditions, important for risk assessment and the protection of aquatic species, is also considered.

Streamflow

The model predictions of streamflow were assessed by comparing the results at the location of gauge 02MC001 with observed values. This gauge provides the only series of continuous observed data for the watershed. Cross plots of simulated and observed average weekly flow at gauge 02MC001, as well as the values of NS and mean error for the periods of calibration and validation are given in Figure 27 and Figure 28. Box plots showing the weekly error in predicted flow are given in Figure 29 and Figure 30.

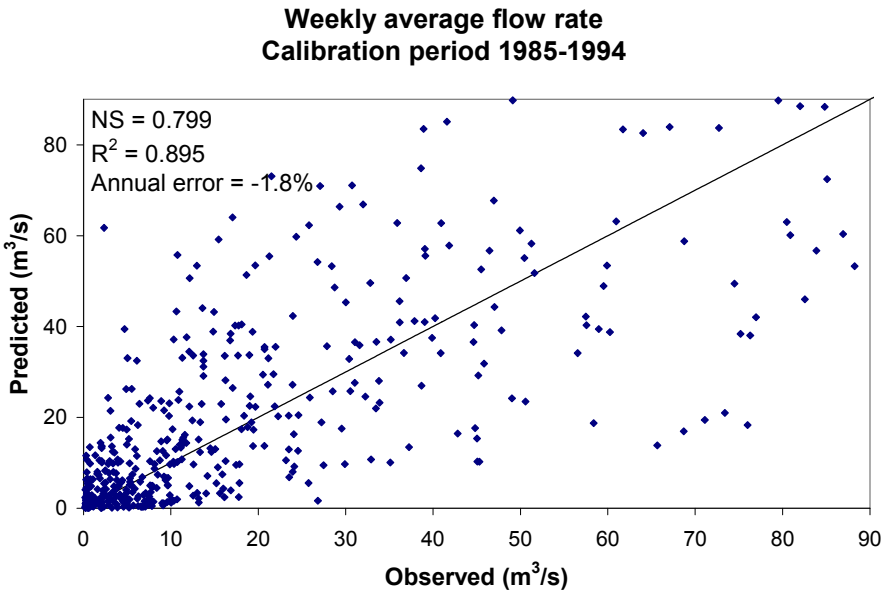

Figure 27 - Weekly average flow at 02MC001, calibration period. Solid line indicates where predicted equals observed.

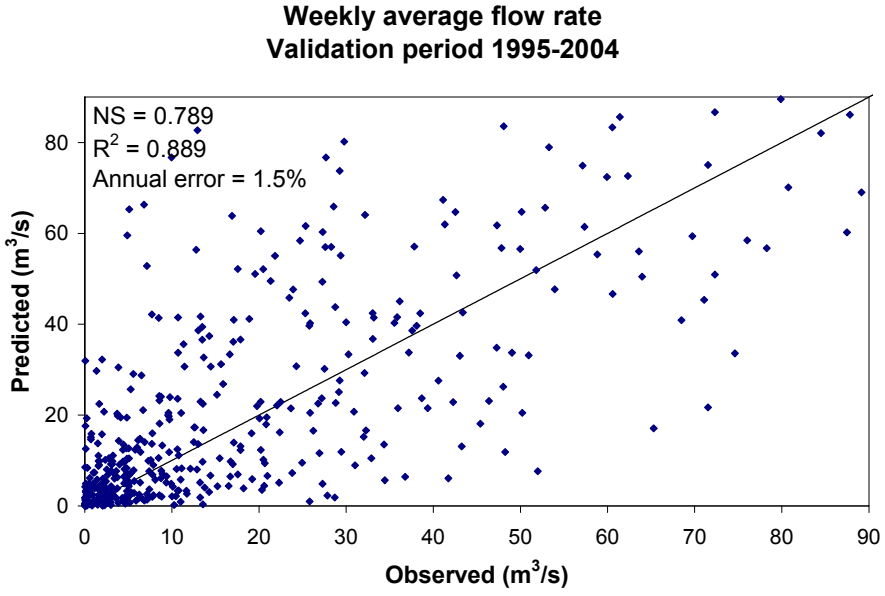

Figure 28 - Weekly average flow at 02MC001, validation period. Solid line indicates where predicted equals observed.

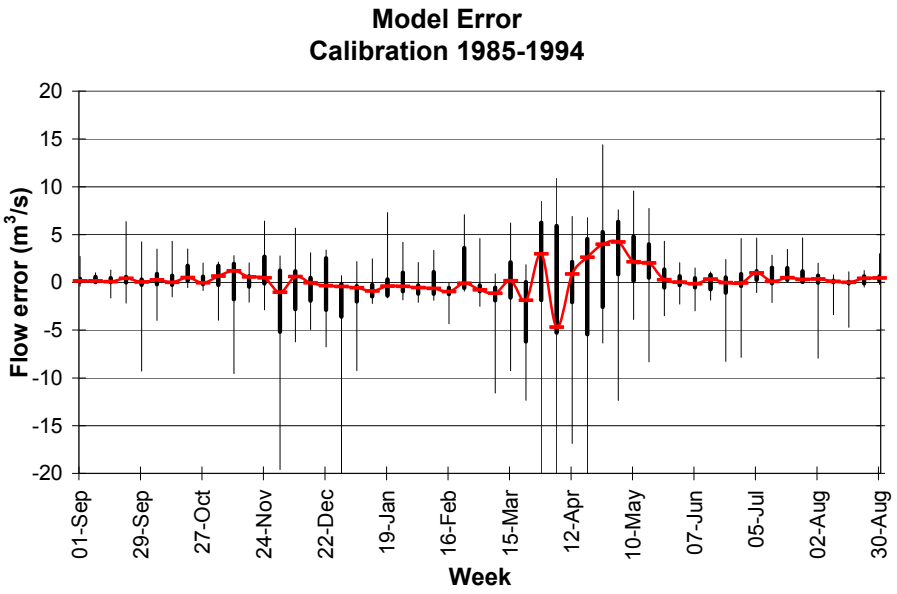

Figure 29 - Weekly model error at 02MC001, calibration period. Boxes illustrate the minimum, first quartile, median, third quartile and maximum weekly prediction error.

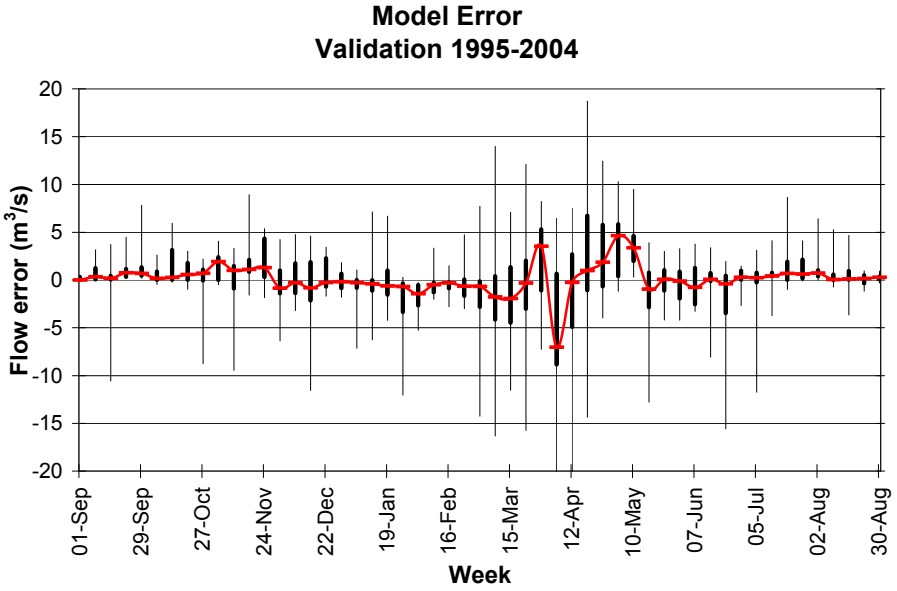

Figure 30 - Weekly model error at 02MC001, validation period. Like the calibration period, prediction errors are greatest during the spring months.

Generally, the median weekly error is very small, suggesting that the model performance is reasonable for most years. During both the calibration and validation period, the model performance is worst during the months of March and April, when snowmelt occurs.

A possible constant source of error is the flow rate reported at the gauge site. Gauge 02MC001, which measures a contributing area of 363km^2, was originally at a point 4.8km downstream of its present location draining an area of 404km^2. The depth to discharge relationship established at the original site is still in use, with no conversion for the different contributing area or possible difference in cross-sectional area[1]. This likely adds some error to the reported values and may have led to incorrectly calibrated parameters.

Two other gauges within the watershed have data which was used to validate the model. Both operate only seasonally, typically from March to May (see Map 5). Gauge 02MC027 has records from 1986 to 1992 and measures a contributing area of 129km^2. Gauge 02MC030 has records from 1986 to 2004 and measures a contributing area of 26km^2. By assessing the model performance at these two sites (i.e. at points different than the calibration site) we can gain some insight into the ability of SWAT to model spatial variability within the watershed. This is tempered by the fact that these gauges record only during the freshet which appears to be the most difficult time period to model.

A comparison of predicted and observed weekly average flow at gauge 02MC027 is shown in Figure 31, representing 64 weeks over the seven years of data. The model tends to overpredict (average error of 14.4%) but the calculated NS of 0.528 suggests the model is a reasonably good predictor.

Records for gauge 02MC030 are sporadic, with many missing data points. It was thus not always possible to determine a weekly average flow at this gauge site. In order to compare our model data, we considered any period where there were continuous records of at least six days in length. This provided 49 periods of average length 6.9 days over the entire 19 year range of data. The average error was -25.0% and NS was 0.308 as shown in Figure 32. It is difficult to assess the validity of these statistics with so many missing data points. However, the numbers are consistent with the simulated hydrograph which appears to under predict peak flows at this site. The spring season of 1990 for which there are the most data points (52) is shown in Figure 33.

[1] Tom Arsenault, Water Survey Canada, personal communication, Dec. 19 2006

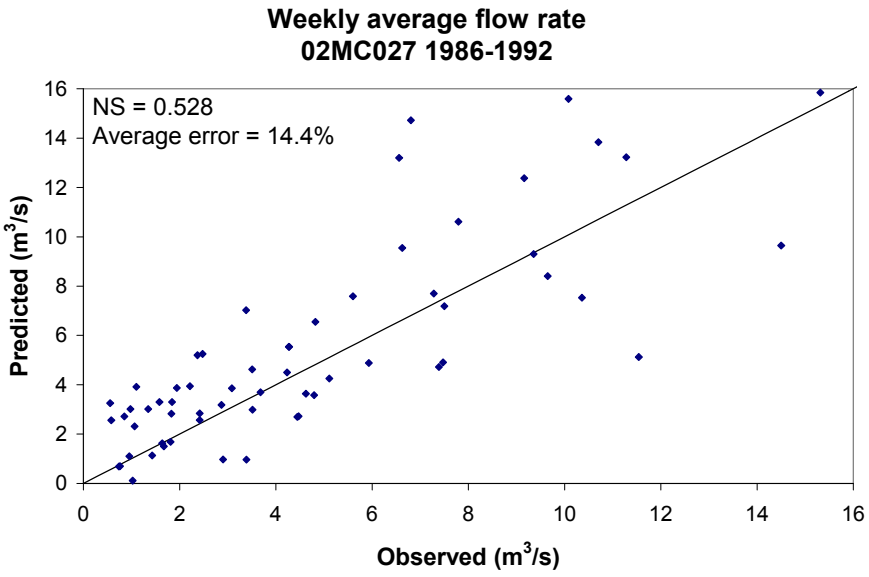

Figure 31 - Weekly flow at 02MC027. Solid line indicates where predicted equals observed.

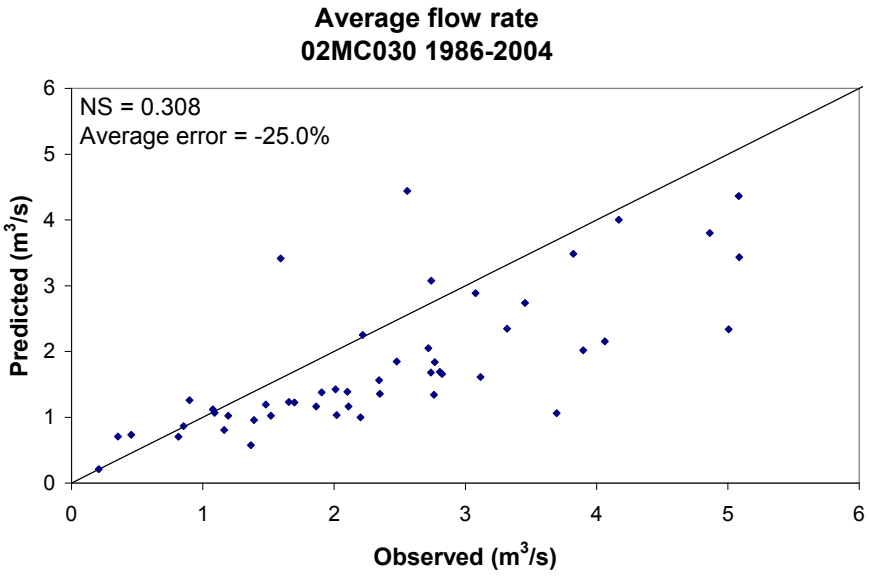

Figure 32 - Weekly flow at 02MC030. Solid line indicates where predicted equals observed.

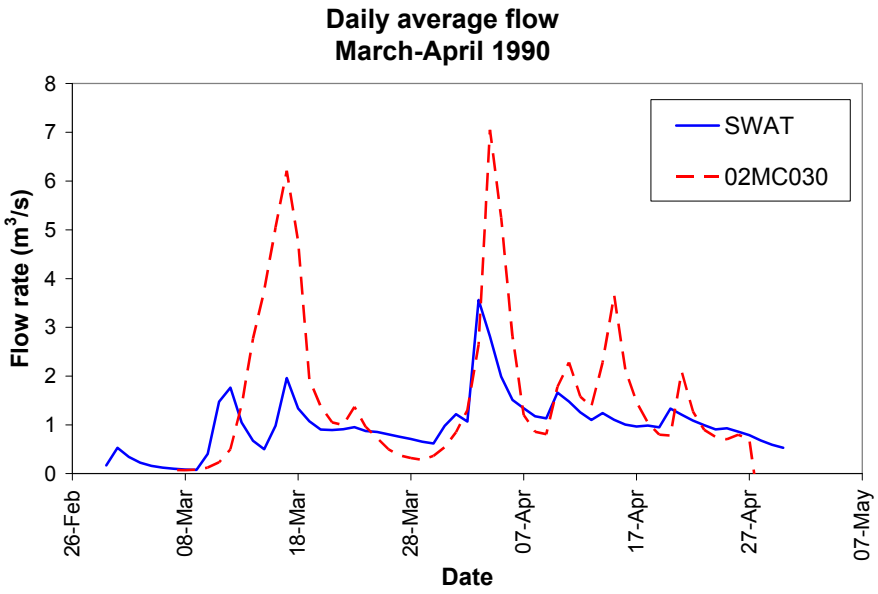

Figure 33 - Hydrograph at 02MC030 for March and April, 1990. Flow peaks at this location are underpredicted by the model.

Some of the underprediction at the location of 02MC030 may be attributable to the ponds and sinks located upstream of it. Within the gauge's contributing area, the model directs roughly 26% of the surface runoff to ponds or inland detention rather than to the stream network. This is notably higher than the amounts found upstream of gauges 02MC001 and 02MC027 (11% and 14% respectively). It is possible that there exists small surface features which would alter the contributing areas of the ponds and sinks. Since this gauge captures a relatively small area compared to the other gauges, a few small topographical differences could have a significant impact. As well, a major highway runs through a portion of this subwatershed, suggesting that there may be detailed anthropogenic changes to the landscape not reflected in the DEM or stream network. More detailed topographical information would be required to account for these potential differences.

Runoff

The portion of streamflow at the location of gauge 02MC001 attributable to runoff was determined using the filter previously described. Predicted and observed average weekly runoff rates are shown in Figure 34. Annual runoff by land use and soil group is shown in

Figure 35. The runoff values are directly related to the curve number coefficients selected for each class.

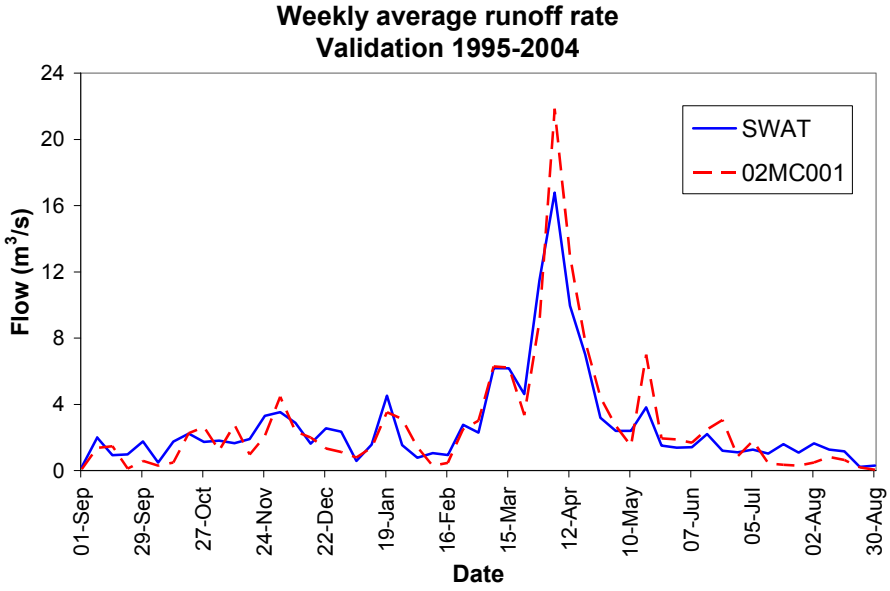

Figure 34 - Weekly average runoff at gauge 02MC001, observed and predicted.

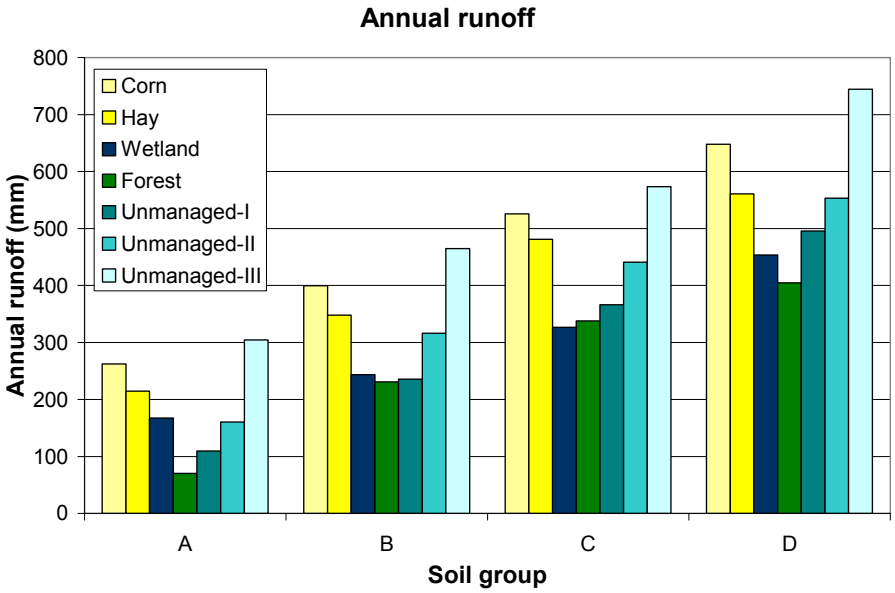

Figure 35 – Predicted annual runoff by land use and soil group

During the summer low flow period, runoff is slightly overpredicted. This is likely due to our increase of CN values in order to obtain satisfactory annual runoff totals. It is also

possible that the model does not sufficiently adjust CN values to account for dry, late summer soil conditions.

Runoff is a clear function of hydrologic group, which is to be expected since the curve numbers were specified based on these groups. Agricultural land and the Unmanaged-III classes produced the most runoff, while the forest and wetland covers produced the least. The land cover seems to be more significant than the hydrologic group: the difference in runoff between the classes is greater than the difference between one soil group.

The model predicts most runoff to be generated from the organic soils located in the northern part of the watershed, and in the lower reaches of the watershed where soils are generally less well drained (Map 9). Much of the area captured by gauge 02MC001 generates lower than average annual runoff, a consequence of the forests and well-drained soils which dominate the watershed.

Baseflow

Baseflow predicted by the model appears more reactive than observed. In autumn, the predicted level of baseflow peaks higher and earlier than observed while winter baseflow is underpredicted. During the freshet, the predicted baseflow peak is also slightly higher than observed, as well as slightly delayed with respect to observed (Figure 36).

Much less is known about the shallow aquifer characteristics such as slope, extent and composition, than about surface features. This limits our ability to model the groundwater system in a more detailed spatial way. As well, other SWAT implementations have identified that the model's simplified groundwater design is limited (Romanowicz et al. 2005, Arabi et al. 2006). Even if our specification of groundwater parameters is sufficiently detailed, the model structure may not be reasonable for this region. The aquifer may also extend outside the watershed which would introduce additional error to our predictions.

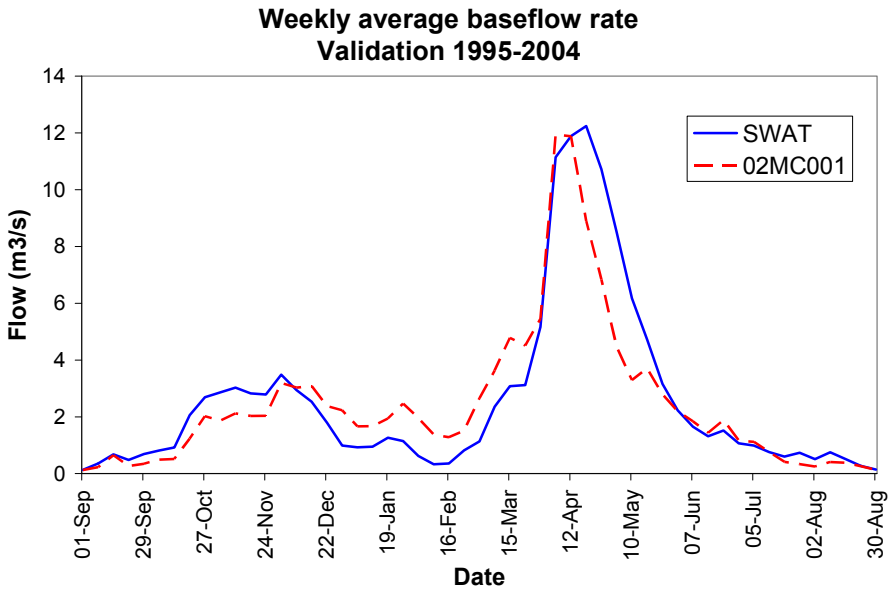

Figure 36 - Weekly average baseflow at 02MC001, predicted and observed

SWAT implements baseflow recession as an exponential decay of storage volume. We can isolate the recession process to periods of no recharge or runoff, such as in winter months when the soil above the aquifer is frozen, or after periods of drought in other times of the year. By observing the natural logarithm of the baseflow during these time periods, we should see a linear decay. However, the observed flow decays at a less than exponential rate suggesting the model structure is incorrect, or that the aquifer is being continually recharged. It is possible that wetlands located in the headwaters of the watershed do not completely freeze in the winter, thus continually recharge the aquifer. If so, the underprediction of baseflow in the winter we observe would reflect the model's failure to account for this.

Snowmelt

Runoff induced from snowmelt is a clear limitation of the SWAT model. At this time of year the flow rates and flow variability are very high. The absolute error of the model has much greater variation in this period of the year than any other.

This limitation of the model was also highlighted by Benaman et al. (2005) who implemented SWAT for a watershed with similar winter characteristics. Wang and Melesse (2005) undertook an evaluation of SWAT in another snowmelt-dominated watershed and

determined that model performance was quite poor when the snowfall received during the season was less than normal.

SWAT does not take in consideration factors such as solar radiation or wind which affects the amount of melt occurring. As well, the river in this study is subject to ice jams during the melt season which can dramatically alter the reported flow rate during the spring: the model does not account for such occurrences. Dunne and Leopold (1978) outline a physically-based, energy balance method for calculating snowmelt which is shown to have a marked improvement over the degree-day method. The energy balance method has been implemented in other watershed models such as HSP-F (Bicknell et al. 1997), but the climate data required to use this method is substantial.

Evapotranspiration

The average monthly potential evapotranspiration (PET) predicted by the model for the validation period is shown in Figure 37, along with estimates of PET derived using the Thornthwaite method (MacIver and Isaac 1989) and the Penman method (CCN 2004) for the Cornwall region. The simulated values, derived using the Priestley Taylor method (1972), amounted to 603mm per year. The Thornthwaite equation, based solely on daily air temperature, estimates 585mm PET per year. The Penman method utilises average temperature, wind speed, solar radiation and humidity to predict 676mm of PET. The Thornthwaite and modeled values are comparable in magnitude, but the Thornthwaite estimates are slightly delayed in the season.

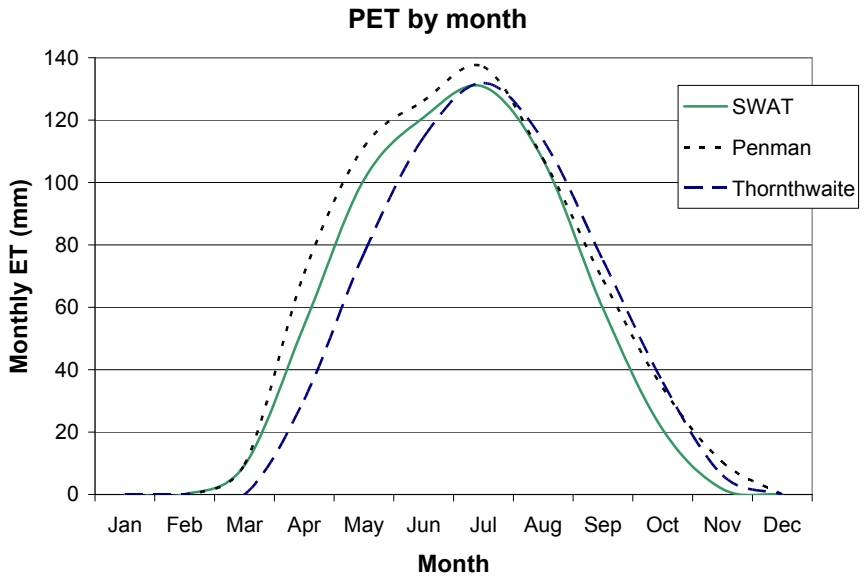

Figure 37 - Monthly estimated PET for the watershed.

Actual ET is highest for the forest and wetland land covers which come close to satisfying the PET demand (Figure 38), while agricultural land exhibits less ability to satisfy PET demands (Figure 39). This inability to satisfy the PET becomes more pronounced in the poorly drained soils. As shown above, the poorly drained soils have been defined to have higher runoff coefficients, and thus less precipitation is predicted to infiltrate into the soil.

ET predictions are sensitive to the climate input and the difference in temperature data between the two climate stations is apparent in the map of annual ET (Map 10). The subbasins in the north west utilising data from the Avonmore station exhibit a lower annual ET than the rest of the basin. This discrete difference in ET prediction highlights the limitations of the Thiessan methodology and the potential benefits of increasing the spatial density of climate stations.

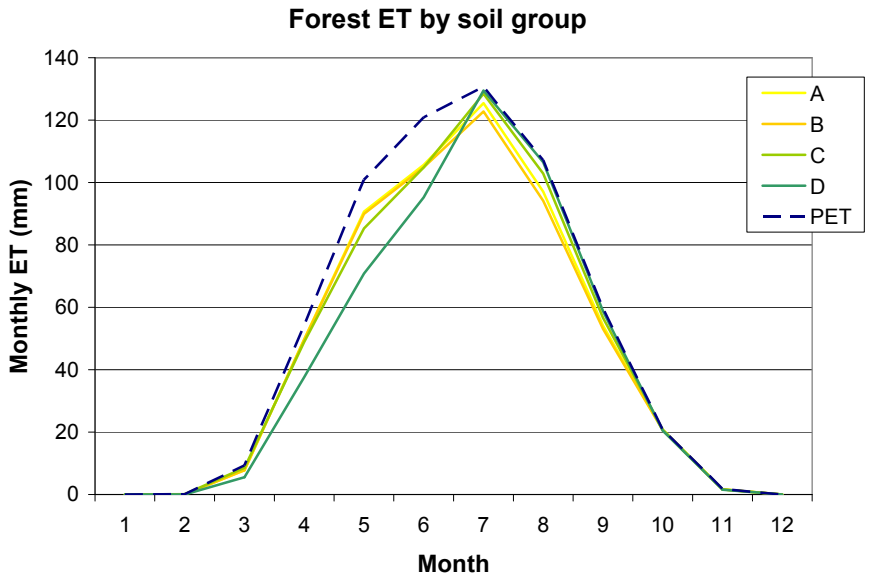

Figure 38 – Monthly model predicted actual ET for forest

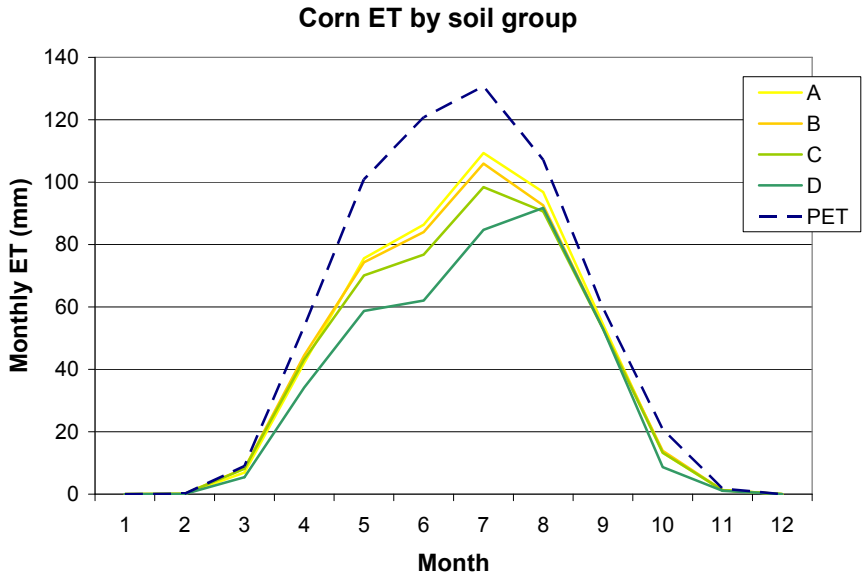

Figure 39 – Monthly model predicted actual ET for corn

Recharge

The average annual deep aquifer recharge is shown for each land use and soil group in Figure 40. Recharge is primarily dependent on CN and infiltration rate, both of which dictate the amount of water reaching the aquifer.

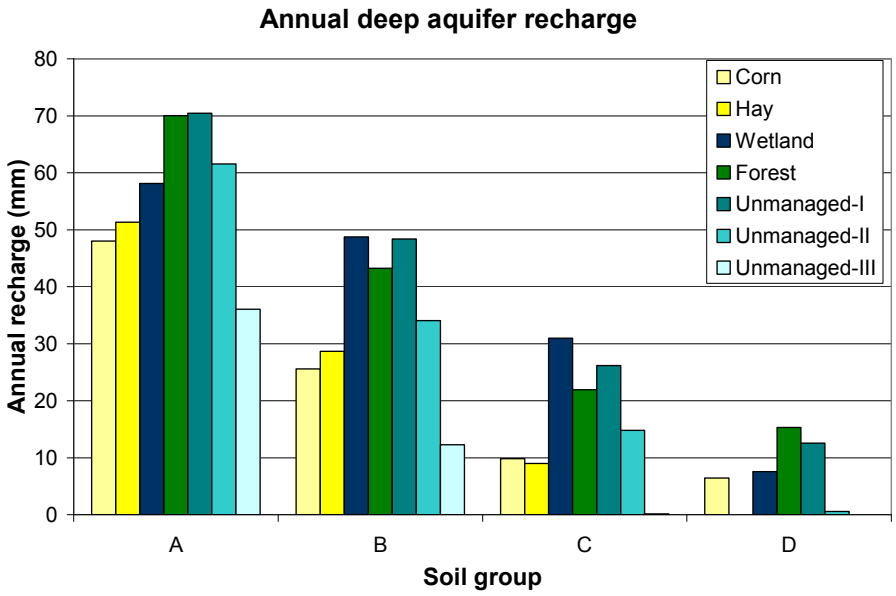

Figure 40 – Predicted annual deep aquifer recharge by land cover and soil group

These numbers must be considered in the context of the areal distribution of soils and land use within the basin (Figure 6). Soil group A makes up the largest part of the watershed (52%). This, combined with its strong contribution to recharge, means that these lands account for 78% of the recharge in the watershed. Conversely, soil group D makes up 17% of the watershed area, but only 5% of the total recharge. The distribution of recharge by subbasin is highlighted in Map 11.

Unlike runoff, the impact of land use on recharge changes throughout the year. In the spring, the dominant contributions come from the forest and unmanaged-I land covers, with the agricultural contribution much lower. However, in the fall agricultural land contributes as much to recharge as the other land use classes (Figure 41). The spring event is the dominant annual event, thus on an annual basis forest contributes the most to recharge.

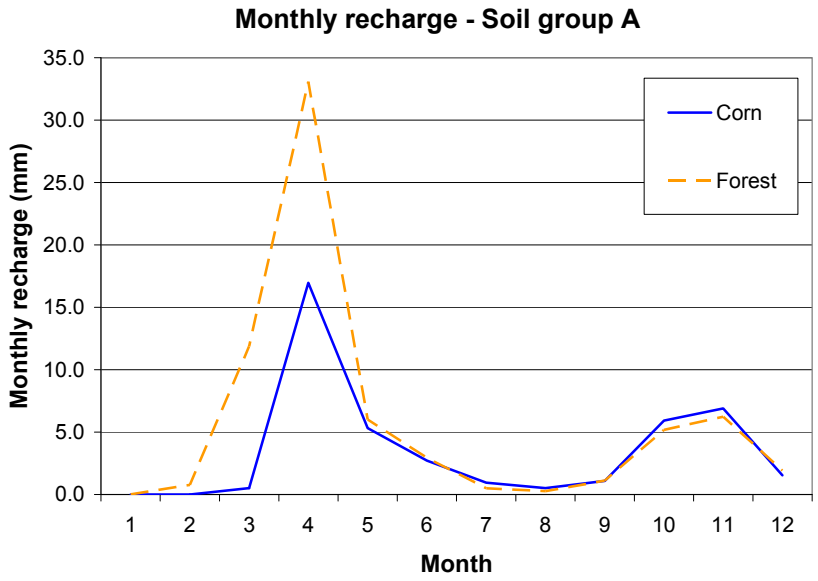

Figure 41 – Model predicted average monthly recharge for soil group A

Water budget and supply

The average annual amounts of the main water budget components over the area of the watershed are shown in Figure 42. Average annual values provide a starting point for a more detailed assessment of available water supply. In the Ontario SPP development process (MOE 2006), groundwater recharge levels are initially analysed on an annual basis. However, surface flow – by nature a faster process than recharge – is initially assessed at a monthly level. More detailed assessment considers shorter time intervals to highlight specific periods with a higher potential threat to availability.

Provincial guidelines for SPP surface flow quantity assessment require initial analysis to be undertaken using median monthly values and more detailed analysis at the weekly level. The use of minimum seven-day moving average (7Q) values is recommended to quantify annual low flow periods. Surface water is not used as a potable water source within the Raisin River watershed, thus the need to assess surface flow for this basin within the SPP framework is reduced. However, the SWAT model implemented does provides sufficient detail to perform an analysis of surface water supply were it required. Weekly flow data indicates that the model overpredicts on average during the summer low flow season (Figure

30), but the mean 7Q flow is less than observed (Figure 43). This is in agreement with our previous observation that the predicted flow seems to be more dynamic than the observed flow.

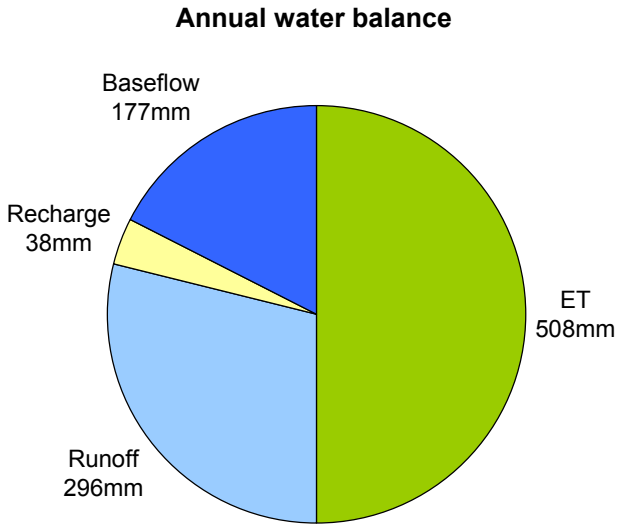

Figure 42 – Model predicted annual water balance for the watershed

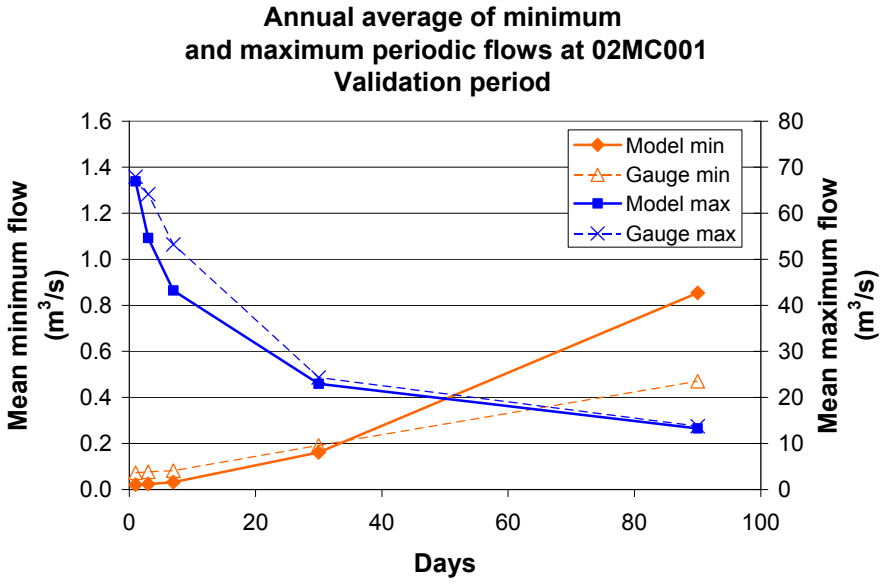

Figure 43 – Annual average periodic minimum and maximum flows at 02MC001

Prediction of flow peaks or low flow levels is not specifically captured by the NS coefficient used for calibration and validation. The coefficient is particularly insensitive to low flow conditions, as detailed in Chapter 6. For the model to reasonably predict low flow conditions, it must be calibrated to do so. Given the limitations of the NS coefficient in this regard, the calibration process undertaken is not appropriate for modeling the minimum surface water availability. A different measurement, such as the range of variability approach (RVA) (Richter et al. 1997) must be used to capture the extreme conditions of the streamflow regime.

The RVA uses several streamflow characteristics which provide insight into the parts of the flow regime masked by the NS coefficient. The range of variability in streamflow is measured by the number, duration and magnitude of flow pulses and recessions. Annual average peak and minimum flows for various time periods have been shown in Figure 43 and flow pulse frequency and duration are given in Table 10. We see that the SWAT model has predicted a greater number of peaks and recessions of shorter duration than observed at the stream gauge. At the same time, the model predicts smaller flow peaks and, for short durations, lower minimum flow rates. These measures also indicate that the model is too dynamic and, as calibrated, may not be suitable for precise estimation of minimum flow levels and periods.

Annual average (1995-2004)	SWAT	02MC001
High pulses (highest quartile)	12.9	9.4
High pulse duration (days)	7.5	12.1
Low pulses (lowest quartile)	11.6	4.0
Low pulse duration (days)	7.4	36.0

Table 10 - Flow pulse characteristics at 02MC001, predicted and observed

Due to the number of measurement values used by the RVA, it cannot be used directly with a calibration process that relies on maximising a single value. However, the approach could be used to place further constraints on the calibration process, which may in turn improve the model performance for particular surface flow regimes.

The Ontario SPP process requires initial analysis of groundwater supply and availability to be based on annual estimations of recharge. Additionally, the identification of areas with

significant surface – groundwater interaction (i.e. high levels of recharge) is necessary. The SWAT model as implemented generates this information. Key recharge areas, primarily forest land, have been identified. The impact of changes to land use on annual recharge levels can be assessed with the information presented. However, we are unable to directly validate recharge predictions due to the lack of independently observed data. As well, the effect or contribution of areas outside the watershed to the aquifer has not been investigated in this study. To gain greater certainty or to perform recharge analysis at a more detailed spatial or temporal scale would require the implementation of a more detailed groundwater model.

8. Conclusions and Summary

The SWAT model implemented for the Raisin River watershed provides a means to assess the hydrology of the basin spatially and temporally. Modeling was facilitated by existing data sources without the need for extensive field data collection. The methodology described permits other regions to implement the model using the same data sources, as well as generate information useful in the development of source water protection plans. The specific objectives of this thesis have been achieved:

1. An implementation of a calibrated and validated SWAT model has been presented. A sensitivity analysis of model parameters has been undertaken.
2. The data used for modeling comes from standardised national data. This, along with the methodology described, would permit this study to be easily replicated for other watersheds.
3. Limitations of the SWAT model, specifically related to snowmelt and groundwater predictions, have been described and their impact on the model results quantified. The limitations of a the Nash Sutcliffe coefficient to measure model performance is also quantified.
4. The results as presented can be used directly in the development of source protection plans

The streamflow predicted at the location of gauge 02MC001 is comparable to observed data and thus we have high confidence in the model to predict these values. Inconsistent results at other stations and the lack of other continuous stream flow data sets limit our certainty that the model is equally accurate across the watershed. Other indications that the model may not be consistent are the parameter values determined during calibration. CN values needed to be increased substantially to sufficiently account for snowmelt. This in turn led to the substantial increases in available water content values in an attempt to reduce runoff during the summer months.

The modeling of the snowmelt period is the most significant limitation of the model. This time of year brings the highest flows and greatest flood risks to the region. It is also the time when most of the erosion and sediment movement occurs within the watershed. Implementation of a snowmelt process which accounts for other climatic factors, particularly solar radiation, would likely improve the performance of the model. Data for a region near to the Raisin River (Dunne and Leopold 1978) shows marked improvement in snowmelt predictions when a degree-day approach is replaced with an energy based approach. A key barrier to implementing this would be the need for daily solar radiation values which are not currently measured (or predicted) at most Canadian climate stations. While such values might be easily synthesised based on historical conditions, the use of synthetic data may limit the ability to validate the model against observed conditions. Nevertheless, the climate data used in this model implementation appears insufficient to accurately predict snowmelt. More information would be needed to improve the model performance during the spring period.

Other components of the model are also sensitive to the climate data available. For example, predictions of evapotranspiration highlight the use of two distinct temperature gauges. PET is notably less in the north west region of the basin where data from the Avonmore climate station was used. The sensitivity of PET predictions to temperature highlights the need to use accurate climate data for all parts of the watershed. Just as the temperature measurements from the two climate stations are different but highly correlated, it may be possible with additional gauges to quantify the temperature variation within the basin. This information would improve the spatial hydrologic predictions of the model.

The region's potable water is sourced from groundwater. Proper assessment of the groundwater supply would require more detailed knowledge of the aquifer. In particular, the extent to which the aquifer is affected by areas outside of the watershed should be investigated. Any attempt to calibrate or validate the groundwater portion of the model (e.g. using well drilling records) would require a more precise groundwater model structure.

New legislation in Ontario has created a requirement to develop a source protection plan which would comprehensively assess this water supply. The SWAT model as implemented provides some of the key information required of a SPP. The Raisin River watershed was described in terms of its surface features, topography and climate. The SWAT model

quantified the runoff, baseflow, recharge and evapotranspiration on a daily basis throughout the basin. We have analysed surface flow at a weekly level and recharge on a monthly basis. The impact of land use and soil type on the components of the hydrologic cycle were investigated.

Assessment of surface water supply must consider periods when availability is at its lowest. The process by which this and other hydrologic models are often calibrated makes use of a single metric to quantify the model performance over the entire period of simulation. However, the commonly used Nash Sutcliffe coefficient does not capture the model behaviour during low flow periods. The coefficient may be altered to place greater weight on these periods of interest. Alternately, a greater number of constraints may be placed on the model during calibration in order to encourage better model behaviour during low flow conditions. A consistent set of objectives for model performance should be developed if the use of watershed models is to be part of the SPP development process. Consistent objectives will help ensure that water quantity assessments are made with a similar level of accuracy and certainty throughout the process.

9. References

Abbott, M.B., Bathurst, J.C., Cunge, J.A., O'Connell, P.E., Rasmussen, J. 1986. "An introduction to the European Hydrological System – Systeme Hydrologique Europeen, "SHE", 2: Structure of a physically-based, distributed modelling system" Journal of Hydrology, 87 p61-77

Al-Abed, N. A., Whiteley, H. R. 2002. "Calibration of the Hydrological Simulation Program Fortran (HSPF) model using automatic calibration and geographical information systems." Hydrological Processes, 36 p3169-3188

ASCE Task Committee on Definition of Criteria for Evaluation of Watershed Models of the Watershed Management Committee, Irrigation and Drainage Division. 1993. "Criteria for evaluation of watershed models" Journal of Irrigation and Drainage Engineering, 119 p429-442

Arabi, M., Govindaraju, R.S., Sophocleous, M., Koelliker, J.K. 2006. "Use of distributed models for watershed management: case studies" in Watershed Models V.P Singh and D.K. Frevert, eds. CRC.

Arnold, J. G., Allen, P. M. 1996. "Estimating hydrologic budgets for three Illinois watersheds." Journal of Hydrology, 176 p57-77

Arnold, J. G., Muttiah, R. S., Srinivasan, R., Allen, P. M. 2000. "Regional estimation of base flow and groundwater recharge in the Upper Mississippi river basin." Journal of Hydrology, 227 p21-40

Arnold, J.G., Williams, J.R. 1995. "SWRRB – A watershed scale model for soil and water resources management" in Computer models of watershed hydrology Water Resources Publications, Colorado.

Arnold, J.G., Williams, J.R., Maidment, D.R. 1995. "Continuous-time water and sediment-routing model for large basins" Journal of Hydraulic Engineering, 121 p171-183

Aspinall, R., Pearson, D. 2000. "Integrated geographical assessment of environmental condition in water catchments: linking landscape ecology, environmental modelling and GIS" Journal of Environmental Management, 59 p299-319

Attwood, J.D., McCarl, B., Chen, C-C., Eddleman, B.R., Nayda, B., Srinivasan, R. 2000. "Assessing regional impacts of change: linking economic and environmental models" Agricultural Systems, 63 p147-159

Bärlund, I., Kirkkala, T., Malve, O., Kämäri, J. 2007. "Assessing SWAT model performance in the evaluation of management actions for the implementation of the Water Framework Directive in a Finnish catchment" Environmental Modelling and Software, 22 p719-724

Bekele, E.G., Nicklow, J.W. 2005. "Multiobjective management of ecosystem services by integrative watershed modeling and evolutionary algorithms" Water resources research, 41, W10406

Benaman, J., Shoemaker, C.A. 2005. "An analysis of high flow sediment event data for evaluating model performance" Hydrological Processes, 19 p605-620

Benaman, J., Shoemaker, C.A., Haith, D.A. 2005. "Calibration and Validation of Soil and Water Assessment Tool on an agricultural watershed in upstate New York" Journal of Hydrologic Engineering, 10 p363-374

Bicknell, B.R., Imhoff, J.C., Kittle, J.L., Jr., Donigian, A.S., Jr., and Johanson, R.C. 1997. Hydrological Simulation Program--Fortran, User's manual for version 11 U.S. Environmental Protection Agency, National Exposure Research Laboratory, Athens, Ga., EPA/600/R-97/080

Bingner, R. L., Garbrecht, J., Arnold, J. G., Srinivasan, R. 1997. "Effect of watershed subdivision on simulation runoff and fine sediment yield." Transactions of the ASAE, 40 p1329-1335

Bingner, R., Theurer, F.D. 2001. AnnAGNPS Pollutant Loading Model United States Department of Agriculture Agricultural Research Service. Retrieved April 10, 2007 from http://www.ars.usda.gov/Research/docs.htm?docid=5222

Borah, D.K., Bera, M. 2003. "Watershed-scale hydrologic and nonpoint-source pollution models: review of mathematical bases" Transactions of the ASAE, 46 p1553-1566.

Borah, D.K., Bera, M. 2004. "Watershed-scale hydrologic and nonpoint-source pollution models: review of applications" Transactions of the ASAE, 47 p789-803.

Box, G.E.P., Cox, D.R. 1964. "An analysis of transformations" Journal of the Royal Statistical Society, Series B, 26 p211-252.

Bradford, A., Maude, S. "Achieving ecological integrity on the Oak Ridges Moraine: Towards ecologically relevant water management" University of Guelph. http://www.soe.uoguelph.ca/webfiles/abradfor/Assets/Text/ORM%20Paper.pdf Accessed April 10, 2007.

Burton, J. 2003. Integrated Water Resources Management on a Basin Level Institut de l'energie et de l'environnement pour la Francophonie. UNESCO.

Cao, W., Bowden, W. B., Davie, T., Fenemor, A. 2006. "Multi-variable and multi-site calibration and validation of SWAT in a large mountainous catchment with high spatial variability." Hydrological Processes, 20 p1057-1073

Chaplot, V. 2005. "Impact of DEM mesh size and soil map scale on SWAT runoff, sediment, and NO3-N loads predictions." Journal of Hydrology, 312 p207-222

Chaplot, V., Saleh, A., Jaynes, D. B. 2005. "Effect of the accuracy of spatial rainfall information on the modeling of water, sediment, and NO3-N loads at the watershed level." Journal of Hydrology, 312 p223-234

Chaubey, I., Cotter, A. S., Costello, T. A., Soerens, T. S. 2005. "Effect of DEM data resolution on SWAT output uncertainty" Hydrological Processes, 19 p621-628

Chen, E., Mackay, D. S. 2004. "Effects of distribution-based parameter aggregation on a spatially distributed agricultural nonpoint source pollution model." Journal of Hydrology, 295 p211-224

Cherrill, A. J., Lane, A., Fuller, R. M. 1994. "The use of classified Landsat-5 Thematic Mapper imagery in the characterization of landscape composition: a case study in northern England." Journal of Environmental Management, 40 p357-377

Chica-Olmo, M., Abarca-Hernandez, F. 2000. "Computing geostatistical image texture for remotely sensed data classification." Computers and Geosciences, 26 p373-383

Chu, T-W., Shirmohammadi, A. 2004. "Evaluation of the SWAT model's hydrography component in the piedmont physiographic region of Maryland." Transactions of the ASAE. 47 p1057-1073

Cihlar, J., Guindon, B., Beaubien, J., Latifovic, R., Peddle, D., Wulder, M., Fernandes, R., Kerr, J. 2003. "From need to product: a methodology for completing a land cover map of Canada with Landsat data." Canadian Journal of Remote Sensing, 29 p171-186

Cihlar, J., Okouneva, G., Beaubien, J., Latifovic, R. 2001. "A new histogram quantization algorithm for land cover mapping." International Journal of Remote Sensing, 22 p2151-2169

Coffey, M. E., Workman, S. R., Taraba, J. L., Fogle, A. W. 2004. "Statistical Procedures for Evaluating Daily and Monthly Hydrologic Model Predictions." Transactions of the ASAE, 47 p59-68

Cosh, M. H., Jackson, T. J., Bindlish, R., Prueger, J. H. 2004. "Watershed scale temporal and spatial stability of soil moisture and its role in validating satellite estimates." Remote Sensing of Environment, 92 p424-435

Crawford, N.H., Linsley, R.K. 1966. Digital simulation in hydrology: Stanford Watershed Model IV Stanford University Technical Report No. 39. Stanford University, California.

Crist, E.P., Kauth, R.J. 1986. "The Tasseled Cap de-mystified" Photogrammetric Engineering and Remote Sensing, 52 p81-86

Di Luzio, M., Arnold, J. G., Srinivasan, R. 2005. "Effect of GIS data quality on small watershed stream flow and sediment simulations" Hydrological Processes, 19 p629-650

Du, B., Arnold, J. G., Saleh, A., Jaynes, D. B. 2005. "Development and application of SWAT to landscapes with tiles and potholes" Transactions of the ASAE, 48 p1121-1133.

Duda, T., Canty, M. 2002. "Unsupervised classification of satellite imagery: Choosing a good algorithm" International Journal of Remote Sensing, 23 p2193-2212

Dunne, T., Leopold, L.B. 1978. Water in environmental planning W.H. Freeman, San Francisco

Dymond, C. C., Mladenoff, D. J., Radeloff, V. C. 2002. "Phenological differences in tasseled cap indices improve deciduous forest classification." Remote Sensing of Environment, 80 p460-472

Eckhardt, K., Arnold, J. G. 2001. "Automatic calibration of a distributed catchment model." Journal of Hydrology, 251 p103-109

Eckhardt, K., Breuer, L., Frede, H. G. 2003. "Parameter uncertainty and the significance of simulated land use change effects." Journal of Hydrology, 273 p164-176

Eckhardt, K., Fohrer, N., Frede, H-G. 2005. "Automatic model calibration" Hydrological Processes, 19 p651-658

Eckhardt, K., Ulbrich, U. 2003. "Potential impacts of climate change on groundwater recharge and streamflow in a central European low mountain range." Journal of Hydrology, 284 p244-252

El-Nasr, A.A.., Arnold, J.G., Feyen, J., Berlamont, J. 2005. "Modelling the hydrology of a catchment using a distributed and semi-distributed model" Hydrological Processes, 19 p573-587

Emerson, J.D., Strenio, J. 1983. "Box plots and batch comparision" in Understanding Robust and Exploratory Data Analysis, D.C. Hoagin, F. Mosteller and J.W. Tukey, eds. John Wiley and Sons, New York.

FitzHugh, T. W., Mackay, D. S. 2000. "Impacts of input parameter spatial aggregation on an agricultural nonpoint source pollution model." Journal of Hydrology, 236 p35-53

Fontaine, T.A., Cruickshank, T.S., Arnold, J.G., Hotchkiss, R.H. 2002. "Development of a snowfall-snowmelt routine for mountainous terrain for the soil water assessment tool (SWAT)" Journal of Hydrology, 262 p209-263

Goetz, S. J., Wright, R. K., Smith, A. J., Zinecker, E., Schaub, E. 2003. "IKONOS imagery for resource management: tree cover, impervious surfaces, and riparian buffer analyses in the mid-Atlantic region." Remote Sensing of Environment, 88 p195-208

Grayson, R., Blöschl, G. 2000. "Spatial modelling of catchment dynamics" in Spatial Patterns in Catchment Hydrology: Observations and Modelling Cambridge University Press, Cambridge.

Grayson, R., Moore, I., McMahon, T.A. 1992. "Physically based hydrological modeling: 2. Is the concept realistic?" Water Resources Research, 26 p2659-2666

Grizzetti, B., Bouraoui, F., Granlund, K., Rekolainen, S., Bidoglio, G. 2003. "Modelling diffuse emission and retention of nutrients in the Vantaanjoki watershed (Finland) using the SWAT model" Ecological Modelling 169 p25-38

Haapanen, R., Ek, A. R., Bauer, M. E., Finley, A. O. 2004. "Delineation of forest/nonforest land use classes using nearest neighbout methods." Remote Sensing of Environment, 89 p265-271

Hargreaves, G.L., Hargreaves, G.H., Riley, J.P. 1985. "Agricultural benefits for Senegal River Basin" Journal of Irrigation and Drainage Engineering, 111 p113-124

Havnø, K., Madsen, M.N., Dørge, J. 1995. "MIKE 11 – A Generalized river modelling package" in Computer models of watershed hydrology V.P.Singh (ed.), Water Resources Publications, Colorado.

Hernandez, M., Miller, S. N., Goodrich, D. C., Goff, B. F., Kepner, W. G., Edmonds, C. M., Jones, K. B. 2000. "Modeling runoff response to land cover and rainfall spatial variability in semi-arid watersheds." Environmental Monitoring and Assessment, 64 p285-298

Heuvelmans, G., Muys, B., Feyen, J. 2006. "Regionalisation of the parameters of a hydrological model: Comparison of linear regression models with artificial neural nets." Journal of Hydrology, 319 p245-265

Hill, M.C. 1998. Methods and guidelines for effective model calibration U.S. Geological Survey, Water Resources Investigations Report 98-4005. Denver, Colorado.

Jayakrishnan, R., Srinivasan, R., Santhi, C., Arnold, J.G. 2005. "Advances in the application of the SWAT model for water resources management". Hydrological Processes, 19 p749-762.

Jetten, V., Govers, G., Hessel, R. 2003. "Erosion models: quality of spatial predictions" Hydrological Processes, 17 p887-900

Jobin, B., Beaulieu, J., Grenier, M., Belanger, L., Maisonneuve, C., Bordage, D., Filion, B. 2003. "Landscape changes and ecological studies in agricultural regions, Quebec, Canada." Landscape Ecology, 18 p575-590

Kang, M.S., Park, S.W., Lee, J.J., Yoo, K.H. 2006. "Applying SWAT for TMDL Programs to a small watershed containing rice paddy fields." Agricultural Water Management v79 p72-92

Kerr, J., Cihlar, J. 2003. "Land use and cover with intensity of agriculture for Canada from satellite and census data." Global Ecology and Biogeography, 12 p161-172

Kinnell, P.I.A. 2004a. "Letter to the Editor on 'The mathematical integrity of some Universal Soil Loss Equation variants'" Soil Science Society of America Journal, 68 p336-337

Kinnell, P.I.A. 2004b. "Sediment delivery ratios: A misaligned approach to determining sediment delivery from hillslopes" Hydrological Processes, 18 p3191-3194

Knisel, W.G. 1982. "Systems for evaluating nonpoint source pollution: an overview" Mathematics and Computers in Simulation, 24 p173-184

Latifovic, R., Zhu, Z.-L., Cihlar, J., Giri, C., Olthof, I. 2004. "Land cover mapping of North and Central America - Global Land Cover 2000." Remote Sensing of Environment, 89 p116-127

Legates, D.R., McCabe, G.J. 1999. "Evaluating the use of 'goodness of fit' measures in hydrologic and hydroclimatic model validation" Water Resources Research, 35 p233-241

Leonard, R.A., Knisel, W.G., Still, D.A. 1987. "GLEAMS: Groundwater loading effects on agricultural mamangement systems" Transactions of the ASAE, 30 p1403-1428

Marzen, L.J., Harrington Jr., J.A., Bhuyan, S.J., Koelliker, J.K. 2000. "Use of satellite imagery to determine land cover input variables in an AGNPS water quality model" ASAE International Meeting, Milwaukee. Paper 002200.

Mein, R.G., Larson, C.I. 1973. "Modeling infiltration during a steady rain" Water Resources Research, 9 p384-394

MOE. 2006. Assessment report: Draft Guidance Modules. Toronto, Ontario Ministry of the Environment, October 2006. Retrieved April 10, 2007 from http://www.ene.gov.on.ca/envision/water/cwa-guidance.htm

Monteith, J.L. 1965. "Evaporation and the environment" In The state and movement of water in living organisms. XIXth Symposium. Society for Exp. Biol., Swansea. Cambridge University Press.

Muleta, M.K., Nicklow, J.W. 2005. "Sensitivity and uncertainty analysis coupled with automatic calibration for a distributed watershed model" Journal of Hydrology, 306 p127-145

Muttiah, R. S., Wurbs, R. A. 2002. "Scale-dependent soil and climate variability effects on watershed water balance of the SWAT model." Journal of Hydrology, 256 p264-285

Nash, J.E., Sutcliffe, I.V. 1970. "River flow forcasting through conceptual models: Part 1 – A discussion of principles" Journal of Hydrology, 10 p282-290

Neitsch, S.L., Arnold, J.G., Kiniry, J.R., Williams, J.R., King, K.W. 2002. Soil and Water Assessment Tool: Theoretical Documentation Grassland Soil and Water Research Laboratory, Temple, Texas.

Nelson. R.G., Ascough II, J.C., Langemeier, M.R. 2006. "Environmental and economic analysis of switchgrass production for water quality improvement in northeast Kansas" Journal of Environmental Management 79 p336-347

O'Connor, D.R. Part 2: Report of the Walkerton Inquiry: A Strategy for Safe Drinking Water. Ontario Ministry of the Attorney General, Queen's Printer. 2002.

Oetter, D. R., Cohen, W. B., Berterretche, M., Maiersperger, T. K., R.E., K. 2000. "Land cover mapping in an agricultural setting using multiseasonal Thematic Mapper data." Remote Sensing of Environment, 76 p139-155

Ontario. Conservation Authorities Act. R.S.O. 1990, c.C.27

Ontario. Clean Water Act, 2006. S.O. 2006, c.22

Ontario. Ontario Water Resources Act. R.S.O. 1990, c.O.40

Ontario. Safe Drinking Water Act, 2002. S.O. 2002, c.32

Parsons, A.J., Wainwright, J., Braizier, R.E., Powell, D.M. 2006. "Is sediment delivery a fallacy?" Earth Surface Processes and Landforms, 31 p1325-1328.

Peng, W., Wheeler, D.A., Bell, J.C., Krusemark, M.G. 2003. "Delineating patterns of soil drainage class on bare soils using remote sensing analysis" Geoderma, 115 p261-279

Philip, J.R. 1957. "The theory of infiltration: 4. Sorptivity and algebraic infiltration equations" Soil Science, 84 p257-264

Pietroniro, A., Leconte, R. 2000. "A review of Canadian remote sensing applications in hydrology, 1995-1999" Hydrological Processes, 14 p1641-1666

Pietroniro, A., Leconte, R. 2005. "A review of Canadian remote sensing and hydrology, 1999-2003" Hydrological Processes, 19 p285-301

Prenzel, B., Treitz, P. 2005. "Comparison of function and structure based schemes for classification of remotely sensed data". International Journal of Remote Sensing, 26 p543-561

Priestley, C.H.B., Taylor, R.J. 1972. "On the assessment of surface heat flux and evaporation using large scale parameters" Monthly Weather Review. 100 p81-92.

Refsgaard, J.C., Storm, B. 1995. "MIKE SHE" in Computer models of watershed hydrology V.P.Singh (ed.), Water Resources Publications, Colorado.

Refsgaard, J.C., Storm, B. 1996. "Construction, calibration and validation of hydrological models" in Distributed Hydrological Modelling Kluwer Academic Publishers, Dordrecht, The Netherlands.

Renard, K.G., Foster, G.R., Weesies, G.A., McCool, D.K, Yoder, D.C. 1997. Predicting soil erosion by water: A guide to conservation planning with teh Revised Soil Loss Equation (RUSLE) US. Department of Agriculture Agricultural Research Service, Washington D.C.

Reungsang, P., Kanwar, R. S., Jha, M., Gassman, P. W., Ahmad, K., Saleh, A. "Calibration and Validation of SWAT for the Upper Maquoketa River Watershed." June 2005. Working Paper 05-WP 396, Iowa State University Center for Agricultural and Rural Development, Ames Iowa.

Richards, J.A., Jai, X. 1999. Remote Sensing Digital Image Analysis (3rd ed.) Springer-Verlag, Berlin.

Richter, B. D., Baumgartner, J. V., Wigington, R. 1997. "How much water does a river need?" Freshwater Biology, 37 p237-249

Romanowicz, A., Vanclooster, M., Rounsevell, M., La Junesse, I. 2005. "Sensitivity of the SWAT model to the soil and land use data parametrisation: a case study in the Thyle catchment, Belgium" Ecological Modelling 187 p27-39

Rosenthal, W.D., Hoffman, D.W. 1999. "Hydrologic modelings: GIS as an aid in locating monitoring sites" Transactions of the ASAE, 42 p1591-1598

Saleh, A., Du, B. 2004. "Evaluation of SWAT and HSPF within BASINS Program for the Upper North Bosque River Watershed in Central Texas" Transactions of the ASAE, 47 p1039-1049

Santhi, C., Arnold, J.G., Williams, J.R., Dugas, W.A., Sirinivasan, R., Hauck, L.M. 2001. "Validation of the SWAT model on a large river basin with point and non point sources" Journal of the American Water Resources Association, 37 p1169-1188

Santhi, C., Srinivasan, R., Arnold. J.G., Williams, J.R. 2006. "A modeling approach to evaluate the impacts of water quality management plans implemented in a watershed in Texas" Environmental Modelling and Software, 21 p1141-1157

Singh, J., Knapp, V., Arnold, J.G., Demissie, M. 2005. "Hydrological modeling of the Iroquois River watershed using HSPF and SWAT" Journal of the American Water Resources Association, 41, p343-360

Singh, V.P. 1988. Hydrologic systems Prentice-Hall, Englewood Cliffs, New Jersey.

Singh, V.P. (ed) 1995. Computer Models of Watershed Hydrology Water Resources Publications, Colorado.

Singh, V.P., Woolhiser, D.A. 2002. "Mathematical modeling of watershed hydrology" Journal of Hydrologic Engineering, 7 p270-292

SCS. 1972. "Section 4: Hydrology – Chapter 10: Estimation of direct runoff from storm rainfall" by V. Mockus, in National Engineering Handbook Soil Conservation Service.

Sophocleous, M. A., Koelliker, J. K., Govindaraju, R. S., Birdie, T., Ramireddygari, S. R., Perkins, S. P. 1999. "Integrated numerical modeling for basin-wide water management: The case of the Rattlesnake Creek basin in south-central Kansas." Journal of Hydrology, 214 p179-196

Sophocleous, M., Perkins, S. P. 2000. "Methodology and application of combined watershed and ground-water models in Kansas." Journal of Hydrology, 236 p185-201

Spruill, C. A., Workman, S. R., Taraba, J. L. 2000. "Simulation of daily and monthly stream discharge from small watersheds using the SWAT model." Transactions of the ASAE, 43 p1431-1439

Srinivastava, P., McNair, J. N., Johnson, T. E. 2006. "Comparison of Process-based and Artificial Neural Network Approaches for Streamflow Modeling in an Agricultural Watershed." Journal of the American Water Resources Association, 42 p545-563

Steele, B. M., Winne, J. C., Redmond, R. L. 1998. "Estimation and mapping of misclassification probabilities for Thematic land cover maps." Remote Sensing of Environment, 66 p192-202

Su, Z. 2000. "Remote sensing of land use and vegetation for mesoscale hydrological studies." International Journal of Remote Sensing, 21 p213-233

Sun, H., Cornish, P. S. 2005. "Estimating shallow groundwater recharge in the headwaters of the Liverpool Plains using SWAT" Hydrological Processes, 19 p795-807

Tarboton, D. G., Bras, R. L., Rodriguez-Iturbe, I. 1991. "On the extraction of channel networks from digital elevation data." Hydrological Processes, 5 p81-100

US-EPA. 2000. National Water Quality Inventory: 2000 Report EPA-841-R-02-001. United States Environmental Protection Agency, Washington D.C.

Van Liew, M. W., Arnold, J. G., Bosch, D. D. 2005. "Problems and potential of autocalibrating a hydrologic model" Transactions of the ASAE, 48 p. 1025-1040.

Van Liew, M.W., Arnold, J.G., Garbrecht, J.D. 2003. "Hydrologic simulation on agricultural watersheds: Choosing between two models" Transactions of the ASAE, 46 p1539-1551.

von Neumann, J., Morgenstern, O. 1953. Theory of Games and Economic Behavior (3rd ed.) Princeton University Press, Princeton.

Wang, X., Melesse, A. M. 2005. "Evaluation of the SWAT model's snowmelt hydrology in a northwestern Minnesota watershed." Transactions of the ASAE, 48 p1359-1376

Williams, J.R. 1969. "Flood routing with variable travel time or variable storage coefficients" Transactions of the ASAE, 12 p100-103

Williams, J.R., Jones, C.A., Dyke, P.T. 1984. "A modeling approach to determining the relationship between erosion and soil productivity" Transactions of the ASAE, 27 p129-144

Williams, J., Nearing, M., Nicks, A., Skidmore, E., Valentine, C., King, K., Savabi, R. 1996. "Using soil erosion models for global change studies." Journal of Soil and Water Conservation, 51 p381-385

Young, R.A., Onstad, C.A., Bosch, D.D., Anderson, W.P. 1989. "AGNPS: A nonpoint source pollution model for evaluating watersheds" Journal of Soil and Water Conservation, 44 p168-173

Appendix A. Additional Tables

Data	Source
Landsat imagery Path 15, Row 29 1992 May 29 1999 Nov 01 2001 Sep 01 2001 Jun 15	GeoGratis (Natural Resources Canada) *URL: geogratis.cgdi.gc.ca* Global Observatory for Ecosystem Services (Michigan State University) *URL: landsat.org*
Digital elevation model Map sheet 031G02 Geographic NAD83 0.75 arcseconds horizontal, 1m vertical	National Topographic Database (NTDB) 1:50000 series, version 3.04, April 26 2001 *URL: www.cits.rncan.gc.ca*
Water layers Mapsheet 031G02 Watercourses Waterbodies Wetlands	National Topographic Database (NTDB) 1:50000 series, version 3.04, April 26 2001 *URL: www.cits.rncan.gc.ca*
Soil data Climate normals Crop heat units Solar radiation	Canadian Soils Information System (CanSIS) database *URL: sis.agr.gc.ca*
Climate station records Cornwall (C6101874) 45° 1' N, 74° 45' W Avonmore (C6100398) 45° 10'N, 74° 58' W	National Climate Archive (Environment Canada) *URL: climate.weatheroffice.ec.gc.ca*
Stream flow records: Williamstown (02MC001) Black River (02MC027) Raisin River South branch (02MC030)	Water Survey Canada *URL: www.wsc.ec.gc.ca*

Table 11 – Data sources

Parameter	Range	Final value
Curve number (CN)	+/- 15%	+10%
Available water content (AWC)	+/- 20%	+20%
Surface lag coefficient (SURLAG)	0.0 – 5.0	0.9
Soil evaporation coefficient (ESCO)	0.1 – 1.0	0.7
Revap coefficient (REVAP)	0.1 – 0.2	0.15
Groundwater delay coefficient	0.0 – 10.0	0.6
Groundwater recession coefficient	0.0 – 0.2	0.05
Deep aquifer loss fraction	0.0 – 0.5	0.18
Snowfall temperature [ºC]	-1.0 – 2.0	0.6
Snowmelt temperature [ºC]	-1.0 – 2.0	0.8
Snowpack temperature lag coefficient (TIMP)	0.0 – 1.0	0.7
December 21 snowmelt rate [mm/(ºC · day)]	0.5 – 3.0	2.1
June 21 snowmelt rate [mm/(ºC · day)]	0.5 – 3.0	2.3

Table 12 - Calibration parameters: the ranges used during calibration and the final values

Appendix B. Additional Figures

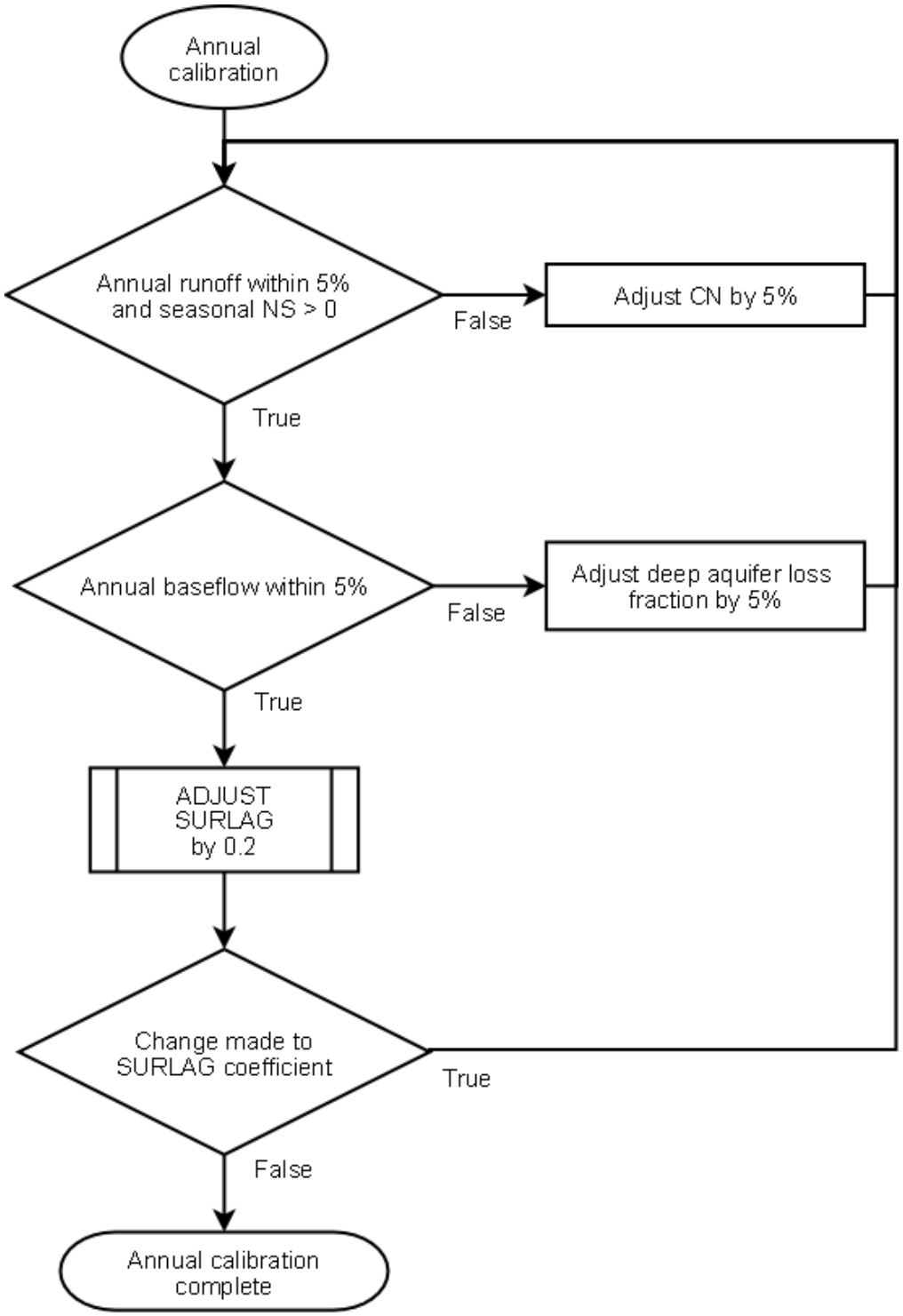

Figure 44 - Annual calibration procedure

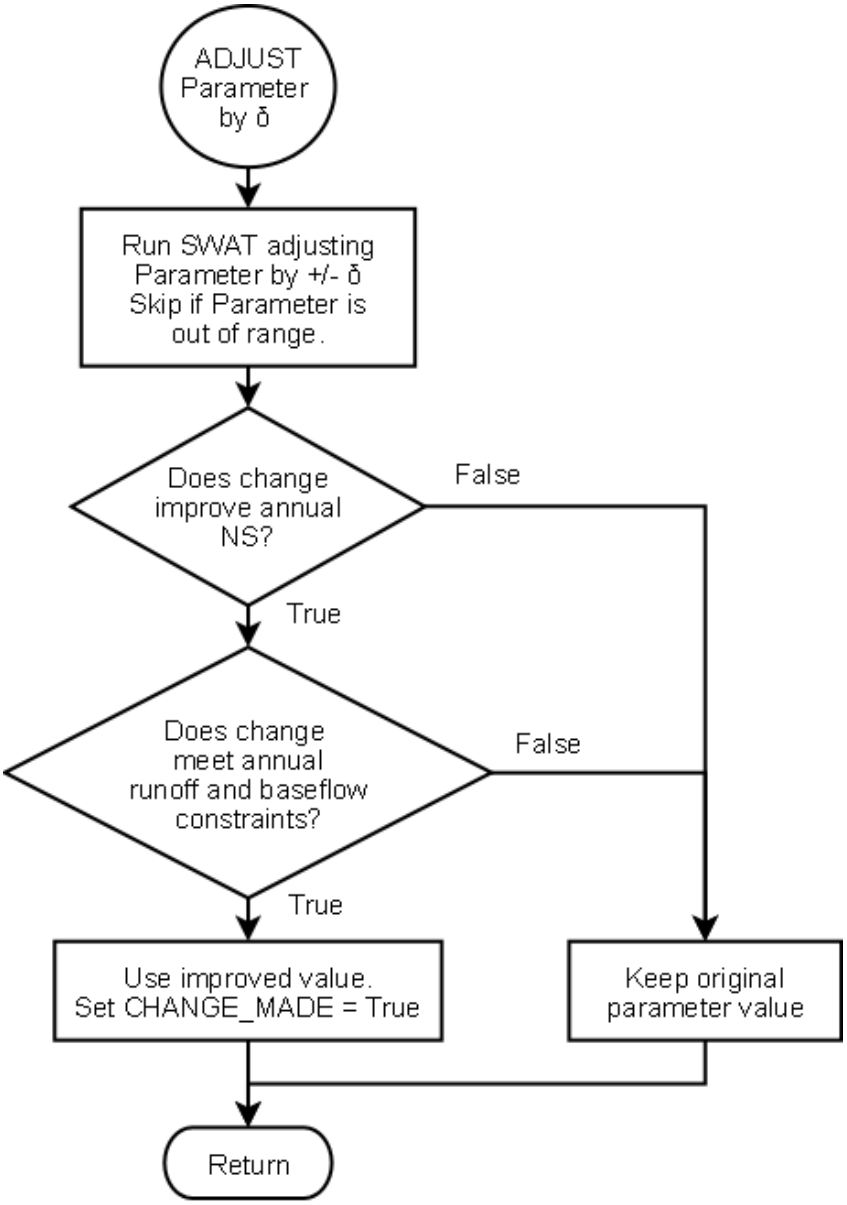

Figure 45 - Variable adjustment procedure

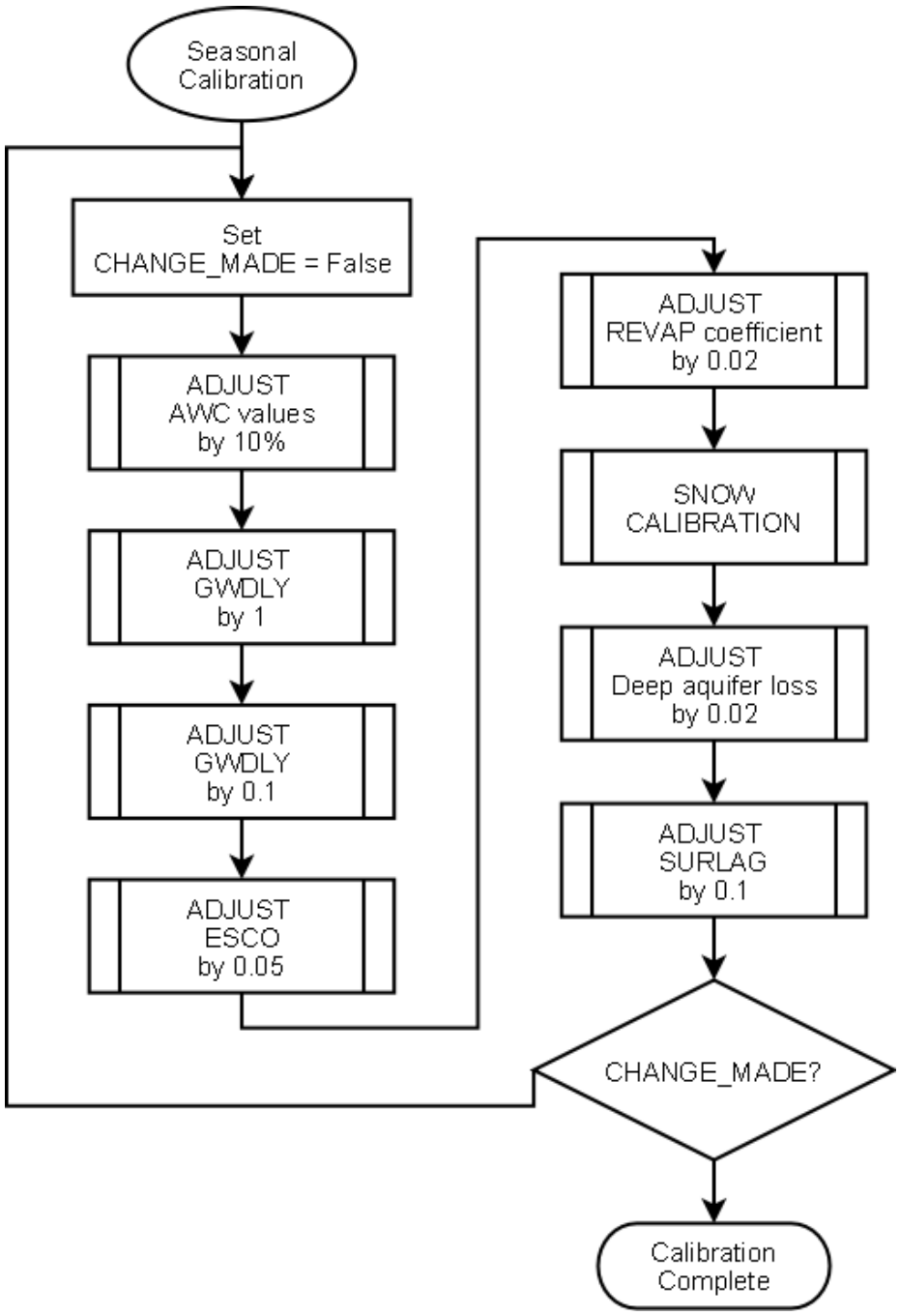

Figure 46 - Seasonal adjustment

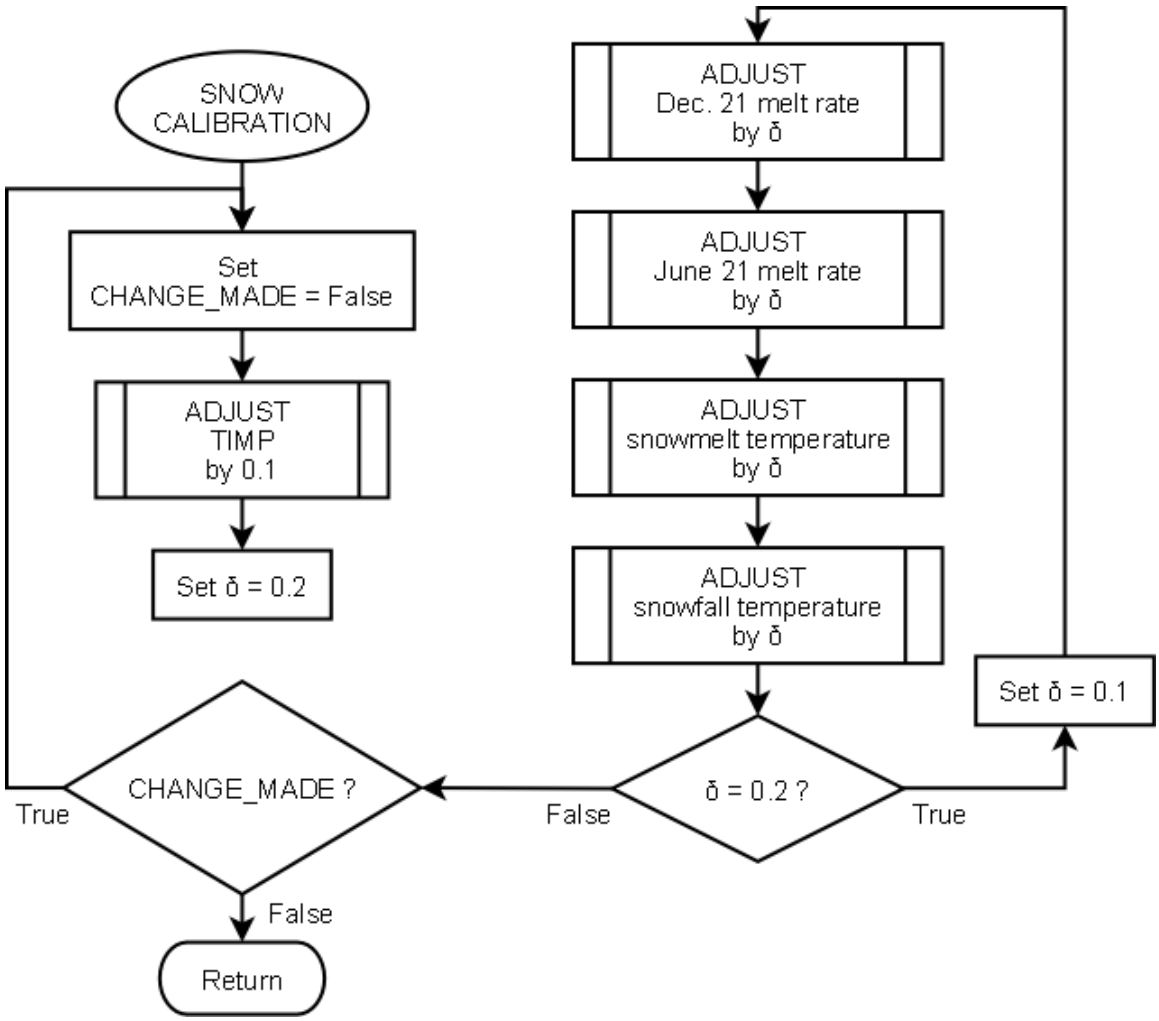

Figure 47 - Snow calibration

Appendix C. Maps

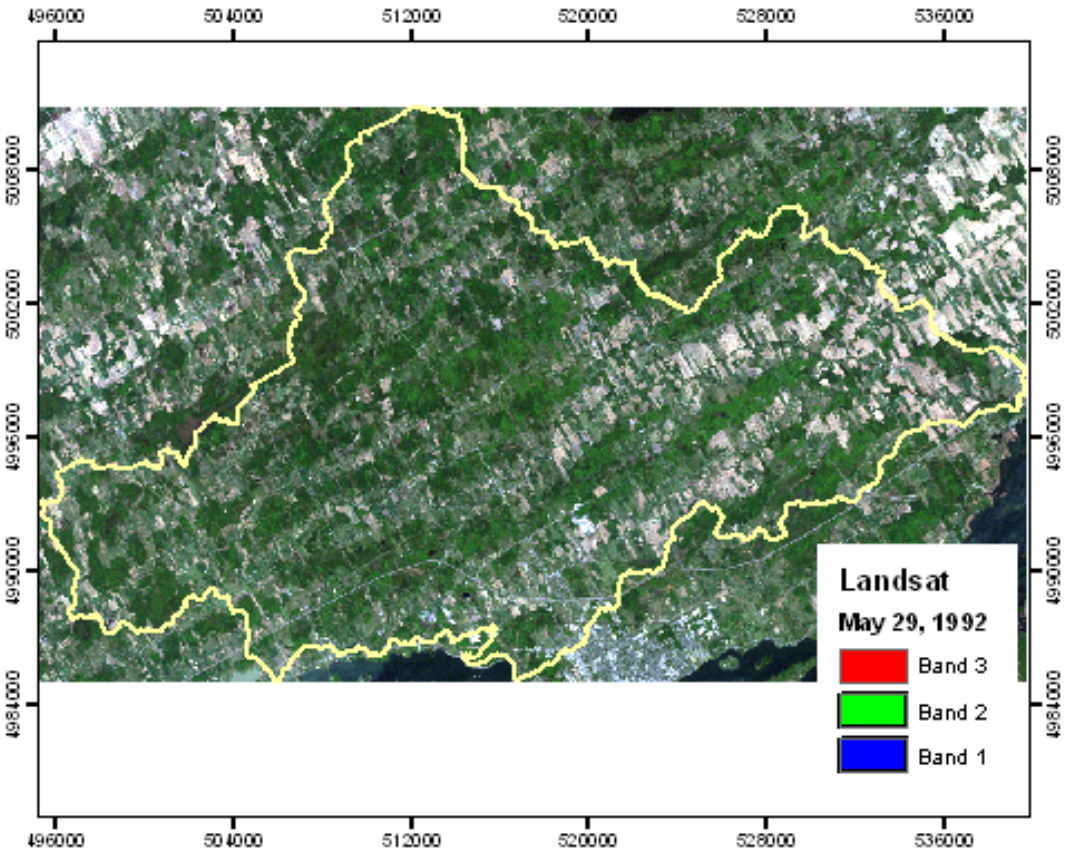

Map 1 - Landsat May 29, 1992

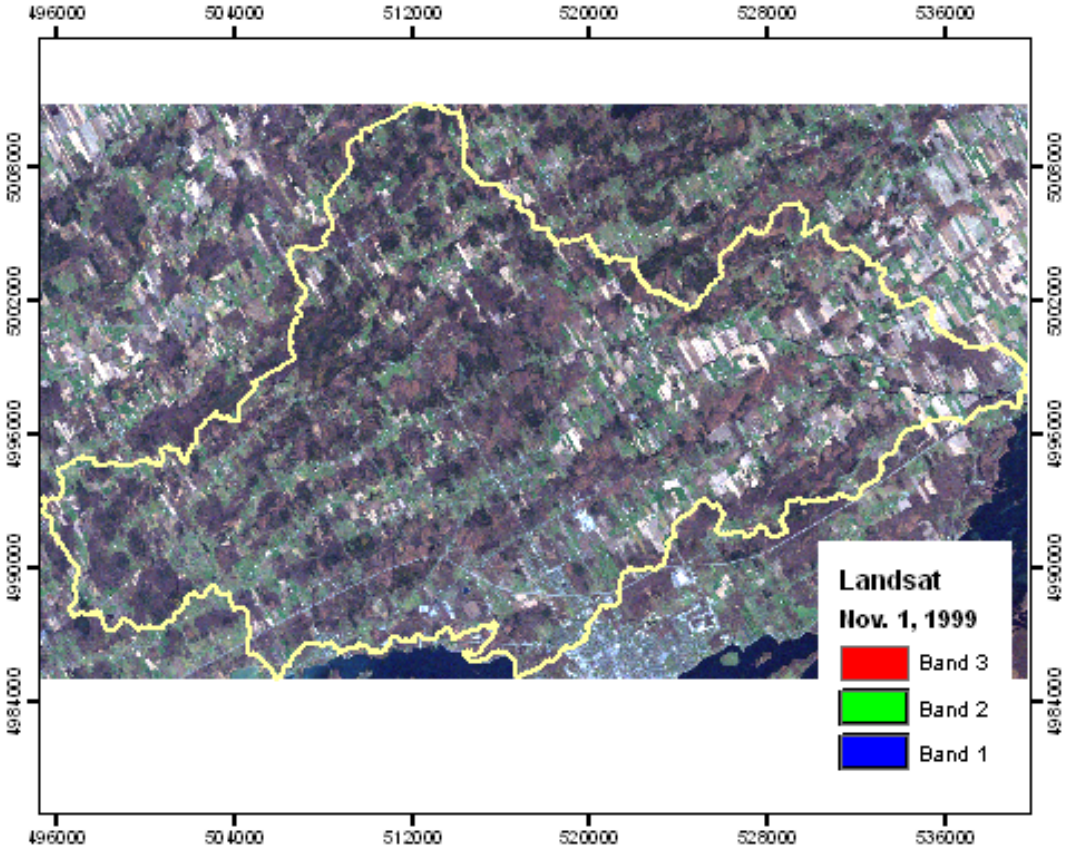

Map 2 - Landsat November 1, 1999

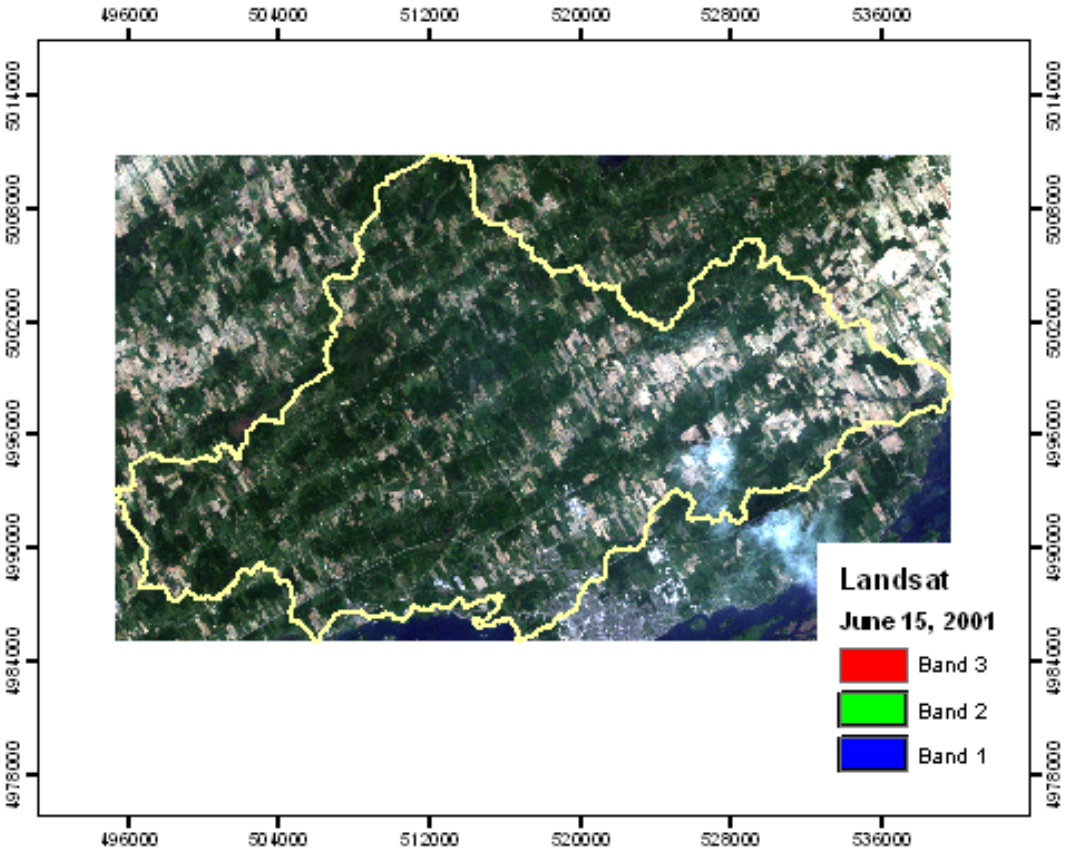

Map 3 - Landsat June 15, 2001

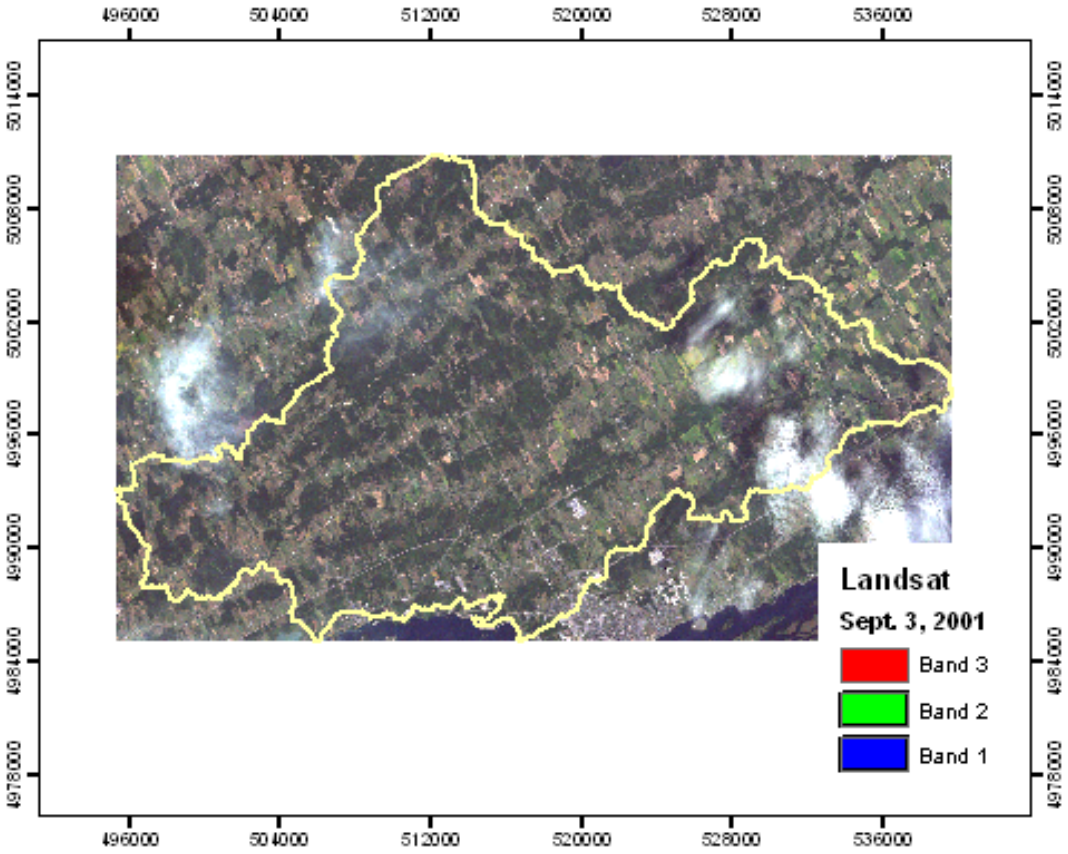

Map 4 - Landsat September 3, 2001

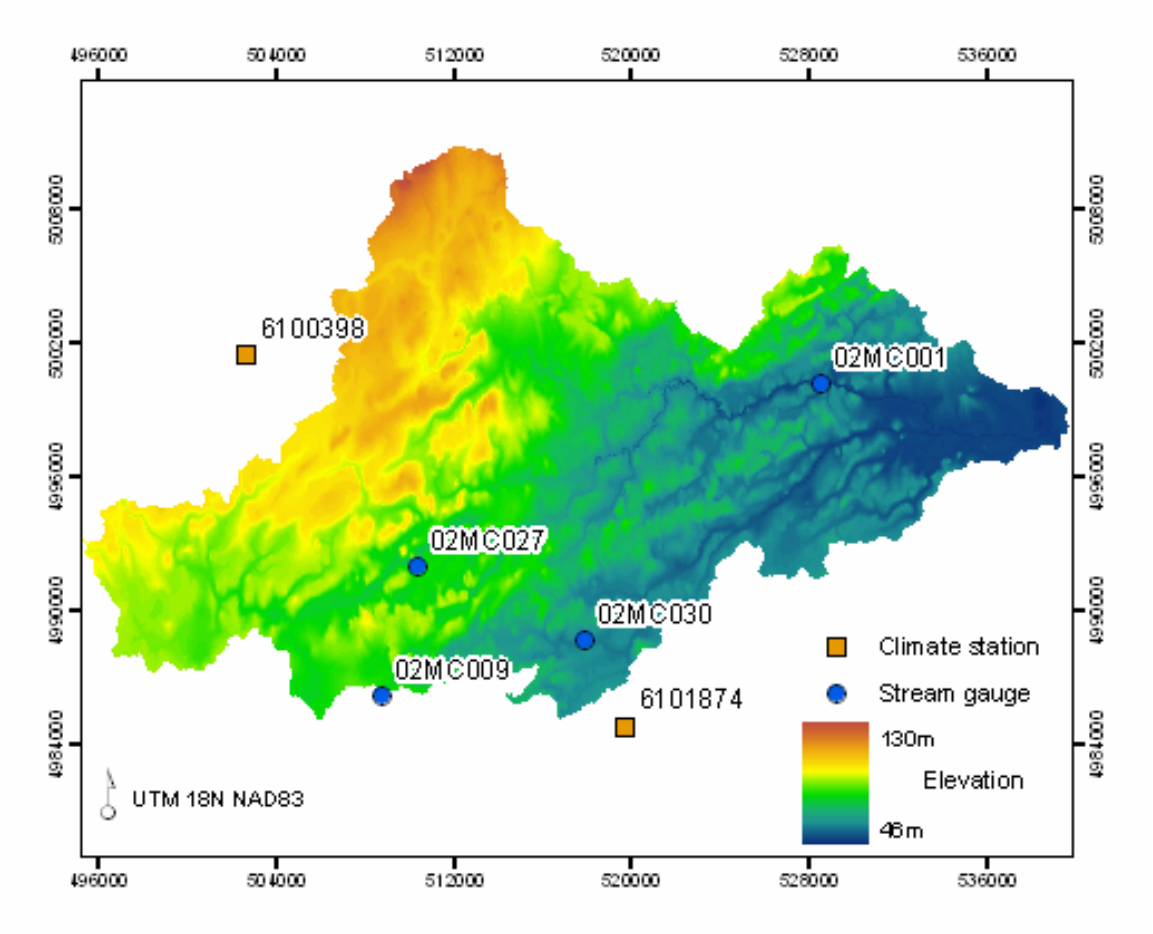

Map 5 - Elevation and location of gauges

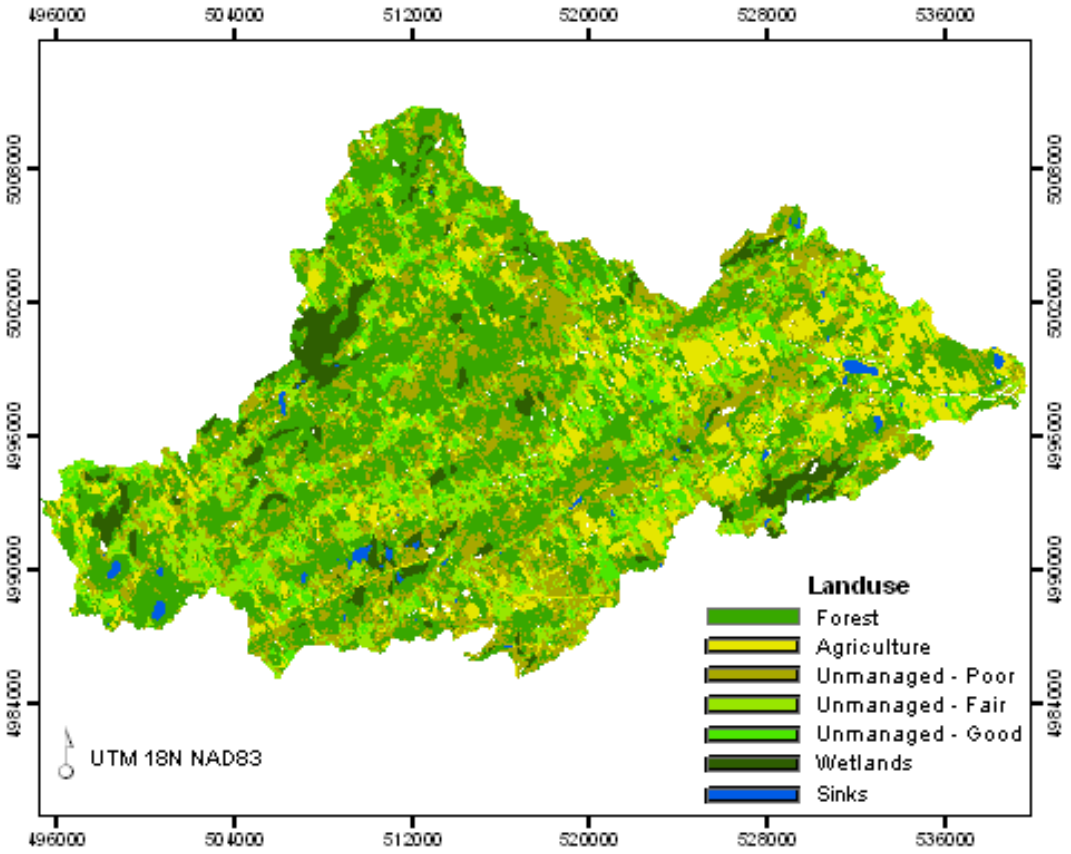

Map 6 - Landuse derived from November 1999 Landsat image

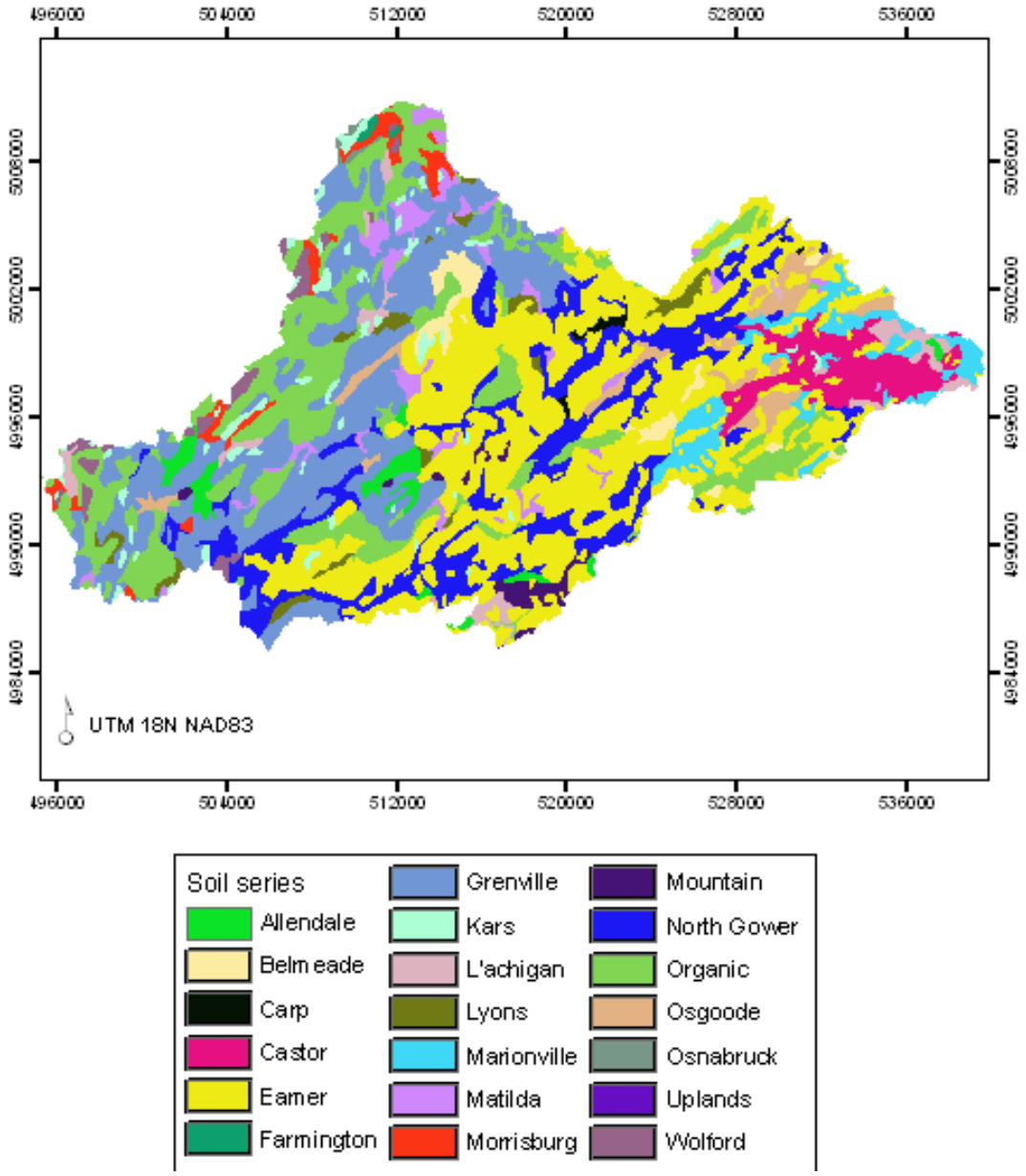

Map 7 - Soil types

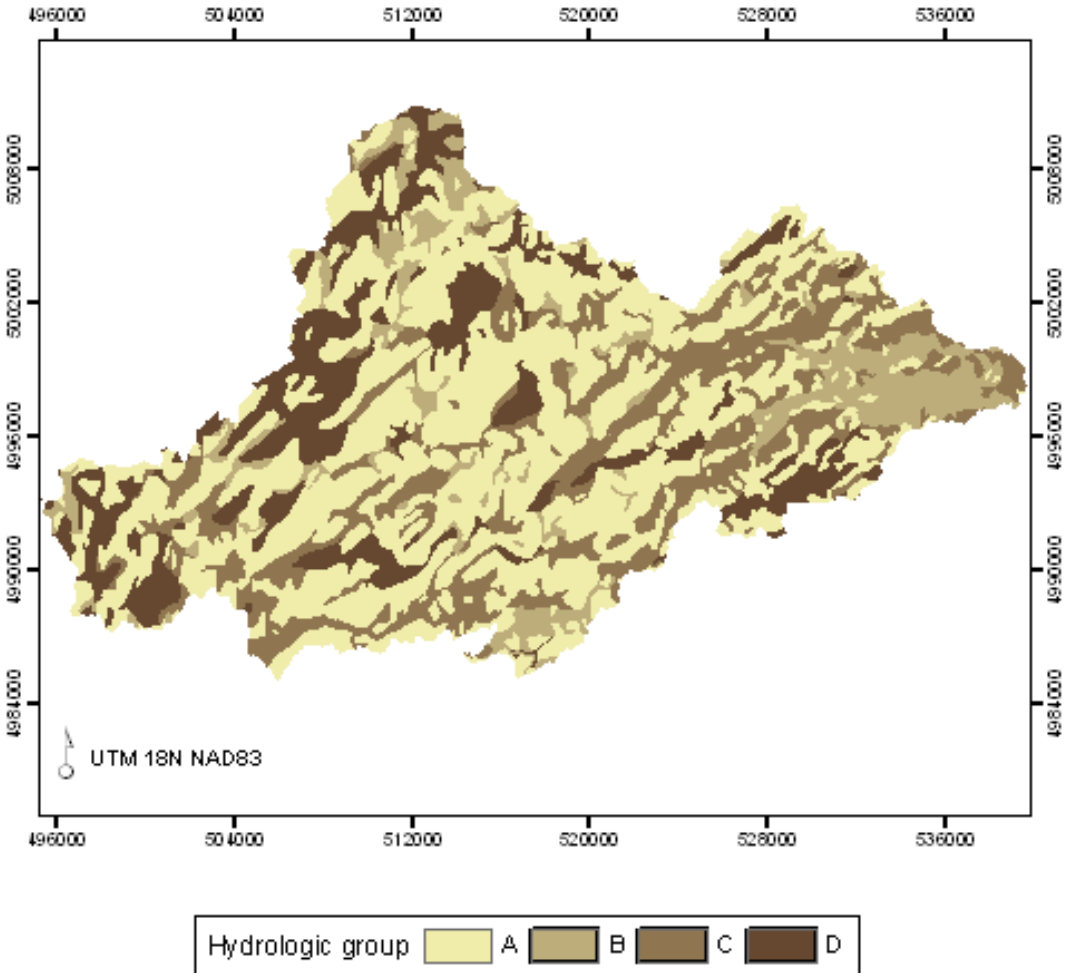

Map 8 - Soil drainage class

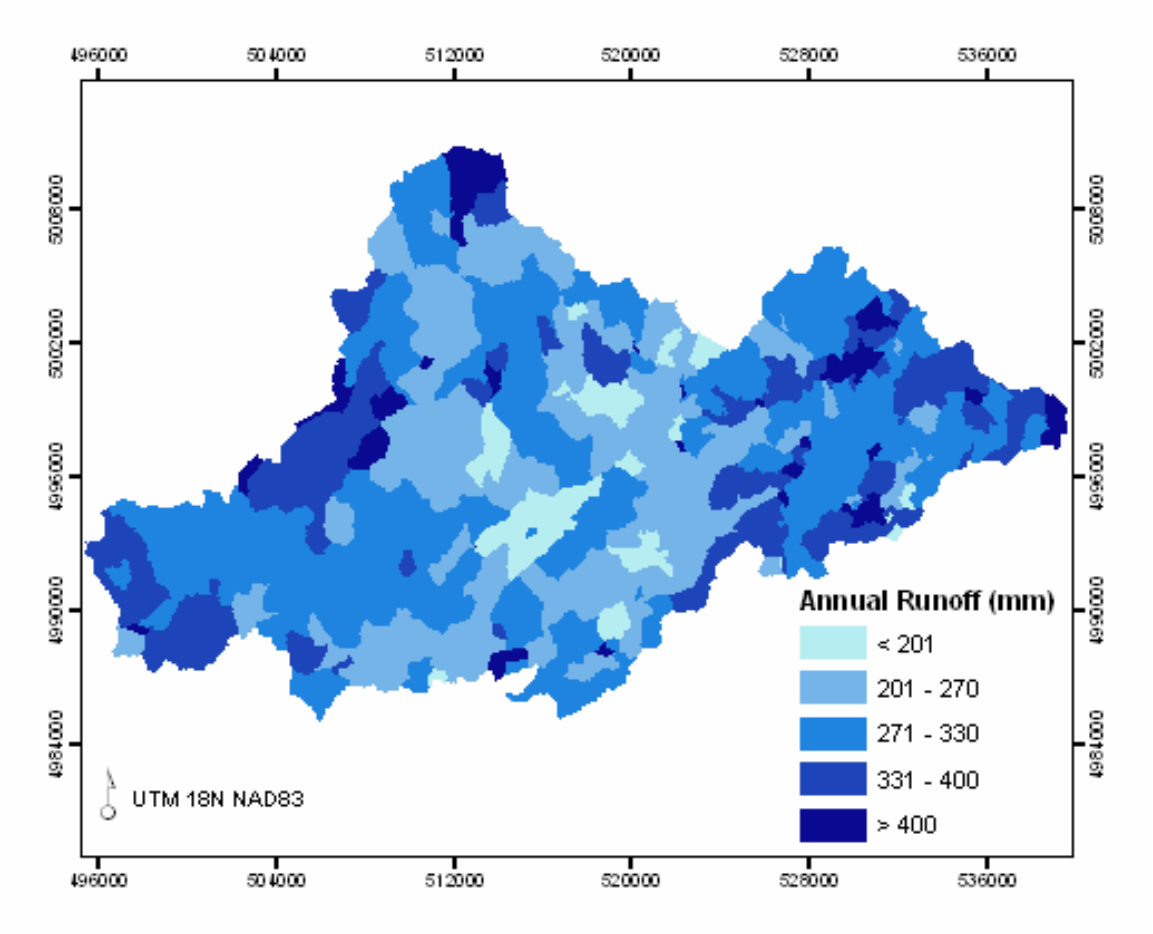

Map 9 - Average annual runoff per subbasin

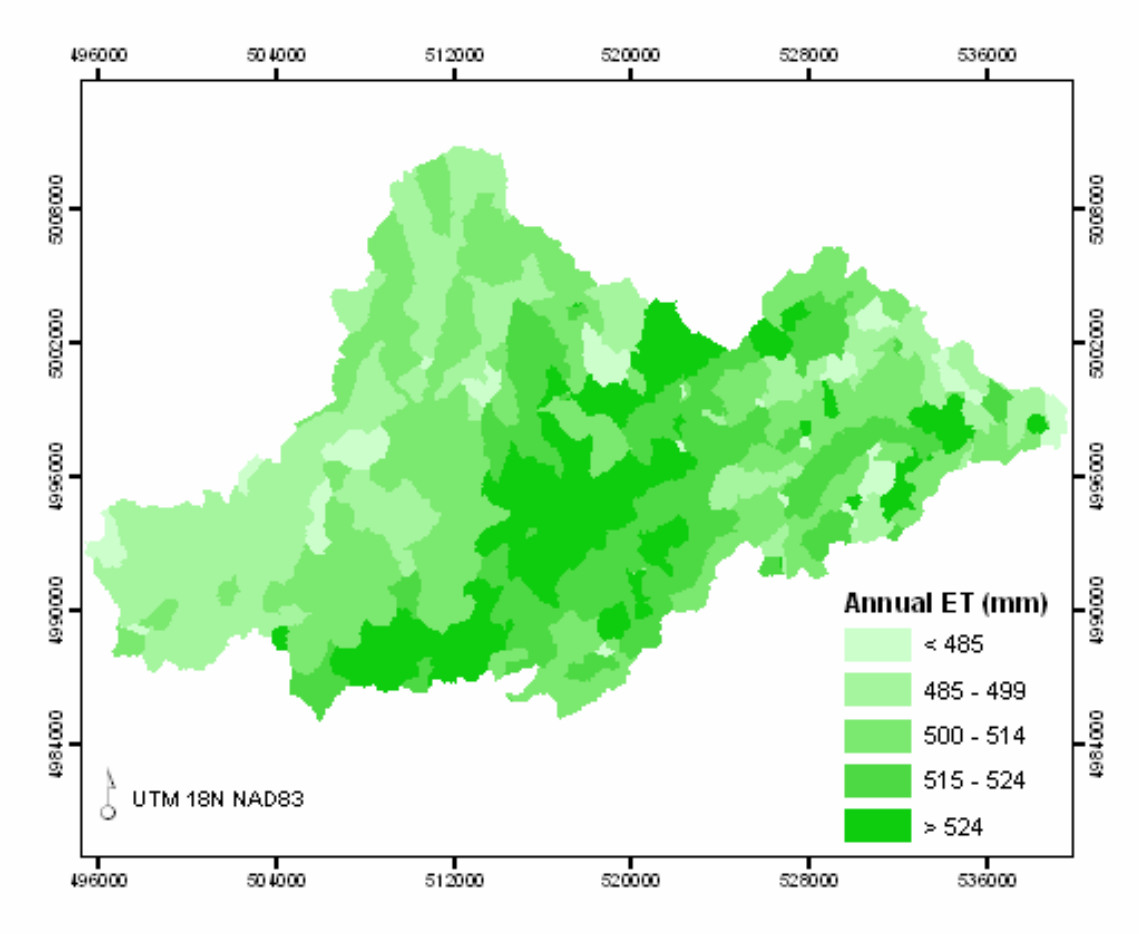

Map 10 - Average annual evapotranspiration

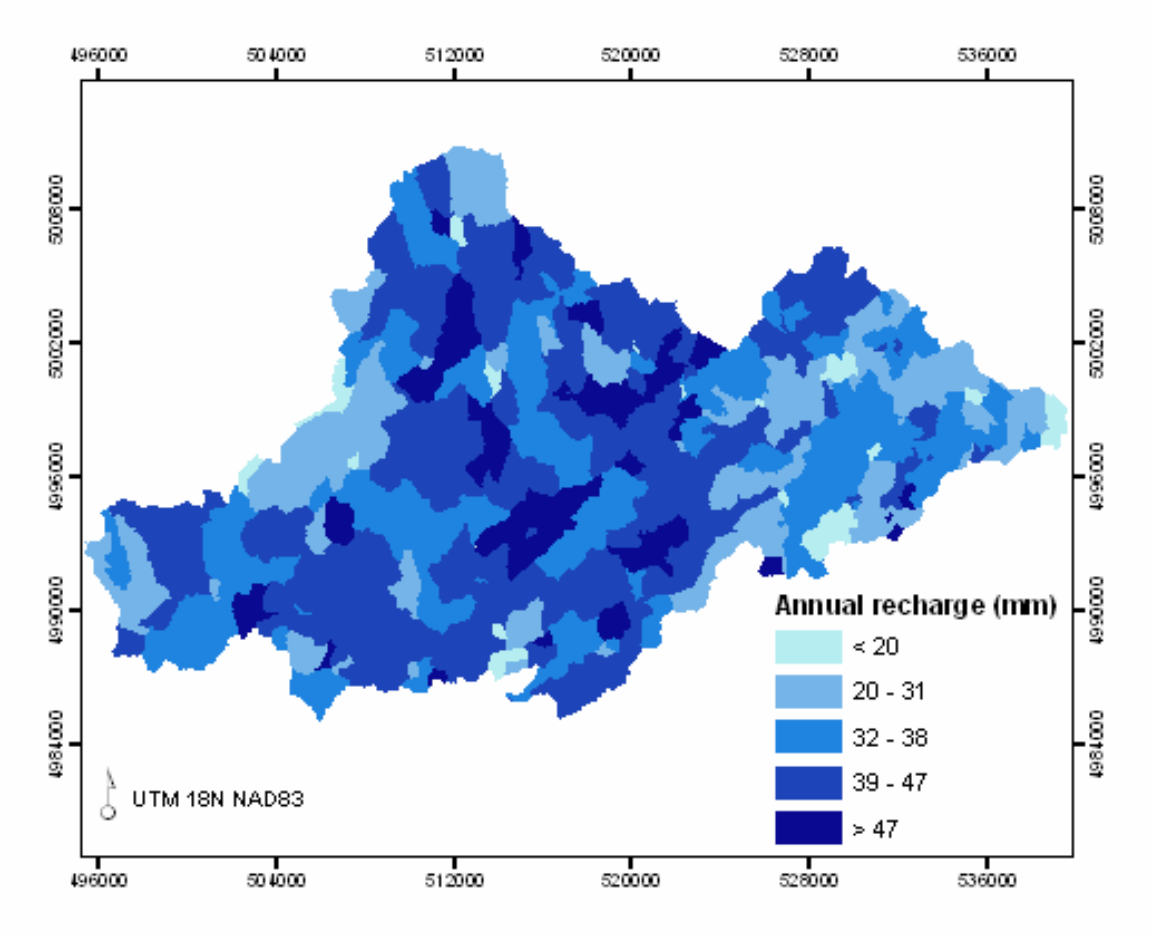

Map 11 - Average annual recharge

Appendix D. Soil Data

L'Achigan AHG

Layer	Depth (mm)	AWC (mm/mm)	K_{sat} (mm/hr)	Carbon (%)	Clay (%)	Silt (%)	Sand (%)	Rock (%)	Albedo
1	30	0.14	25.9	11	12	19	69	0	0.05
2	100	0.12	61.0	10	8	9	83	0	0.17
3	230	0.12	61.0	1	2	15	83	0	0.13
4	582	0.12	61.0	1	3	11	86	0	0.13
5	770	0.10	210.0	1	3	10	88	0	0.17

Allendale ALL

Layer	Depth (mm)	AWC (mm/mm)	K_{sat} (mm/hr)	Carbon (%)	Clay (%)	Silt (%)	Sand (%)	Rock (%)	Albedo
1	186	0.14	25.9	4	8	26	66	0	0.01
2	384	0.12	61.0	0	7	11	82	0	0.17
3	568	0.20	13.2	0	26	29	46	0	0.17
4	932	0.25	0.9	0	42	45	13	0	0.17
5	1000	0.20	13.2	0	25	28	47	0	0.17

Marionville BIV

Layer	Depth (mm)	AWC (mm/mm)	K_{sat} (mm/hr)	Carbon (%)	Clay (%)	Silt (%)	Sand (%)	Rock (%)	Albedo
1	163	0.20	6.8	8	13	54	33	0	0.05
2	367	0.14	25.9	0	3	39	59	0	0.13
3	524	0.20	13.2	0	14	48	38	0	0.17
4	990	0.25	0.9	0	46	45	9	0	0.17
5	1000	0.20	6.8	1	26	55	19	0	0.17

Belmeade BMD

Layer	Depth (mm)	AWC (mm/mm)	K_{sat} (mm/hr)	Carbon (%)	Clay (%)	Silt (%)	Sand (%)	Rock (%)	Albedo
1	177	0.23	1.5	20	35	51	14	0	0.01
2	337	0.23	1.5	1	35	51	14	0	0.13
3	697	0.23	1.5	1	34	50	16	0	0.17
4	1000	0.23	1.5	0	35	45	20	0	0.17

Carp CRP

Layer	Depth (mm)	AWC (mm/mm)	K_{sat} (mm/hr)	Carbon (%)	Clay (%)	Silt (%)	Sand (%)	Rock (%)	Albedo
1	253	0.23	2.3	6	30	45	25	0	0.09
2	377	0.23	2.3	2	28	46	26	0	0.17
3	633	0.23	1.5	0	34	48	18	0	0.13
4	883	0.23	1.5	0	35	51	14	0	0.13
5	1083	0.23	1.5	0	36	50	14	0	0.17

Castor CST

Layer	Depth (mm)	AWC (mm/mm)	K_{sat} (mm/hr)	Carbon (%)	Clay (%)	Silt (%)	Sand (%)	Rock (%)	Albedo
1	168	0.20	6.8	5	13	62	25	0	0.05
2	418	0.20	2.5	2	4	82	14	0	0.17
3	713	0.20	6.8	1	3	63	34	0	0.13
4	903	0.14	25.9	0	7	35	58	0	0.17
5	1067	0.23	2.3	0	36	32	32	0	0.17

Eamer EMR

Layer	Depth (mm)	AWC (mm/mm)	K_{sat} (mm/hr)	Carbon (%)	Clay (%)	Silt (%)	Sand (%)	Rock (%)	Albedo
1	130	0.20	13.2	3	16	38	47	5	0.05
2	250	0.14	25.9	2	12	32	56	5	0.09
3	460	0.20	13.2	1	11	39	51	15	0.05
4	580	0.20	13.2	0	20	37	43	15	0.13
5	1000	0.20	13.2	0	19	33	49	15	0.13

Farmington FRM

Layer	Depth (mm)	AWC (mm/mm)	K_{sat} (mm/hr)	Carbon (%)	Clay (%)	Silt (%)	Sand (%)	Rock (%)	Albedo
1	134	0.20	13.2	3	20	39	41	5	0.09
2	376	0.14	25.9	2	12	31	57	15	0.13
3	797	0.20	13.2	1	11	39	50	95	0.17
4	931	0.23	2.3	0	28	34	38	95	0.17
5	1000	0.23	2.3	0	28	34	38	95	0.17

Grenville GVI

Layer	Depth (mm)	AWC (mm/mm)	K_{sat} (mm/hr)	Carbon (%)	Clay (%)	Silt (%)	Sand (%)	Rock (%)	Albedo
1	136	0.14	25.9	3	15	33	52	5	0.05
2	235	0.14	25.9	2	12	33	55	5	0.17
3	461	0.20	13.2	1	10	39	51	5	0.09
4	657	0.20	13.2	0	12	40	47	15	0.09
5	841	0.14	25.9	0	9	32	59	15	0.13

Kars KRS

Layer	Depth (mm)	AWC (mm/mm)	K_{sat} (mm/hr)	Carbon (%)	Clay (%)	Silt (%)	Sand (%)	Rock (%)	Albedo
1	180	0.14	25.9	3	9	26	65	5	0.09
2	335	0.14	25.9	1	11	22	67	5	0.13
3	530	0.12	61.0	2	6	15	79	5	0.09
4	1000	0.10	210.0	1	2	9	89	20	0.13

Lyons LYS

Layer	Depth (mm)	AWC (mm/mm)	K_{sat} (mm/hr)	Carbon (%)	Clay (%)	Silt (%)	Sand (%)	Rock (%)	Albedo
1	184	0.14	25.9	6	9	21	71	15	0.01
2	342	0.14	25.9	1	7	21	73	15	0.13
3	746	0.14	25.9	0	8	30	62	15	0.17
4	1000	0.14	25.9	0	7	34	59	15	0.17

Morrisburg MBG

Layer	Depth (mm)	AWC (mm/mm)	K_{sat} (mm/hr)	Carbon (%)	Clay (%)	Silt (%)	Sand (%)	Rock (%)	Albedo
1	150	0.23	2.3	2	34	33	33	5	0.09
2	250	0.23	2.3	1	34	33	33	5	0.09
3	380	0.23	2.3	0	34	33	33	5	0.09
4	1000	0.23	2.3	0	34	33	33	15	0.17

Matilda MTD

Layer	Depth (mm)	AWC (mm/mm)	K_{sat} (mm/hr)	Carbon (%)	Clay (%)	Silt (%)	Sand (%)	Rock (%)	Albedo
1	142	0.20	13.2	4	14	35	51	5	0.13
2	240	0.14	25.9	1	6	33	61	5	0.13
3	401	0.20	13.2	1	13	36	51	5	0.13
4	617	0.14	25.9	0	8	30	62	15	0.13
5	880	0.14	25.9	0	6	31	62	15	0.17

Mountain MUA

Layer	Depth (mm)	AWC (mm/mm)	K_{sat} (mm/hr)	Carbon (%)	Clay (%)	Silt (%)	Sand (%)	Rock (%)	Albedo
1	195	0.12	61.0	2	6	12	82	0	0.09
2	313	0.12	61.0	1	4	9	87	0	0.17
3	493	0.10	210.0	0	4	8	89	0	0.17
4	653	0.23	2.3	0	32	37	31	0	0.17
5	970	0.18	4.3	0	29	23	49	0	0.17

North Gower BDO

Layer	Depth (mm)	AWC (mm/mm)	K_{sat} (mm/hr)	Carbon (%)	Clay (%)	Silt (%)	Sand (%)	Rock (%)	Albedo
1	150	0.23	2.3	8	32	38	30	0	0.05
2	326	0.25	0.9	1	41	40	19	0	0.13
3	567	0.28	0.6	0	44	36	20	0	0.13
4	686	0.25	0.9	0	53	40	7	0	0.17
5	1000	0.28	0.6	0	54	37	10	0	0.17

North Gower NGW

Layer	Depth (mm)	AWC (mm/mm)	K_{sat} (mm/hr)	Carbon (%)	Clay (%)	Silt (%)	Sand (%)	Rock (%)	Albedo
1	182	0.20	6.8	4	27	51	22	0	0.05
2	424	0.23	2.3	1	31	46	23	0	0.13
3	628	0.23	2.3	0	38	40	22	0	0.13
4	924	0.23	1.5	0	36	44	19	0	0.17
5	1000	0.23	1.5	0	36	44	20	0	0.17

Osnabruck OBK

Layer	Depth (mm)	AWC (mm/mm)	K_{sat} (mm/hr)	Carbon (%)	Clay (%)	Silt (%)	Sand (%)	Rock (%)	Albedo
1	250	0.28	0.6	8	48	37	15	5	0.01
2	400	0.23	1.5	0	36	50	14	5	0.17
3	1000	0.23	1.5	0	36	50	14	20	0.17

Osgoode OGO

Layer	Depth (mm)	AWC (mm/mm)	K_{sat} (mm/hr)	Carbon (%)	Clay (%)	Silt (%)	Sand (%)	Rock (%)	Albedo
1	239	0.20	13.2	5	22	36	43	0	0.09
2	523	0.20	13.2	0	20	36	44	0	0.17
3	939	0.20	13.2	0	24	41	35	0	0.13
4	1000	0.20	13.2	0	23	45	32	0	0.13

Organic ORG

Layer	Depth (mm)	AWC (mm/mm)	K_{sat} (mm/hr)	Carbon (%)	Clay (%)	Silt (%)	Sand (%)	Rock (%)	Albedo
1	537	0.20	2.5	50	25	50	25	0	0.1
2	1059	0.20	2.5	50	25	50	25	0	0.1
3	1401	0.20	2.5	50	25	50	25	0	0.1
4	1600	0.20	2.5	50	25	50	25	0	0.1

Uplands UPD

Layer	Depth (mm)	AWC (mm/mm)	K_{sat} (mm/hr)	Carbon (%)	Clay (%)	Silt (%)	Sand (%)	Rock (%)	Albedo
1	120	0.10	210.0	4	5	7	88	0	0.05
2	185	0.12	61.0	2	4	10	87	0	0.13
3	295	0.10	210.0	1	2	7	92	0	0.13
4	528	0.10	210.0	1	2	3	95	0	0.13
5	780	0.10	210.0	0	2	2	96	15	0.13

Wolford WFD

Layer	Depth (mm)	AWC (mm/mm)	K_{sat} (mm/hr)	Carbon (%)	Clay (%)	Silt (%)	Sand (%)	Rock (%)	Albedo
1	150	0.23	2.3	4	34	33	33	10	0.01
2	225	0.23	2.3	2	34	33	33	5	0.09
3	400	0.23	2.3	1	34	33	33	15	0.05
4	500	0.23	2.3	0	34	33	33	15	0.09
5	1000	0.23	2.3	0	34	33	33	15	0.17